Spring 2016

Geophysical Imaging of Karst Features in Missouri

Jeremiah Chukwunonso Obi

Department: Geosciences and Geological and Petroleum Engineering

GEOPHYSICAL IMAGING OF KARST FEATURES IN MISSOURI

By

JEREMIAH CHUKWUNONSO OBI

A DISSERTATION

Presented to the Faculty of the Graduate School of the

MISSOURI UNIVERSITY OF SCIENCE AND TECHNOLOGY

In Partial Fulfilment of the Requirements for the Degree

DOCTOR OF PHILOSOPHY

In

GEOLOGICAL ENGINEERING

2016

Approved by

Neil L. Anderson, Advisor

J. David Rogers

Kelly Liu

Evgeniy V. Torgashov

Mao Chen Ge

ABSTRACT

Automated electrical resistivity tomography (ERT) supported with multichannel analysis of surface waves (MASW) and boring data were used to map karst related features in Missouri in order to understand karst processes better in Missouri. Previous works on karst in Missouri were mostly surficial mapping of bedrock outcrops and joints, which are not enough to define the internal structure of karst system, since most critical processes in karst occur underground. To understand these processes better, the density, placement and pattern of karst related features like solution-widened joints and voids, as well as top of bedrock were mapped. In the course of the study, six study sites were visited in Missouri. The sites were in Nixa, Gasconade River Bridge in Lebanon, Battlefield, Aurora, Protem and Richland. The case studies reflect to a large extent some of the problems inherent in karst terrain, ranging from environmental problems to structural problems especially sinkhole collapses. The result of the study showed that karst in Missouri is mostly formed as a result of piping of sediments through solution-widened joints, with a pattern showing that the joints/fractures are mostly filled with moist clay-sized materials of low resistivity values. The highest density of mapped solution-widened joints was one in every one hundred and fifty feet, and these areas are where intense dissolution is taking place, and bedrock pervasively fractured. The study also showed that interpreted solution-widened joints trend in different directions, and often times conform with known structural lineaments in the area. About 40% of sinkhole collapses in the study areas are anthropogenic. Karst in Missouri varies, and can be classified as a combination of kI (juvenile), kIII (mature) and kIV (complex) karsts.

ACKNOWLEDGEMENTS

My immense gratitude and appreciation go to my advisor Dr. Neil Anderson for guiding and supporting me throughout my study. He always finds a way of funding me even when things are tight. I would also want to thank Dr. J. David Rogers, Dr. Mao Chen Ge, Dr. Evgeniy Torgashov and Dr. Kelly Liu who are members of my dissertation committee. Their comments, suggestions and overall contributions towards the completion of my dissertation were great.

Also worthy to mention is Mr. James Vandike; he tutored me specifically on karst in Missouri and provided valuable materials to me. I would also want to appreciate my fellow graduate students and all the members of our applied geophysics laboratory who are too numerous to mention for their help, efforts and team work especially in data acquisition during harsh weather conditions. I also thank the Chancellor Dr. Cheryl Schrader for awarding me the Chancellor's fellowship throughout my PhD. years of study. All members of the graduate studies department are also highly appreciated. My special thanks also go to Patty Robertson and Paula Cochran for their administrative help all these years. My special thanks and appreciation go to my family and friends who are always there for me, their prayers, moral and financial supports were unflinching. I am grateful for the special support of Dr. and Mrs. Josiah Ekunno from the very first time I came to the US.

Finally, I dedicate everything to God Almighty who made all things possible.

TABLE OF CONTENTS

Page

LIST OF ILLUSTRATIONS

Page

LIST OF TABLES

Page

1. INTRODUCTION

Karst can be defined as any terrain or landscape where the dissolving of soluble bedrock such as limestone, dolomite, gypsum, marble and salt by both groundwater and surface water has played a dominant role in the development of the area. Typical karst terrain is dominated by the presence of caves, sinkholes, losing/disappearing streams and springs. These features are known to have caused structural and infrastructural problems such as road and highway subsidence, building-foundation collapse, dam leakage and groundwater contamination and pollution. Karst problems worldwide cause huge annual costs as a result of insufficient understanding of karst processes. Missouri is mostly underlain by carbonate rocks and is recognized as a karst state (Veni et. al., 2001), but karst proceses in Missouri are not well understood. Due to complex nature of karst terrain (very strong lateral and vertical changes of physical and lithological properties), subsurface investigation in this area has been a challenge over the years. Typical surficial studies using geological, hydrological and geomorphological methods which have been the case in Missouri are not enough to provide information on degree of karst development, and will not determine the internal structure of karst system. For a better understanding of karst processes in Missouri, geophysical technique is deemed the right technique to use in mapping karst features since most critical processes in karst occur underground.

The objective of the study is to use automated electrical resistivity tomography (ERT) technique supported with multichannel analysis of surface waves (MASW) technique and boring control to image karst-related features like solution widened joints and clay/sediment-filled voids in parts of Missouri (Figure 1.1). Most karst features occur in Southern Missouri.

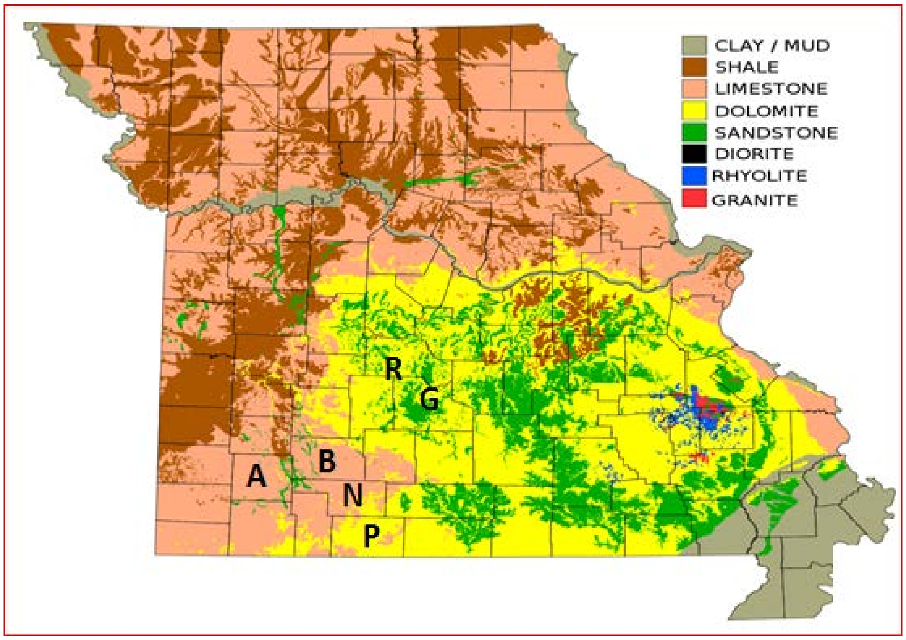

Figure 1.1. Study sites locations showing the distribution of bedrock in the study areas, A- Aurora study site, B- Battlefield study site, G- Gasconade River bridge study site, N- Nixa study site, P- Protem study site, and R-Richland study site. This map shows that karst related features are formed in dolomite and limestone bedrocks in Missouri. The presence of clay/mud and shale with low permeabilities impede downward movement of surface water and slows the development of solution cavities in the underlying carbonate rock, hence fewer sinkholes and caves are found in Northern Missouri compared to Southern and Central Missouri.

The pattern, density and placement of these features would be determined and used to define karst processes better in Missouri. The author would also classify Missouri karst using the “general criteria for engineering classification of karsts” as published in literature. To achieve these stated objectives, six sites were visited in the course of the study and the case studies are presented here. The case studies reflect to a large extent some of the problems inherent in karst terrain, and are a threat to life, property and the environment. The case studies cited are; the Nixa case study in Greene County, the Gasconade river bridge case study in Lebanon area, in Laclede County, the Aurora case study in Lawrence County, the Protem case study in Taney County, the Battlefield case study in Greene County and the Richland case study in Pulaski County.

The study has socio-economic implications such as minimizing loss of life and properties through gradual subsidence and sinkhole collapse because people would be enlightened more on karst processes and features.

About 40% of sinkhole collapses recorded in Missouri are caused by man-made features including roads, parking lots, ponds, hedges and drainage ditches. These man-made features retain water which percolates into the subsurface through pre-existing fractures which result to sinkhole or subsidence.

The study would also help in decision making while siting boreholes for drinking water to minimize groundwater contamination and pollution through sinkholes, since sinkholes have direct access to groundwater.

The study would create awareness to residents on the need to have the type of insurance that would cover their properties in the event of sinkhole disaster. Even insurance policy makers and administrators would benefit from the study during policy formulation for residents, and in drawing geohazard maps of the area.

It would serve as a good source of information in geotechnical and civil engineering works related to sinkhole mitigation and remediation.

2. OVERVIEW OF KARST PROCESSES AND FEATURES

The term “Karst” was used first to describe the region of Carso in northeastern Italy and western Slovenia, where the landform was first noticed and studied in the 19th century. Karst can be defined as a landform that is formed primarily as a result of dissolution of rocks such as limestone, dolomite, marble, gypsum and salt. The concept of karst was expanded further which led to the introduction of the term "pseudokarst" to designate karst-like terrain produced by processes other than the dissolution of rocks (Burger and Dubertret, 1975). Features inherent in karst landscapes are sinkholes, caves, springs, dry valleys and loosing/disappearing streams. Karst regions constitute about 25% of the land surface around the world. About twenty states in the United States are regarded as major karst areas, among them are Missouri, Florida, Texas, Alabama, Kentucky, Tennessee, and Pennsylvania; although there are numerous smaller karst regions nationwide. The World’s deepest cave as at December 2006 is the Mammoth cave in Kentucky USA with a length of 590 km and depth of 116 Km according to the National Speleological Society of America.

Karsts occur primarily on carbonate rocks, and ground cavities develop best on competent, fractured rocks whose intact unconfined compressive strength is around 30-100 MPa. In general, weaker limestones, dolomites, chalk and unlithified carbonate sediments lack the strength to span large cavities, thus they develop suites of karst features that are generally smaller than those on stronger limestones and dolomites (Higginbottom, 1966; Jennings, 1968; White, 2000). Regional climate strongly influences karstic landforms in that it controls the recharge to water flow regimes, and dissolution of calcium carbonate in water is largely dependent on the availability of biogenic carbon dioxide. Biogenic carbon dioxide is highly concentrated in deep soils and in tropical areas where decomposition of organic matter is rapid.

As a result, the most mature karst occurs in wet tropical environments. Dissolution of limestone is reduced in temperate regions, and less in arid glacial areas.

2.1. STRUCTURAL LINEAMENTS/ FAULTING IN MISSOURI

Because Missouri karst is more structurally controlled (solution-widened joints), there is need to understand faulting in Missouri. The New Madrid fault system is the most prominent fault system in Missouri; it has one of the highest rates of seismic energy release in an intraplate setting, and has been regarded as a zone of significant earthquake hazard. The fault system crosses state lines of Missouri, Mississippi, Arkansas, Tennessee, Kentucky and Illinois.

A powerful earthquake of up to 8.0 moment magnitude occurred within a three month period in this zone between December 1811 and February 1812. The New Madrid Fault is hidden beneath 100-200-foot thick layers of alluvium, unlike the San Andreas Fault in California areas where rocks are at or near the ground surface, and are much easier to study because the faults are readily found, seen, measured and analyzed.

There are three general fault trends in Missouri, the general northeast-southwest trend of the New Madrid, the southeast-northwest trend of the Reelfoot fault and the third trend that extends northeast from the northwestern end of the Reelfoot fault; the New Madrid North. These faults have been inactive for millions of years, but they have produced a pattern of northwest-trending (Figure 2.1) solution-widened joints and fractures as a result of weathering of bedrock along them.

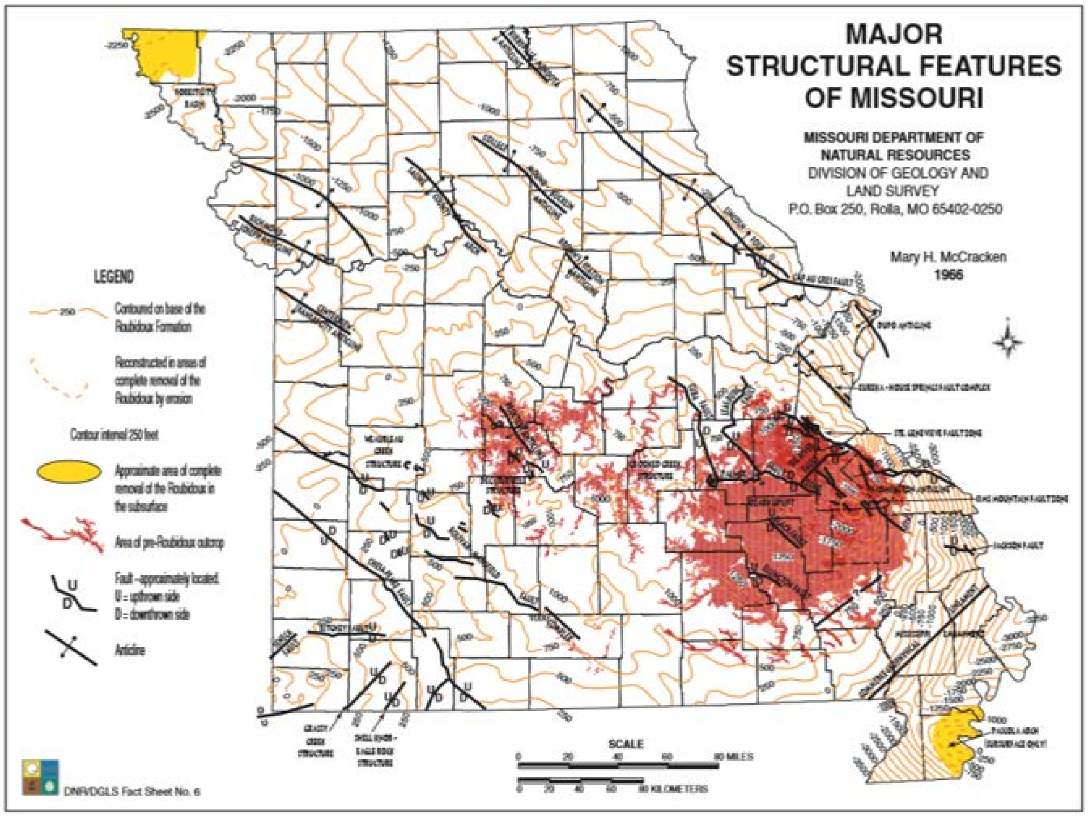

Figure 2.1. Structural lineaments in Missouri (Mary H. McCracken, Missouri Department of Natural Resources, 1966). Faults in Missouri trend mostly in NW-SE direction, and a few in NE-SW directions, and a few in NE-SW directions

2.2. HOW KARST IS FORMED

Karst is formed when rain falls and carbon dioxide in the atmosphere is dissolved making the rainwater to be acidic and consequently dissolving soluble rocks. It is worthy to note that the acidic rainwater passes through dead plant materials/debris in the soil and even becomes more acidic as it percolates through cracks, and consequently dissolving the bedrock (limestone, dolostone, marble, gypsum and salt). Dissolution continues as the water moves sideways along bedding planes and joints/fractures in the rock, forming conduits in the rock. The primary reaction sequence in limestone dissolution is as follows;

$$H_2O + CO_2 \rightarrow H_2CO_3$$

$$CaCO_3 \rightarrow Ca^{2+} + CO_3^{2-}$$

$$CO_3^{2-} + H_2CO_3 \rightarrow 2\ HCO_3^{-}$$

$$CaCO_3 + H_2CO_3 \rightarrow Ca^{2+} + 2\ HCO_3^{-}$$

These conduits enlarge over time (Figure 2.2) as water moves via a combination of hydraulic pressure and gravity. As time goes on, the conduits enlarge further through a combination of solution and abrasion of water on the surrounding rock. Through this process, a solution sinkhole is formed.

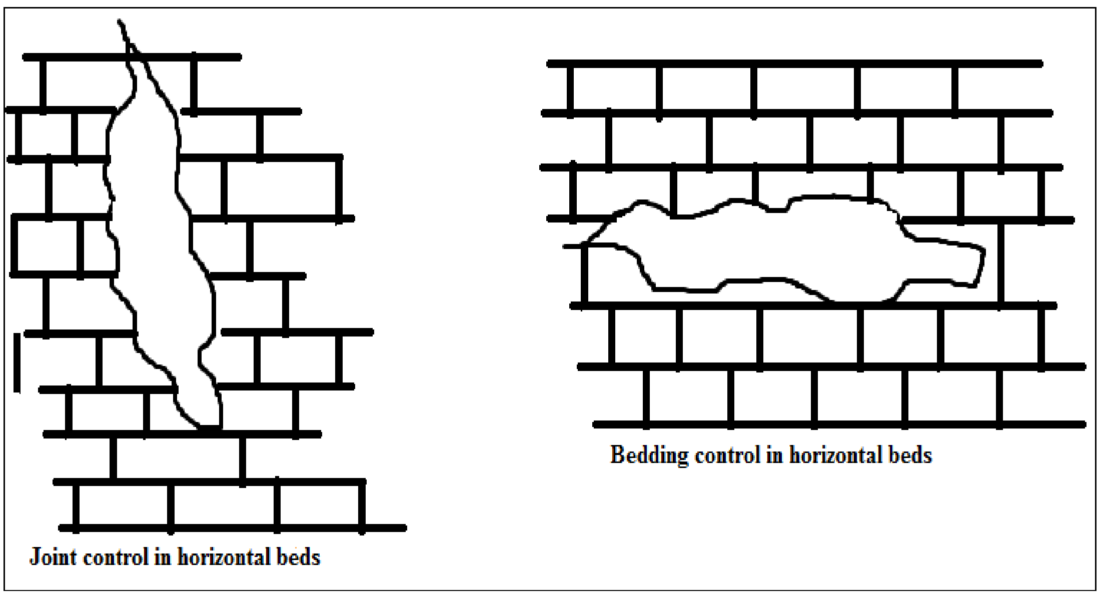

Figure 2.2. Structural control of carbonate dissolution as shown by the passages. Water preferentially dissolves bedrock along planar features such as bedding, joints, or fractures, whichever is the easier path.

In Missouri though, dissolution is generally through joints, and the joints are often in-filled with piped fine-grained sediments such as clays and silts (Figure 2.3), a process known as “piping”.

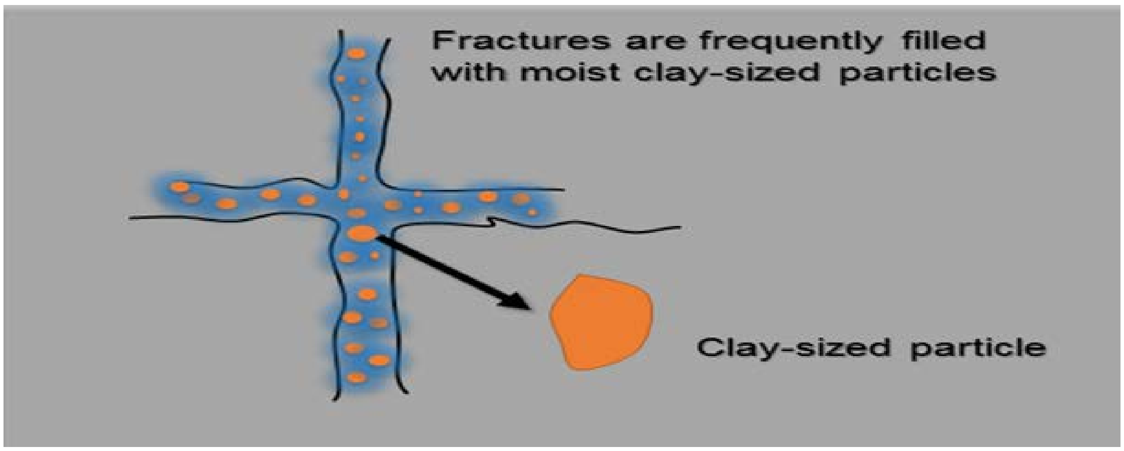

Figure 2.3. A schematic Illustration of sediment piping during sinkhole formation in Missouri.

Piping is a process whereby fine grained soils (fine sand, silt and coarse clay) are eroded and transported downward by infiltrating surface water through solution-widened joints.

Further dissolution of rock continues as a result of water movement, thereby enlarging the conduits which results to increased water pressure. When much of the water under pressure gets to the land surface, spring eventually forms. Spring emergence could be high on a cliff or forced upward from below the level of surrounding surface streams depending on factors such as the base level of the controlling stream in the drainage area and the nature of the surrounding rock. In most karst areas, groundwater movement is so much that springs have a little relationship to surface drainage.

Most flow and enlargement take place at or just below the water table where bedrock dissolution and water circulation are greatest. If groundwater levels in the area drop, more underground passages become air-filled. When these passages are sufficiently filled with air, springs become cave entrances passable by humans. As chemical equilibrium underground changes, the resulting caves begin to fill with dissolved minerals called speleothems or cave deposits (stalactite and stalagmite). Caves can be water-filled, dry, or even cycle several times in response to changes in water levels.

As erosion continues underground, caves get hollow enough and the roofs thin and eventually collapse to form a sink. In a karst terrain, karst features like sinkholes, springs, caves and disappearing streams are dependent on one another (Figure 2.4), and therefore either serve as recharge or discharge areas depending on certain geological and hydrogeological factors.

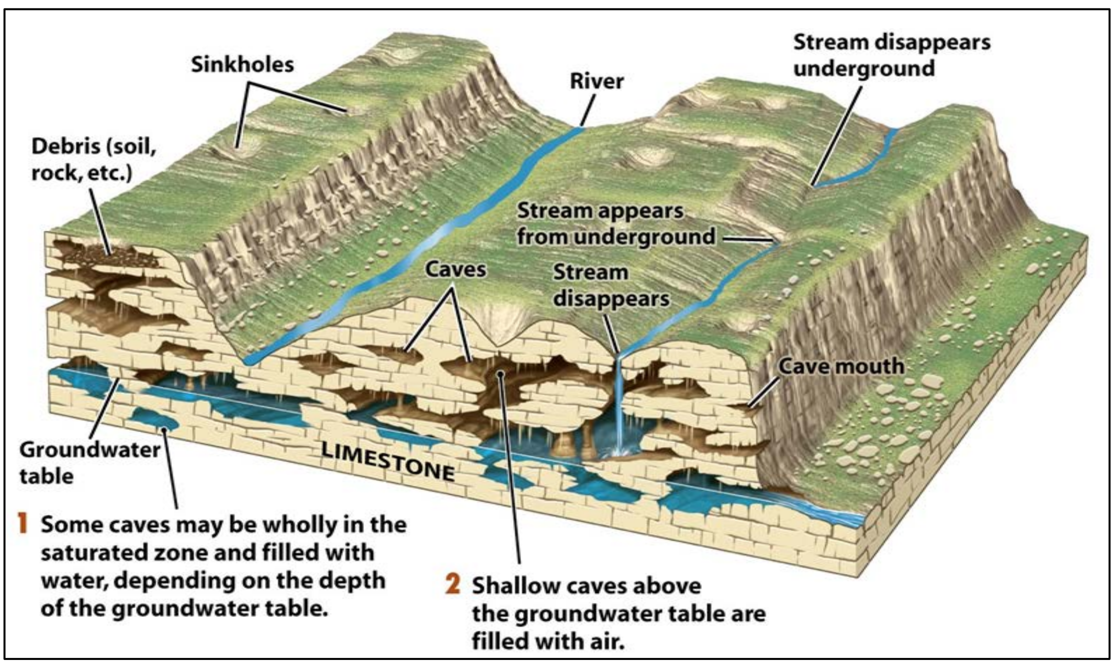

Figure 2.4. Typical example of karst topography showing the karst features in play in a karst terrain (https://cetologydotorg.files.wordpress.com/2015/01/karst_topography.jpg).

The resistant remnants of cave collapse can form natural bridges and tunnels, and may be filled with clay. In some karst areas reversible sinks are formed, especially where the water table is shallow. In such a scenario, declines in the water table change springs into recharge areas, and rises in the water table convert sinkholes into springs. These reversible sinks are called estavelles. In a type of karst where the contact between bedrock and soil overburden is very irregular, it is referred to as cutter and pinnacle karst. Cutters or grikes are roughly vertical solution-widened joints, and are generally filled with soil. The bedrock that remains between cutters may be reduced to relatively narrow ridges of rock called pinnacles especially where cutters are closely spaced. Pinnacle karsts pose a great problem to building foundations due to differential settling of the building. Differential settling often produces cracks in the walls, foundations and floors of buildings, thereby compromising the structural integrity of the structures.

Karst landforms are different because the erosional forms which karst takes is dependent on so many factors such as the mechanical structure and chemical composition of the rock, the local climate, temperature range, amount of vegetation and rainfall in the region. Karst along a seaside is different from that inland, and tropical karst differs from those in sub-arctic or temperate zones. Pseudokarst or false karst areas also occur, especially in the western United States. A typical example is the state of Idaho. These regions contain karst-like features which have developed in poorly soluble rocks. Although pseudokarst areas are formed by different processes, they are often similar to karst areas in terms of how they are used and affected by human activities. The type of karsts that are buried under the rocks and sediments, and are not exposed at the surface are called ancient or paleokarsts, they may also have an effect on surface land use. Some karsts are unusually formed as a result of sulfuric acid welling up from below instead of carbonic acid percolating down from above, as found in New Mexico, US.

2.3. ENGINEERING CLASSIFICATION OF KARSTS

According to Ford and Williams (1989), different landforms relate to each other but the local geological, hydrological and climatic conditions create suites of karstic features with almost infinite variety. Because karst landforms are influenced by specific features that affect ground conditions such as caves, sinkholes and the rockhead morphology, an engineering classification of karstic ground conditions is very useful in providing guidelines to the potential variations in landforms encountered in engineering and geotechnical works on karst. In the classification, five classes of karsts are recognized (Figure 2.5), they are; the Juvenile karst kI, the Youthful karst kII, the Mature karst kIII, the Complex karst kIV and the Extreme karst kV.

Study has shown that the processes and landforms of karsts formation are the same. For example, gypsum karst are broadly comparable to those on limestone, except that gypsum is dissolved more rapidly in natural waters and is mechanically weaker than most limestones. The engineering classification of karst is applicable to gypsum terrains, though extreme karst of class kV does not develop in the terrain. Generally, caves formed in gypsum collapse before they reach very large dimensions, and it is easily eroded before it can mature into the extreme karst landforms. So, the class of karst found in a particular terrain also depends on the type of rock that is dissolved during the formation process of the landform.

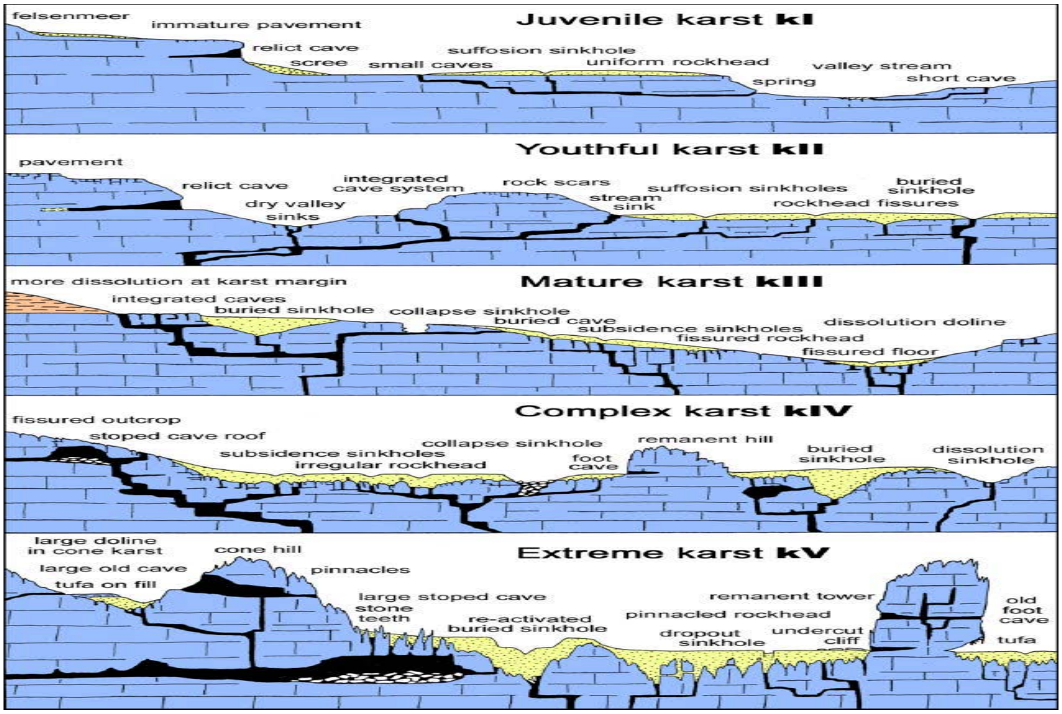

Figure 2.5. Diagrammatic representation of the five classes in engineering classification of karsts (Waltham and Fookes, 2003). This shows horizontal bedding of the limestone, dipping bedding planes and inclined fractures. The dotted ornament represents any type of clastic soil or surface sediment.

kI (Juvenile karst): This type of karst occurs only in deserts and periglacial zones, or on carbonates that mixed with other rock types. Sinkholes and caves are rarely found in this area, and where they are found, they are usually small in size. Some isolated relict features are also found in the area.

kII (Youthful karst): Many small caves are found in this area (mostly less than 9ft. wide), and fissuring is widespread. Small subsidence sinkholes are also common in the area.

kIII (Mature karst): This type of karst is common in temperate regions but sometimes is rarely found in wet tropics. Most fissures here have extensive secondary openings with many caves. All kinds of sinkholes (subsidence, collapse and dissolution sinkholes) are found in numbers in the area.

kIV (Complex karst): This type of karst is localized in temperate regions, but is also found in tropical regions. Wide caves (mostly more than 15ft. wide) are common in the area. There are also pinnacled rockhead and loose blocks in the area. Large dissolution sinkholes, and many subsidence and buried sinkholes are common in the area, and there are a lot scattered collapse features.

kV (Extreme karst): This type of karst is found only in wet tropics with very large sinkholes of different types. There are tall pinnacled rockheads and abundant dissolution cavities in this area coupled with many complex caves.

Based on the author’s judgment, Missouri karst is wide and varied, and has different classes of karst such as; kI (juvenile), kIII (mature) and kIV (complex) karsts. For example, the karst in Northeast Missouri, along the Lincoln Fold can be classified as juvenile. The Salem plateau region that comprises the Ozarks can be classified as complex and mature karst. Karst in Southeast Missouri, along Mississippi river can be classified as complex karst.

2.4. PROBLEMS WITH KARSTS

Karst areas are very complex and problematic, and pose a great threat to human life and the environment. The landscape is most vulnerable to environmental pollution and structural failures (Figure 2.6). Groundwater in the terrain is the most easily polluted since sinkholes have direct access to groundwater.

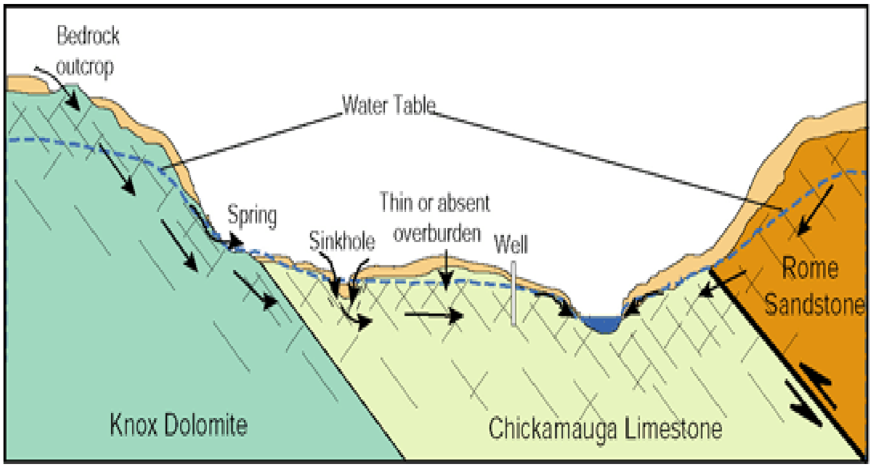

Figure 2.6. Aquifer/groundwater contamination due to direct access to sinkhole (http://pubs.usgs.gov/circ/circ1205/major_findings.htm).

When sinkholes flood as a result of rainfall, it results to urban pollution of groundwater by sewage, runoff containing petrochemicals, pollutants derived from paved areas, domestic and industrial chemicals, and trash. Also, surface events (storms and stream flooding) can trigger changes in water level in wells and springs, and sinkholes located miles away from rivers can flood homes and offices in response to these events. These can lead to sinkhole collapse or development of new one.

The terrain also poses a great challenge to civil and geotechnical engineering practice, and therefore needs special considerations to ensure stable foundation design. For example, in pinnacle karst, part of the foundation may be supported by a bedrock pinnacle and part may be supported by a cutter. This can result to differential settling of the building, which may produce cracks in the walls, foundation, and floor, thereby compromising the structural integrity of the bearing walls and place the safety of the whole structure in danger. Building collapses, road subsidence and dam failures are some of the structural problems encountered in karst terrain, and have caused enormous economic losses around the world (Figure 2.7).

Figure 2.7. Bridge and building collapses caused by sinkhole collapse (http://www.amusingplanet.com/2013/09/disastrous-sinkholes)

2.5. ECONOMIC IMPORTANCE OF KARST

Despite the complex, vulnerable and variable nature of karst areas, their economic importance cannot be over-emphasized. They are among the world's most diverse, resource-rich and fascinating areas. Karst areas contain the largest springs and the most productive groundwater supplies on earth. Resources like minerals, oil, limestone quarries and natural gas are abundant in karst areas. Many oil and gas fields throughout the world tap highly porous and permeable paleokarst reservoirs where tremendous volumes of petroleum are naturally stored.

Caves are a good habitat to rare animals, and many species of bats, including those that form some of the world's largest colonies, roost in caves. Fragile prehistoric materials are preserved in caves and many of the world's greatest archaeological sites have also been found in caves.

Karst areas provide a good recreation for people and enhance economic development of the host states and communities through tourism and caving. There are commercial caves, wild caves and scenic caves which serve different purposes to different people. The Mammoth cave in Kentucky, the world's longest cave with over 355 miles (572 km) mapped is one of the US national parks with huge revenue returns. Some caves are privately owned, such as the Caverns of Sonora in Texas which is internationally recognized as one of the most beautiful show caves in the world. Some artificial caves have been built for tourism purpose while some natural caves have been modified and beautified to further attract people and increase revenue earnings through tourism. Missouri is home to more than 6,000 caves, making the state the second largest state in terms of caves, second to only Tennessee.

Some of the parks found in Missouri for interested cavers are the Meramec state park, Lake of the Ozarks state park and the Onondaga state park. Because of this, there are many scientific organizations in Missouri that help in tourism and development of caves. Some of the organizations are;

- Missouri Speleological Survey
- National Speleological Society
- Cave Research Foundation
- Missouri Caves and Karst Conservancy

3. KARST PROCESSES AND FEATURES IN MISSOURI

The general representation of U.S. karst areas published by American geological institute (AGI) (Veni et. al., 2001) (Figure 3.1) indicates that Missouri is mostly underlain by carbonate rocks and is recognized as a karst terrain.

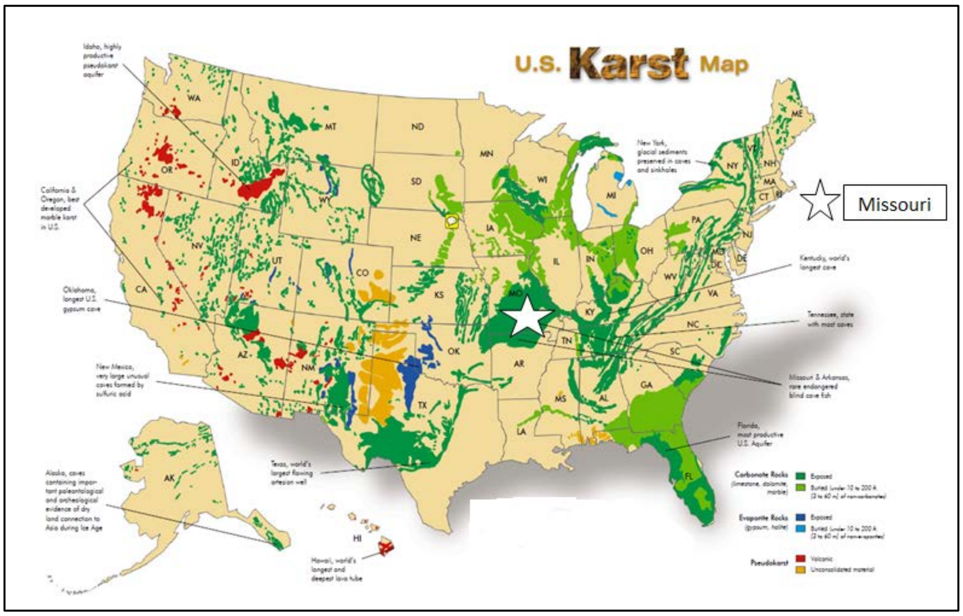

Figure 3.1. Karst Map of the US published by AGI (Veni et al., 2001). The map shows that Missouri karst is mainly formed on exposed carbonate rocks as indicated by the dark green color. Light green color represents buried carbonates rocks (10-200ft.). Other rocks shown in the map are evaporite rocks (gypsum and halite) shown as blue color; dark blue is exposed and light blue is buried. Red and yellow colors represent pseudokarst; red is volcanic and yellow is unconsolidated material.

Most of the states of Missouri is underlain by rocks that contain carbonate units, for example, in the Southeast Missouri, these rocks lie under thick sediments in the Mississippi embayment region. In northern Missouri, west of the Lincoln Hills, the area is mantled by glacial sediments (Figure 3.2), and karst occurences in the region are small and isolated which is also the case in western Missouri.

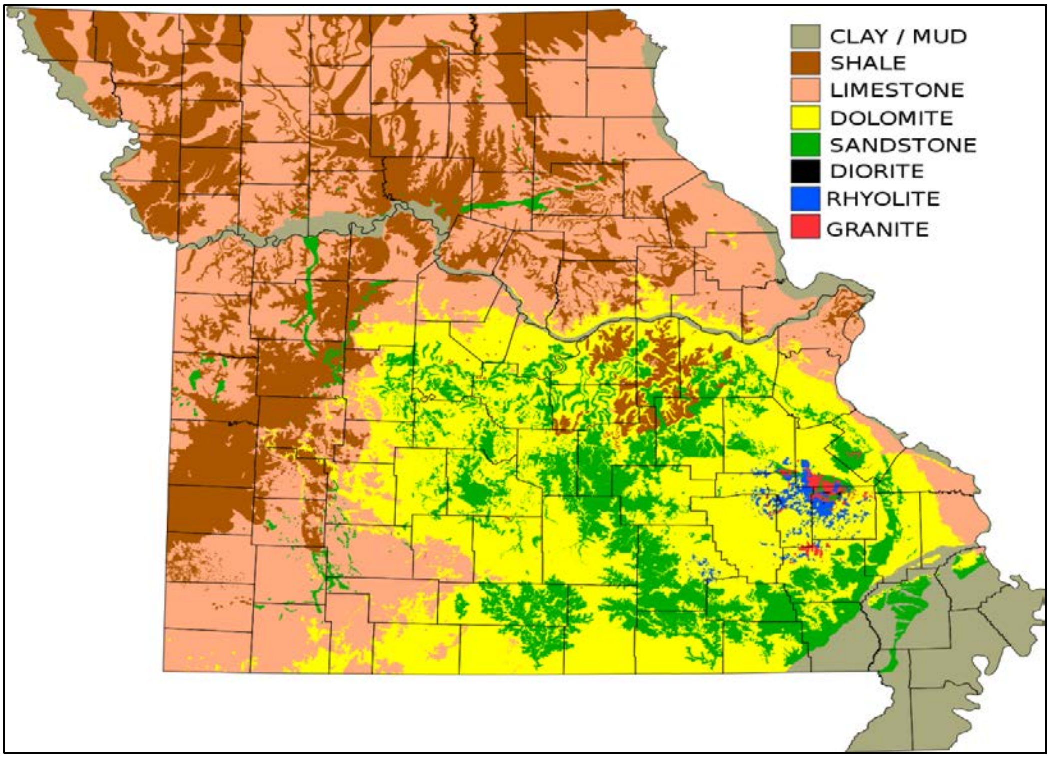

Figure 3.2. Geologic map of Missouri showing distribution of different rock units (http://upload.wikimedia.org/wikipedia/commons/a/a1/Missouri_Geology_Primary_Rock_Types_v1.png). About 59% of the state is underlain by thick carbonate rock units that host a wide variety of karst features

In Missouri, the areas covered by shale as shown in Northern Missouri do not show significant karst development because shale has low permeability and does not allow much surface water to drip into the subsurface to dissolve the carbonate rocks. This is not to say that karst will not develop in these areas, but the rate of development will be very slow. There is significant karst development in Southeastern and Southwestern Missouri where carbonate rocks are more exposed, and when covered, are covered by permeable rocks.

3.1. CAVE FORMATION PROCESS

Cave simply means an underground opening or void formed as a result of dissolution of soluble rocks like limestone, dolostone, marble, gypsum and salt, and is large enough for human entry. Dissolution starts when water falling through the atmosphere dissolves carbon dioxide in the process to form carbonic acid. The carbonic acid formed becomes more acidic when it passes through soil and rock thereby dissolving minerals that form the rock, for example calcite and aragonite minerals. As this acidic groundwater moves through fractures and other spaces within the rock, large passages and openings are created. Where these openings are large enough for human entry, they are called caves. Cave formation could take place below or above the water table. Most caves form at or just below the water table, and form passages that are generally horizontal and looks elliptical when viewed in cross section. Vertical cave passages are formed above the water table, usually along fractures. In cross section, they look narrow and tall.

An important aspect of cave is the formation of cave minerals collectively called speleothems, for example stalactite and stalagmite. A stalactite is formed as a result of precipitation of minerals from water dripping through the cave ceiling. It usually hangs on the ceiling of a cave with pointed tips. When the water dripping from the end of stalactites falls to the floor of a cave, more calcites are deposited into a mound to form a cone-like feature called stalagmite. Most stalagmites have flattened or rounded tips. Stalactites and stalagmites are usually found in pairs, and sometimes they grow together to form a pillar or column.

3.2. CAVES IN MISSOURI

Missouri is known as “The Cave State”. Caves are the most familiar karst feature to most people and forms in a manner similar to sinkholes. In the state, Caves are found almost everywhere (Figure 3.3); with the exception of the areas north of the Missouri River where Pennsylvanian rocks are covered by glacial drift.

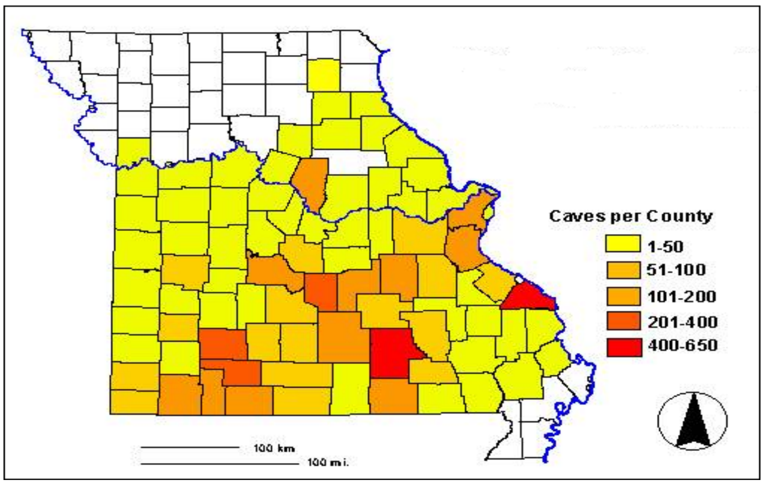

Figure 3.3. Missouri cave density (William Elliot, 1998, based on 5,668 caves recorded in July 1998).

There are more than 6,400 known caves located within Missouri. Some caves in Missouri are active groundwater conduits and have sizeable cave streams that transport significant volumes of water but most are relatively dry and do not transport significant quantities of water unless briefly after intense precipitation. The highest concentration of caves is in Perry County; with 656 known caves as of 2009. The longest caves are also registered in Perry County: Crevice Cave is the longest cave in Missouri (28.2 miles), and the eighth longest in the United States. Most caves are deep below the surface (200-300feet), others are located at shallower depths, with thinner "roofs" and are more subject to collapse.

3.3. SINKHOLE FORMATION PROCESS

Sinkholes, also called dolines form in the same manner caves are formed (dissolution of soluble rocks by surface water and groundwater to create a void or an opening in the soil or rock). Sinkholes are the most diagnostic surface expression of karst landscapes. They are important near-surface indicators of active karst features at depths such as dissolution-enlarged fractures, caves and conduits. Sinkholes can vary from a few feet to hundreds of acres and from less than 1 to more than 100 feet deep. Some are rounded in shape whereas others have vertical walls. Although most sinkholes drain rapidly, some have natural plugs and may hold water for many years. There are three types of sinkholes, Solution-sinkholes, Cover-collapse sinkholes and Cover-subsidence sinkholes.

3.3.1. Solution Sinkholes. Solution-sinkholes occur in areas where carbonate rocks like limestones and dolostones are exposed at land surface (Figure 3.4) or are covered by thin layers of soil and permeable sand.

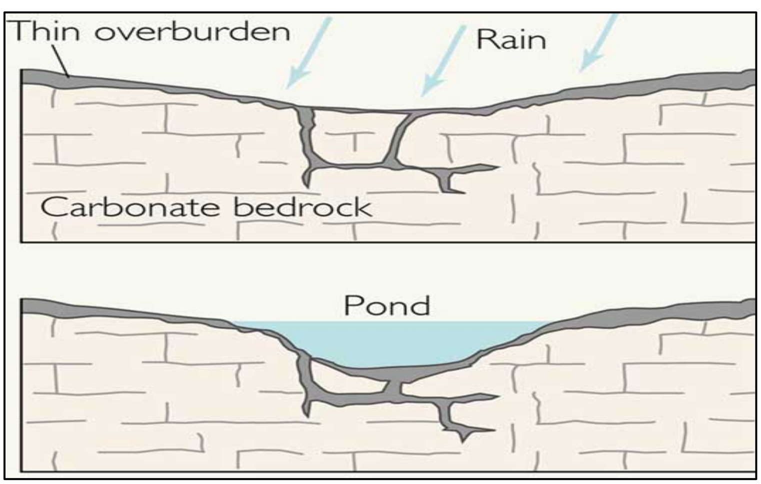

Figure 3.4. Formation of solution-sinkhole (http://www.sinkholes.com/causes/sinkhole-types/)

Dissolution is most active at the limestone surface and along joints, fractures or other openings in the rock that permit water to move easily into the subsurface. When rain falls, surface water percolates through joints in the carbonate rock and the dissolved rock is carried away from the surface and a small depression is formed.

Further drainage of the carbonate surface accelerates dissolution process and enlarges the depression. As more debris are carried into the developing sinkhole, water outflow may be plugged to form pond and may hold water for years. Solution sinkholes tend to have gently sloping sides, and seldom pose a hazard by collapsing.

3.3.2. Cover-Collapse Sinkholes. Cover-collapse sinkholes (Figure 3.5) occur where the covering sediments contain a significant amount of clay or cohesive materials.

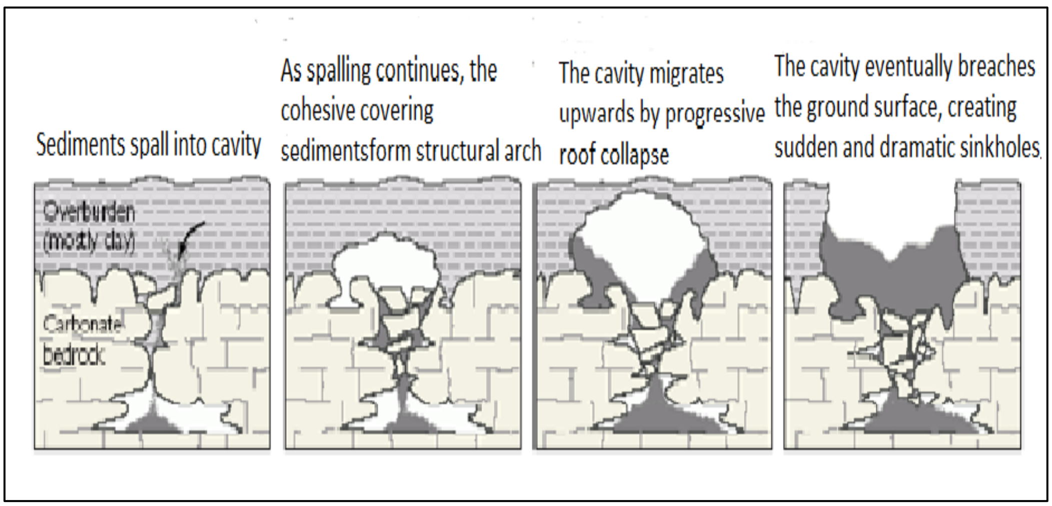

Figure 3.5. Formation of cover-collapse sinkhole (https://water.usgs.gov/edu/ Sinkhole.html Cover-collapse sinkhole)

After the formation of solution cavity by infiltrating surface water, sediments spall into the cavity. As spalling continues, the cohesive cover material forms a structural arch. As the cavity enlarges and progresses upward, it gets to a stage where the cover material can no longer support its own weight and a sudden collapse occurs to form this type of sinkhole.

Heavy rainfall, drought or mechanical loading can trigger this type of sinkhole. The collapse is generally abrupt, and in some cases catastrophic. The sinkhole formed in this manner is often fairly circular with steeply sloping sides.

3.3.3. Cover-Subsidence Sinkholes. Cover-subsidence sinkholes occur where Limestone lies beneath a cover of soil and other unconsolidated material, such as sand and clay. When the limestone dissolves, grains of sand move downward in sequence (Figure 3.6) to occupy the space created by the dissolved limestone, a process termed piping.

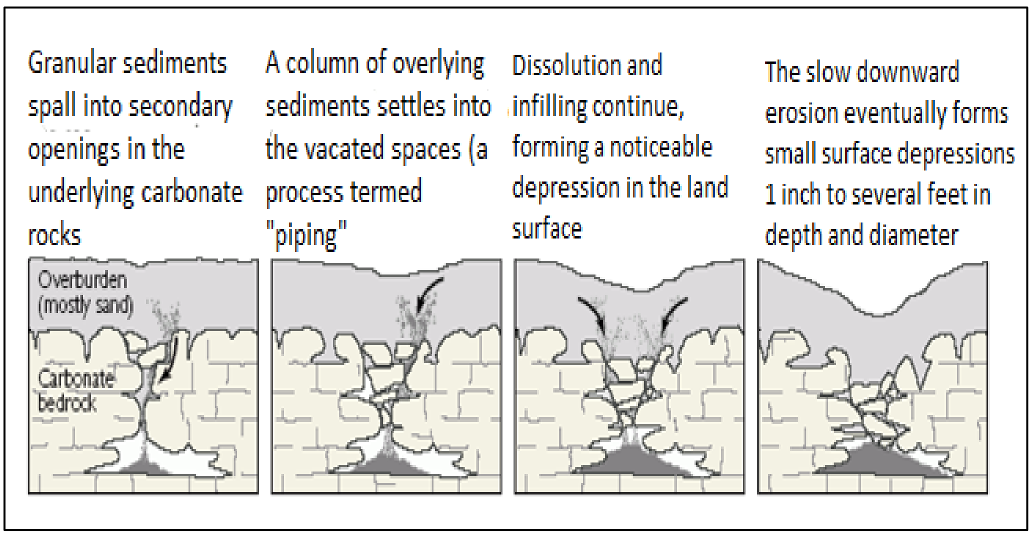

Figure 3.6. Formation of cover-subsidence sinkhole (https://water.usgs.gov/edu/sinkholes.html Cover-subsidence sinkhole)

Dissolution and infilling of the transported sediments cause a depression in the land surface. The collapse is more gradual and circular than the cover collapse. The variable thickness and composition of this cover is important in sinkhole development. In areas where limestones are buried beneath a sufficient thickness of unconsolidated material, few sinkholes generally occur. If the overburden is dense plastic clay, its low permeability may impede downward movement of surface water and slows the development of solution cavities in the underlying limestone. In Missouri, this type of sinkhole is common than the other types based on the mechanism of its formation and nature of overburden materials.

3.3.4. Causes of Man-Made Sinkholes. Sinkholes can form naturally or as a result of human activities that impact on land and groundwater. Man-made sinkholes can occur due to the following reasons:

- Drilling and vibration during mining activity
- Alteration of natural water drainage condition during roads and building construction
- Dewatering and over-pumping of groundwater which destabilizes the equilibrium between the buried cavity and the overburden sediment that is delicately balanced by groundwater fluid pressure
- Surface event like Storm water
- Vehicular traffic which can substantially increase the weight of the overlying material beyond what the underlying supporting material can bear

3.3.5. Sinkhole Indicators. Although in most cases, sinkhole collapse occurs with little or no advanced warning and unknown triggering mechanisms or causes, some of the following signs sometimes serve as a warning or precursor to sinkhole formation especially in karst areas;

- Formation of Small conical holes that appear in the ground over a relatively short period of time
- General slumping, sagging, or tilting of trees, roads, rails, fences, pipes, poles, signboards, and other vertical or horizontal structures in an area
- Structural failure signs such as fractures in foundations and walls, often accompanied by jammed doors and windows
- Ponding of water as a result of subsidence in soil or pavement
- Circular and linear cracks in soil, asphalt, and concrete paving and floors
- Lowering of water table as a result of vegetative stress (wilting of small area of vegetation)

It is worthy to note that these signs are not exclusive to sinkholes alone, they can happen for some other reasons, and also in non-karst areas. However, they are good indicators of sinkholes and needs to be paid a good attention.

3.4. SINKHOLES IN MISSOURI

According to US Geological Survey, about 15,981 sinkholes have been surveyed in Missouri, and many more exist that have not been reported or documented (Figure 3.7). The largest known sinkhole in the state is in western Boone County southeast of where interstate 70 crosses the Missouri River, and covers about 700 acres (approximately 30.5 million square feet). There are no records about the depth but some are known to be greater than 100feet deep. At times sinkholes that form in remote areas are not reported by members of the public; this has been one of the setbacks in sinkhole inventory. In Missouri, the areas covered by shale such as Northern Missouri do not show significant karst development because shale has low permeability and does not allow much surface water to drip into the subsurface to dissolve the carbonate rocks to create cavities.

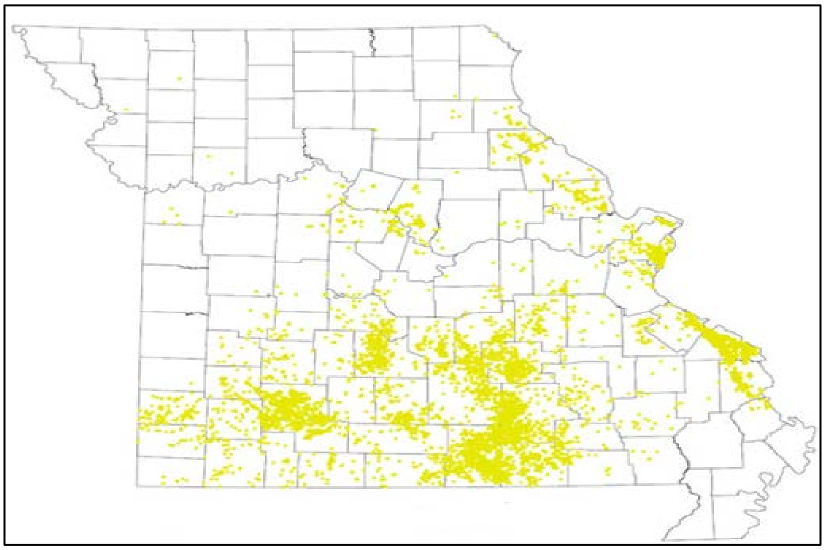

Figure 3.7. Sinkholes in Missouri (http://dnr.mo.gov/geology/geosrv/envgeo/ sinkholes.htm). This shows that sinkholes are more concentrated in the southern and central parts of Missouri than in the northern parts.

Most sinkholes in Missouri are formed through “piping” process. Piping is a process whereby fine grained soils (fine sand, silt and coarse clay) are eroded and transported downward by infiltrating surface water through solution-widened joints. The process is illustrated using the following steps;

1. When rain falls, rainwater seeps more-or-less uniformly into the subsurface through the porous permeable soil and the fractures in the underlying limestone (Figure 3.8). Sinkholes are sparsely located in northern parts of Missouri due to the nature of surficial materials in the area.

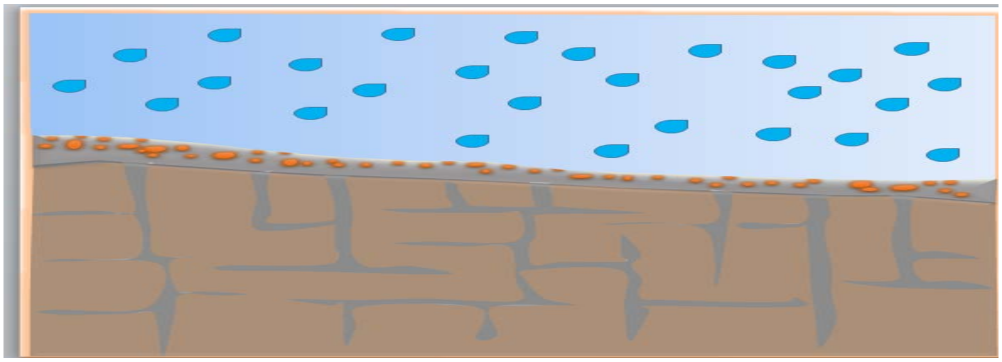

Figure 3.8. . Rainwater seeping uniformly into the subsurface

2. Each droplet of downward percolating rainwater is slightly acidic and dissolves a small amount of limestone. Over time (literally thousands of years), the fractures within the limestone are widened. Each droplet of downward percolating rainwater also contains clay-sized particles (mostly) that were removed from the soil. These clay-sized particles are filtered out of the rainwater as it passes through the fractured limestone. This process is referred to as “piping” (Figure 3.9). As a consequence, the fractures within the limestone are typically in-filled with moist clay.

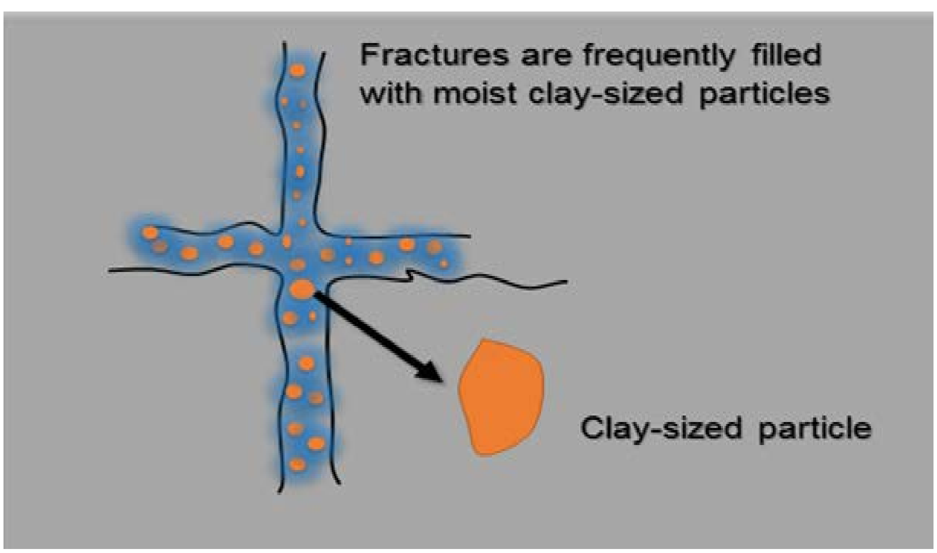

Figure 3.9. Schematic illustration of sediment piping during sinkhole formation

3. In areas where surface run-off is not constrained, rainwater seeps more-or-less uniformly into the soil and underlying rock (Figure 3.10). As a result of the piping process, some of the finer grained particles are removed from the soil. The piping process can cause the ground surface elevation to decrease-imperceptibly (to the human eye) and uniformly.

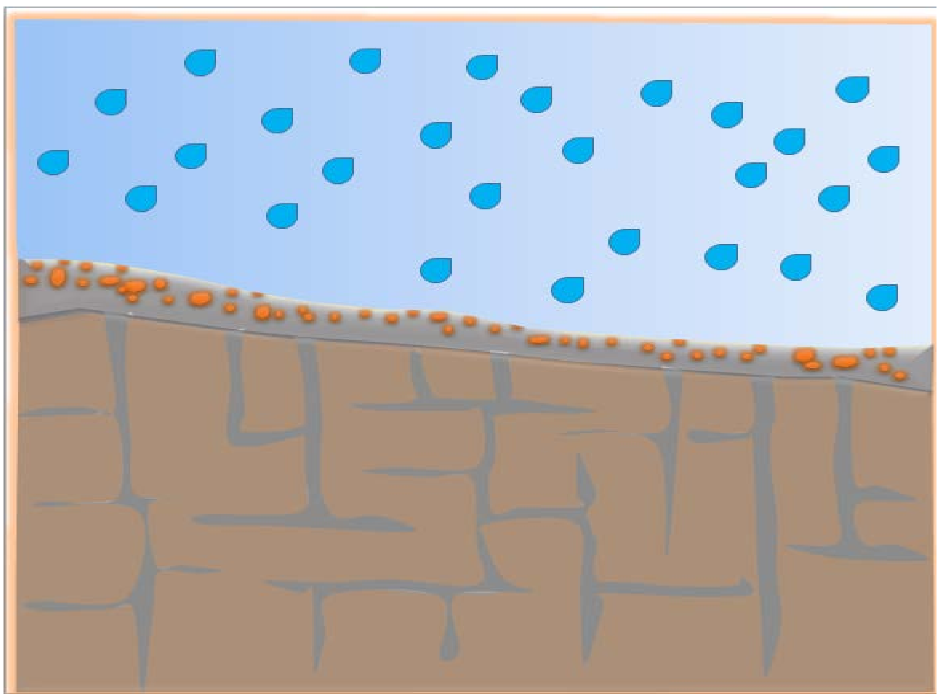

Figure 3.10. Schematic illustration of uniform seepage of rainwater when surface water is not constrained

4. In areas where surface run-off is constrained (by natural or anthropogenic causes), the volume and rate of water seepage can be increased significantly thereby increasing the rate of karst formation in the area (Figure 3.11).

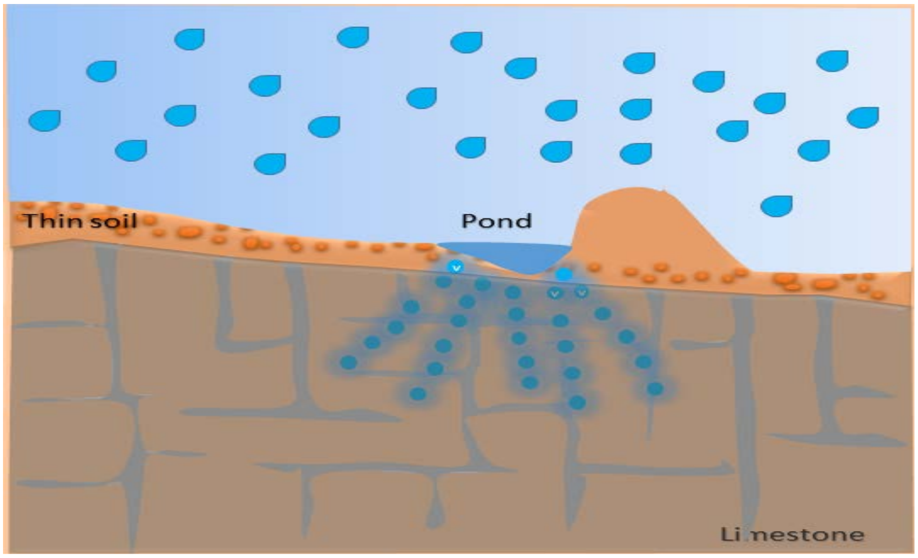

Figure 3.11. Schematic illustration of irregular seepage when surface run-off is constrained. This results in sinkhole formation with natural plugs to form a pond.

As a result of the piping process, the elevation of the ground surface below can drop rapidly and significantly forming sinkholes. Most sinkholes drain rapidly, some have natural plugs and may hold water for many years to form a pond or lake.

It is a fact that the same processes that cause sinkholes to develop-often cause them to increase in size over time. Two limiting factors are the thickness of the soil layer and the percentage of clay-sized particles in that soil. Important facts about sinkholes are that they do not develop randomly; rather they develop mostly where surface run-off is constrained by natural (e.g. fallen trees, slumps) or man-made features, and they will not form where water does not seep into the subsurface.

3.5. DISAPPEARING/LOOSING STREAM

One of the features of karst topography is a disappearing/losing stream, which is a surface stream that loses a significant amount of its flow to the subsurface through bedrock openings. The stream channels surface water into the groundwater system.

Typically, the water table along losing streams is below stream elevation. Water in the stream penetrates bedrock through solution-enlarged openings in and below the stream bed. Some losing streams have the capability of flowing much of the year but at some point lose a significant part of their flow into the bedrock through solution-enlarged channels while others can carry water only briefly after intense precipitation and then dries after a short while. Losing streams or influent streams are common in regions of karst topography where the stream water may be completely captured by an underground cavern system to become a subterranean river.

3.6. DISAPPEARING/LOOSING STREAMS IN MISSOURI

There are a lot of disappearing / loosing streams in Missouri (Figure 3.12). Some notable losing streams in Missouri are as follows; Asher streams, Dry fork creek, Gasconade river losing section, Goodwin creek, Howell creek, Logan creek, Norman creek, North Cobb creek and Spring creek.

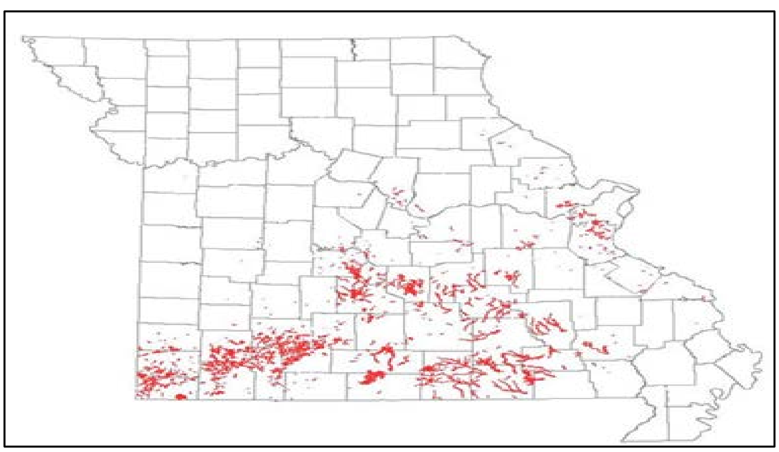

Figure 3.12. Loosing streams in Missouri (http://dnr.mo.gov/env/wrc/losing-streams.htm)

This map shows that there are more loosing streams in southern and central parts of Missouri than in the northern parts.

3.7. SPRINGS

Another interesting feature of karst topography is spring. Spring is formed as a result of natural discharge of water from a rock or soil to the surface. It acts as outflow point for groundwater recharge. Every spring has an area on the land surface through which it is recharged. Springs can be recharged by water from rainfall moving downward through soil and rock openings or water within the recharge area that seeps or flows underground through sinkholes and losing streams. In a karst terrain, the whole features are interconnected.

3.8. SPRINGS IN MISSOURI

Springs are abundant in Missouri, especially in the Ozarks region (Western Missouri). This region contains one of the highest concentrations of springs in the nation and in the world, and hundreds of them flow all year (perennial flow). The current largest spring in Missouri is the Big spring in Carter County with an average discharge of 288 million gallons per day (445ft^3/sec). It is a 1st magnitude spring (spring with average discharge greater than 100ft^3/sec of water). Spring being one of the features of karst terrain is abundant in southern parts of Missouri (Figure 3.13) compared to the northern part. This is as a result of the factors that control the formation of sinkholes and caves such as type of surficial materials, temperature, organic materials and rainwater. The temperature of spring water is fairly constant in a year and is close to the mean annual surface temperature (- 58 to 59 degrees Fahrenheit). The water qualities from the springs are dependent on the mineralogy of the rocks in the area, but are generally good. The water is “hard” if there is significant concentration of dissolved minerals resulting from recharge and discharge of both surface and groundwater

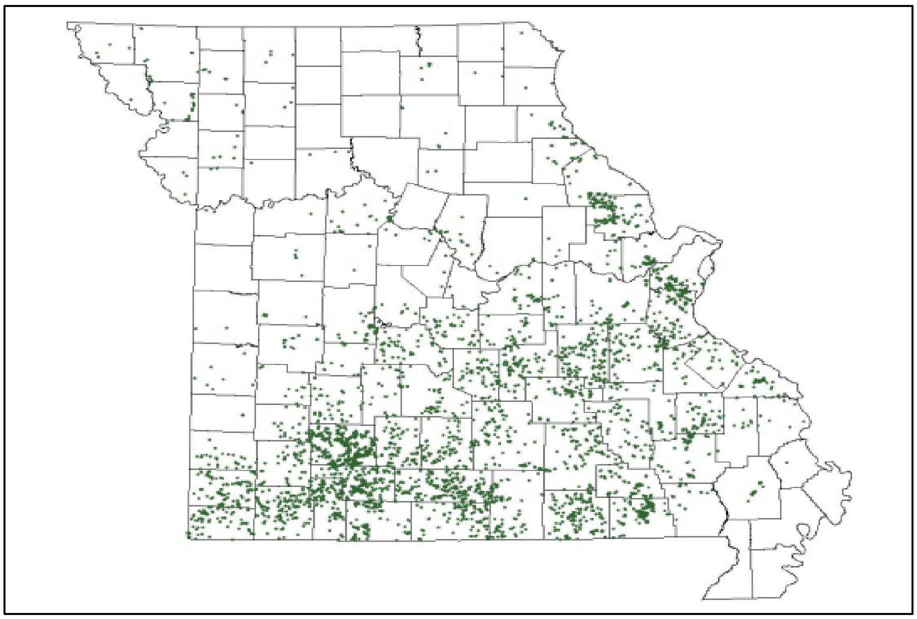

Figure 3.13. Springs in Missouri (http://dnr.mo.gov/env/wrc/springs.htm). This shows that there are more springs in southern and central parts of Missouri than in the northern parts

The spring flows correlate with seasonal rainfall. Large volumes of water flowing from these springs because of the underground channels which are complex networks, they serve as drainage systems for the rainfall on large areas of land surface.

Springs with average discharge between 6.64 million and 64.6 million gallons per day (10 and 100ft^3/sec.) are 2nd magnitude Springs. Other commonly known springs in Missouri are the Alley Spring, Bennett Spring, Blanchard Spring and the Blue Spring.

4. BASIC THEORY OF ELECTRICAL RESISTIVITY

Electrical current flow in the subsurface is primarily electrolytic. Electrolytic conduction involves passage of charged particles by means of groundwater. Charged particles move through liquids that infill the interconnected pores of permeable materials (Robinson, 1988). When an electrical resistivity tomography survey is conducted in karst terrain, current flow is generally assumed to be electrolytic rather than electronic.

4.1. OHM'S LAW AND RESISTIVITY

In 1872, George Simon Ohm derived empirical relationship between the resistance (R) of a resistor in a simple series circuit, the current passing through the resistor (I), and the corresponding change in potential (Δ V) :

$$\Delta V = I R \tag{4.1}$$

A simple series circuit that consists of a battery connected to a resistor by a wire demonstrates this relationship (Figure 4.1).

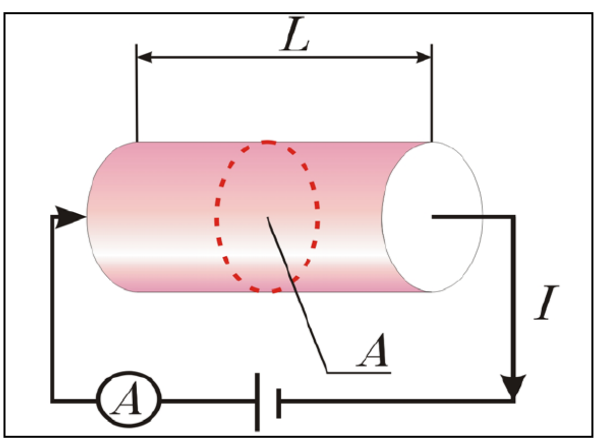

Figure 4.1. Electric circuit for illustration of Ohm's Law

By using Ohm's Law, the value of resistance (R) can easily be calculated by plugging values of voltage (Δ V) and current (I) in the equation (4.1). The last two values are given because they can be measured. The electrical resistivity tomography concept is based on this relationship (Equation 4.1), with the assumption that the resistor in the circuit is the Earth. There is another relationship that defines resistance (R) as a function of geometry of a resistor and the resistivity of the cylindrical-shaped body:

$$R = \rho L/A \quad (4.2)$$

This equation shows that the magnitude of resistance is affected by the length (L) and the cross-sectional area (A) of the cylindrical-shaped body through which electrical current flows (resistor). A factor that defines the ease with which electrical current flows through the media is known as resistivity (ρ). By rearranging equation (4.2), the resistivity can be expressed as:

$$\rho = R\,A/L \quad (4.3)$$

The electrical resistivity of any material is the resistance between the opposite faces of a unit cube of the material. Resistivity is an internal parameter of the material through which current is compelled to flow and describes how easily this material can transmit an electrical current. High values of resistivity imply that the material making up the wire is very resistant to the flow of electricity. Low values of resistivity show that the material making up the wire transmits electrical current very easily. So, while resistivity is an intrinsic property of a material, resistance depends on the shape and composition of the material.

4.2. THEORETICAL DETERMINATION OF RESISTIVITY

The estimation of the apparent resistivity of the earth is relatively simple if several assumptions are made. The first assumption is that a model-Earth is uniform and homogeneous, thus it possesses constant resistivity throughout the entire earth.

The second assumption is that the Earth is a hemispherical resistor in a simple circuit consisting of a battery and two electrodes (the source and the sink electrodes) pounded into the ground (Figure 4.2). The battery generates direct electrical current that enters the Earth at the source electrode connected to the positive portal of the battery. The current exists at the sink electrode coupled to the negative portal of the battery.

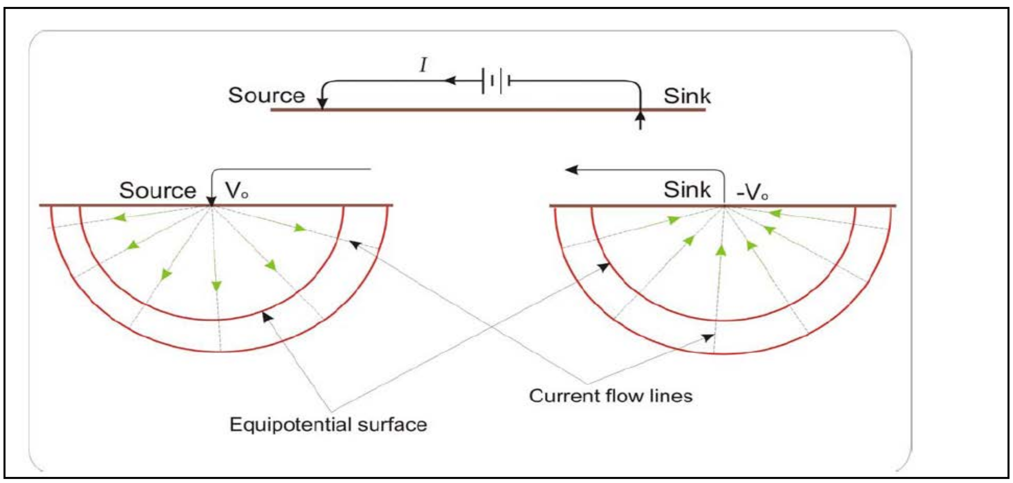

Figure 4.2. Current lines radiating from the source and converging on the sink electrodes (Edwin S. Robinson, 1989)

The battery generates direct electrical current that enters the Earth at the source electrode connected to the positive portal of the battery. The current exists at the sink electrode coupled to the negative portal of the battery. When the current is introduced to the ground, it is compelled to move outward from the source electrode. Due to the assumption that the earth is homogeneous, the current spreads outward in all directions from the electrode, and at each moment of time, the current front will move through a hemispherical zone. The area of such a hemispherical zone can be found from the relationship:

$$A = 2\pi d^2 \tag{4.4}$$

Where d, is the distance from the source electrode to the point on the hemispherical surface defined by Equation 4.4. By substituting equation (4.4) into equation (4.3), we can obtain an expression that defines the resistance of the media at a point separated from the source by distance d:

$$R = \rho / 2\pi d \tag{4.5}$$

The potential difference resulting from the flow of current through the hemispherical resistor can be found from combining Ohm's law expressed by Equation (4.1) and Equation (4.5):

$$V = I\rho / 2\pi d = V_0 - V_d \tag{4.6}$$

Where V_0 is a potential at the source electrode and V_d is a potential at the surface of the hemisphere with radius d. This equation demonstrates that for any point located at the hemispherical surface with radius d, the potential between this point and the source electrode is the same. Such a hemisphere is a surface of constant potential and is called an equipotential surface. In other words, the potential difference between a source and any point on the equipotential surface has the same numerical value.

When the two electrodes are at a finite distance from each other, the potential at any point M separated by distance d_1 from the source electrode, and distance d_2 from the sink electrode, can be found as the sum of the potential contributions from source and sink electrodes for point M (Figure 4.3).

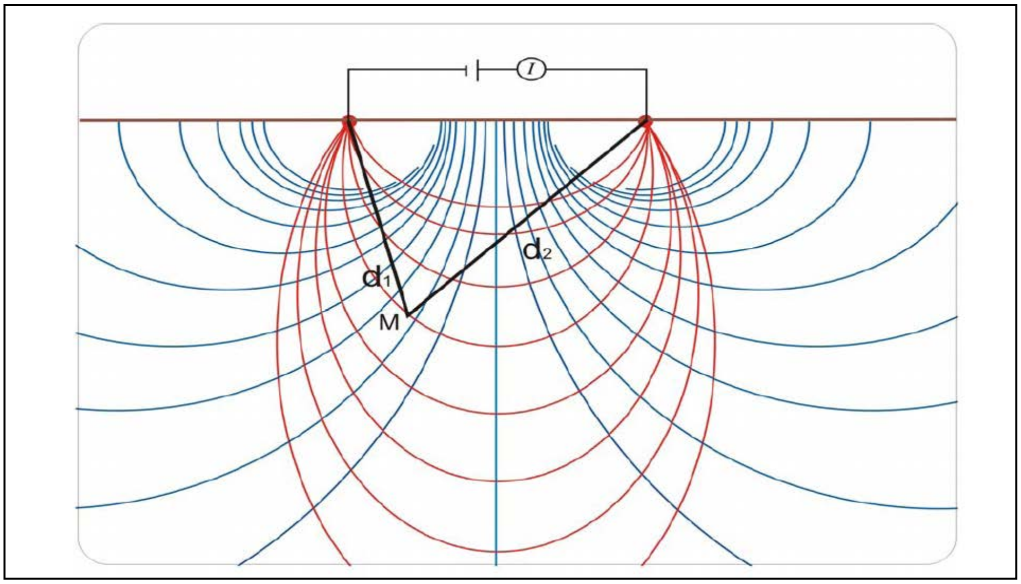

Figure 4.3. Current lines and equipotential surfaces in a medium of uniform resistivity (Edwin S. Robinson, 1989)

$$I\rho/2\pi\ [1/d_1 - 1/d_2] \tag{4.7}$$

This equation can be employed to calculate the potential point by point throughout the earth. By plotting these points and connecting those that are equal, the equipotential surfaces can be obtained.

4.3. RELATIONSHIP BETWEEN GEOLOGY AND RESISTIVITY

Variations in the resistivity of subsurface materials are mostly a function of lithology. Information about resistivity variations within the subsurface can be associated with different materials. The resistivity values of some common earth materials (Figure 4.4) show that there is an overlap in resistivity values of earth materials, and this calls for additional information or ground truth to confirm the particular type of material.

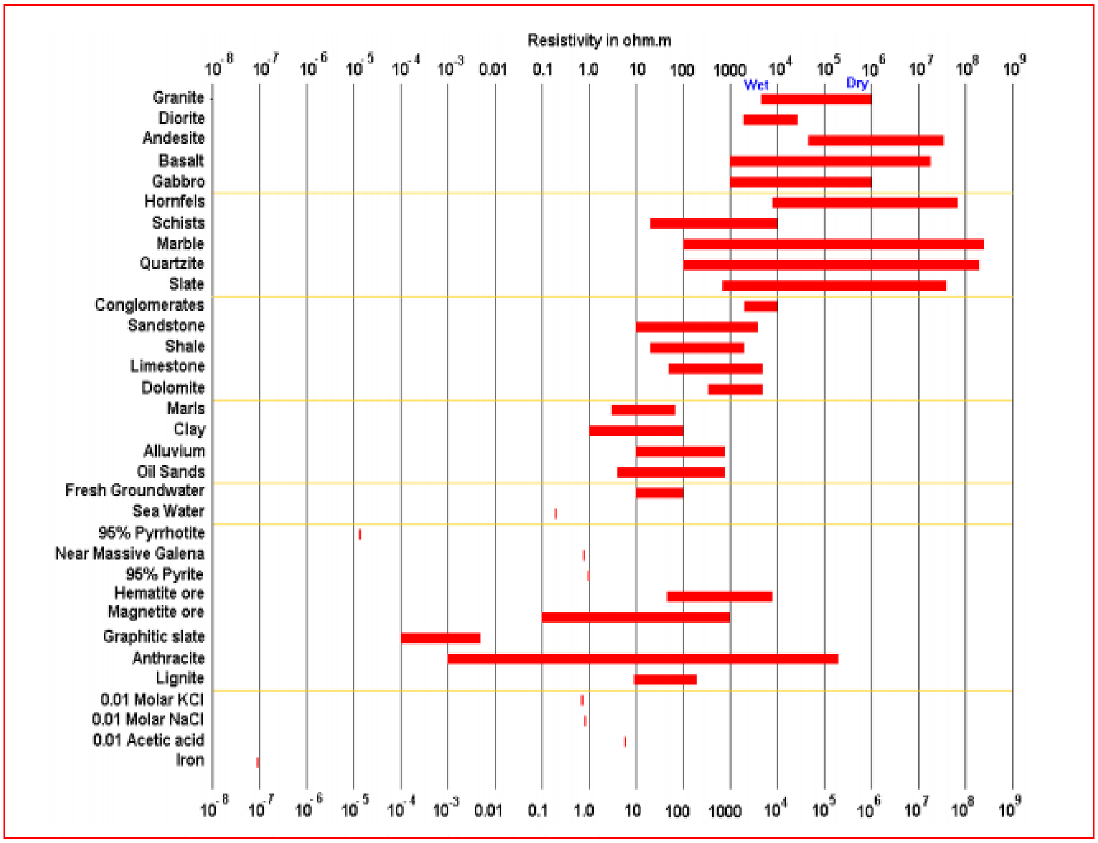

Figure 4.4. The resistivity of common rocks, soil materials and chemicals (Keller and Frischknecht 1966).

Most minerals are considered to be insulators or resistive conductors. So in the majority of rocks, electrical current flow is accomplished by passage of ions in pore fluids (electrolytic conduction). The conductivity, which is the inverse of resistivity, is mostly affected by porosity, saturation, salinity, lithology, clay content and to some degree by temperature. Accordingly, materials with constant mineralogical composition can possess different resistivity values, depending on all the above mentioned parameters.

4.4. APPARENT RESISTIVITY

To acquire 2-D electrical resistivity tomography data in the field, a four- electrode array can be used. Two of these electrodes are used to inject electrical current into the ground and are referred to as current electrodes (Figure 4.5; indicated by letters A and B), and the other two electrodes are connected to a voltmeter and are used to measure the potential difference between electrodes; shown by letters N and M).

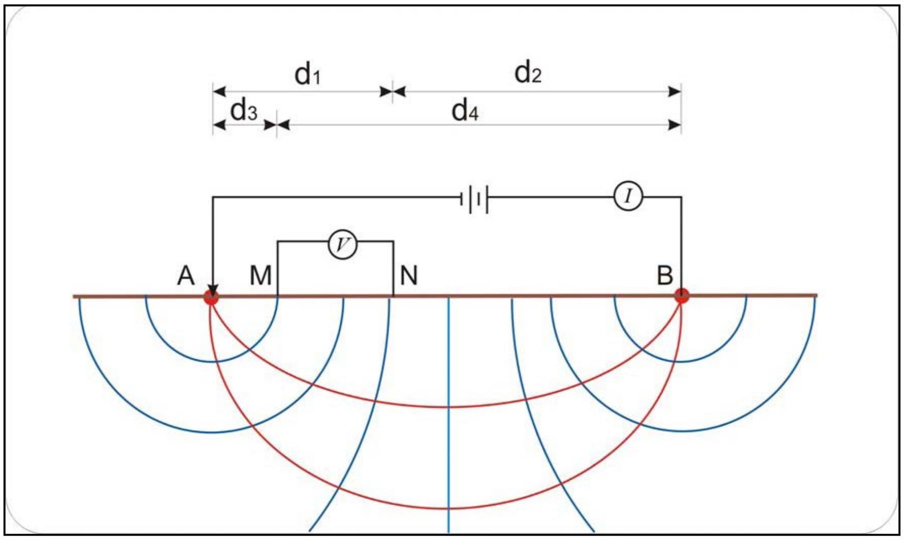

Figure 4.5. Current electrodes A and B and potential electrodes M and N

Current flow direction is shown by red lines and equipotential surfaces are indicated by blue lines. The assumption that the media through which the current is compelled to flow is homogeneous provides for a constant value of resistivity irrespective of where the voltmeter electrodes are placed.

Taking into account the geometry of the electrodes' configuration as illustrated, the electric potential at point M can be deduced from the equation:

$$V_M = I\rho/2\pi\ [1/d_1 - 1/d_2] \quad (4.8)$$

$$V_N = I\rho/2\pi\ [1/d_3 - 1/d_4] \quad (4.9)$$

Therefore, the potential gradient between these two points, $V_{MN,}$ is

$$V_{MN} = V_M - V_N = I\rho/2\pi\ [1/d_1 - 1/d_2 - 1/d_3 + 1/d_4] \quad (4.10)$$

In practice, subsurface materials possess different physical characteristics, and the assumption that resistivity is the same everywhere is not true. Thus, resistivity values that are measured in the field are average resistivity values between two equipotential surfaces, and are known as apparent resistivity values ρ_a.

It can be expressed as:

$$\rho_a = K * V_{MN}/I \tag{4.11}$$

Where K is the geometric factor that depends on the electrode array configuration.

$$K = 2\pi / [1/d_1 - 1/d_2 - 1/d_3 + 1/d_4] \tag{4.12}$$

4.5. ELECTRICAL RESISTIVITY ARRAY CONFIGURATION

For modern electrical resistivity tomography surveys, multi-electrode systems are preferred. The greater the number of electrodes permanently attached to multi-core cable, the higher the investigation capabilities, and less time is spent in the field. Use of multi-electrode system allows combination of vertical sounding and horizontal profiling data to be collected simultaneously. Also it allows the generation of a two-dimensional model of resistivity distribution (Lateral and Vertical).

For 2-D imaging using a modern multi-electrode system, the spacing between electrodes stays fixed for the entire survey. Measurements are taken sequentially using different sets of four electrodes controlled by switching device. The depth of investigation is a function of the array type, the length of array and the physical parameters of material underlying the area of interest, and typically ranges from one-third to one- fifth of the length of the entire array (Robinson et al., 1988).

4.6. 2-D RESISTIVITY ARRAYS

Some of the commonly used electrode configurations are Wenner array, Schlumberger array and Dipole-dipole array. Most electrical resistivity tomography surveying is done with one of the electrode geometries mentioned. The general arrangement of current and potential electrode (Figure 4.6) shows that the potential electrodes (M and N) are placed between the current electrodes (A and B).

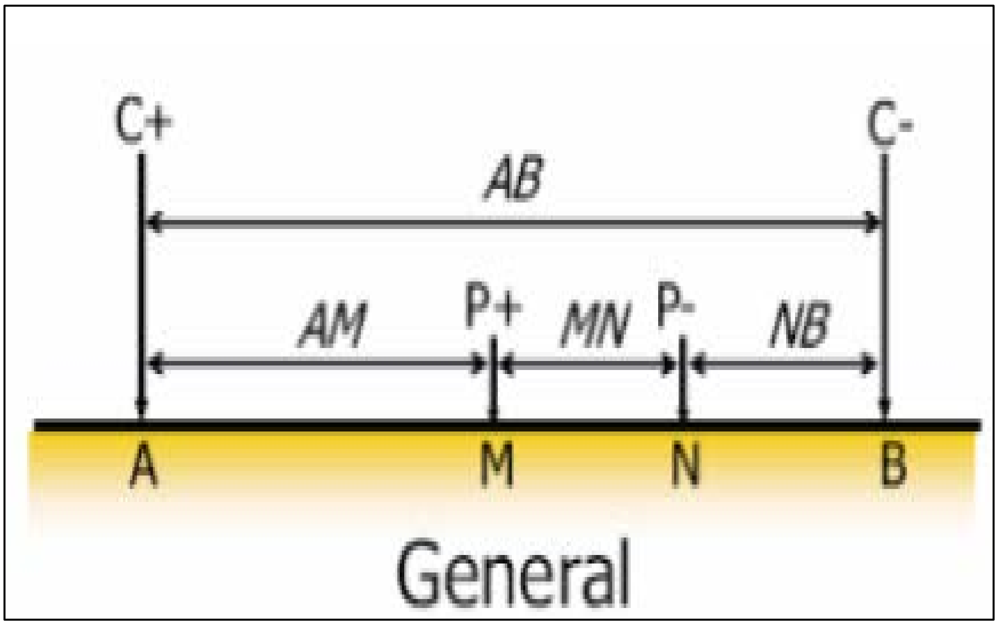

Figure 4.6. General configuration of current and potential electrodes

For the 2-D Wenner Array (Figure 4.7), current and potential electrodes are separated by equal distance ‘a’, such that,

$$AM = MN = NB = a \tag{4.13}$$

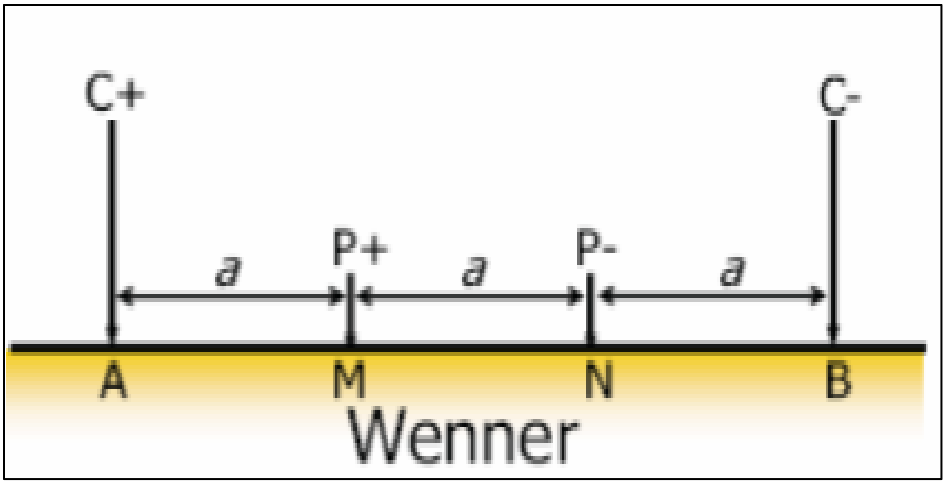

Figure 4.7. Werner array electrode configuration

All the electrodes are arranged along a continuous line, also known as survey line or traverse. The geometric factor for Wenner array can be expressed as,

$$K_W = 2 * \pi * a \quad (4.14)$$

For the 2-D Schlumberger array (Figure 4.8), the potential electrodes M and N are placed between the current electrodes A and B.

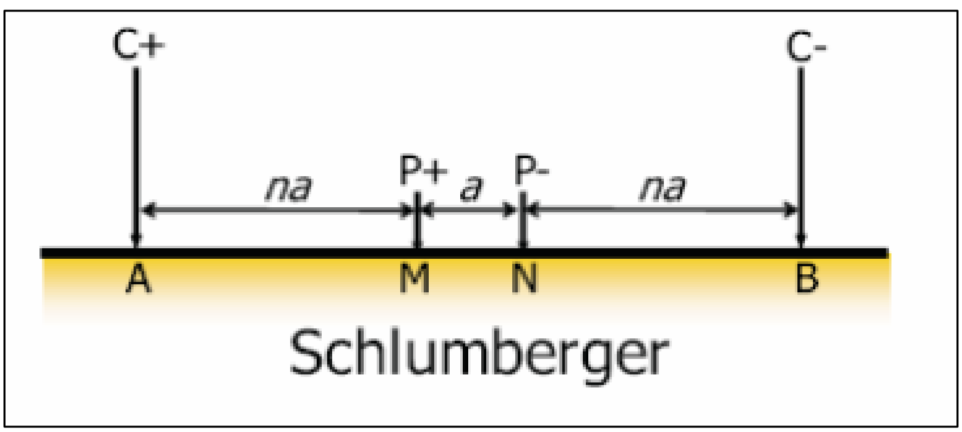

Figure 4.8. Schlumberger array electrode configuration

Suppose the current electrodes A and B are separated by distance ‘L ‘, and the potential electrodes M and N are separated from the center by distance ‘b’, the geometric factor for Schlumberger array can be given by the expression:

$$K_S = \pi (L^2 - b^2) /2b \quad (4.15)$$

For the Dipole-dipole array, the potential electrodes M and N are not placed between the current electrodes A and B (Figure 4.9).

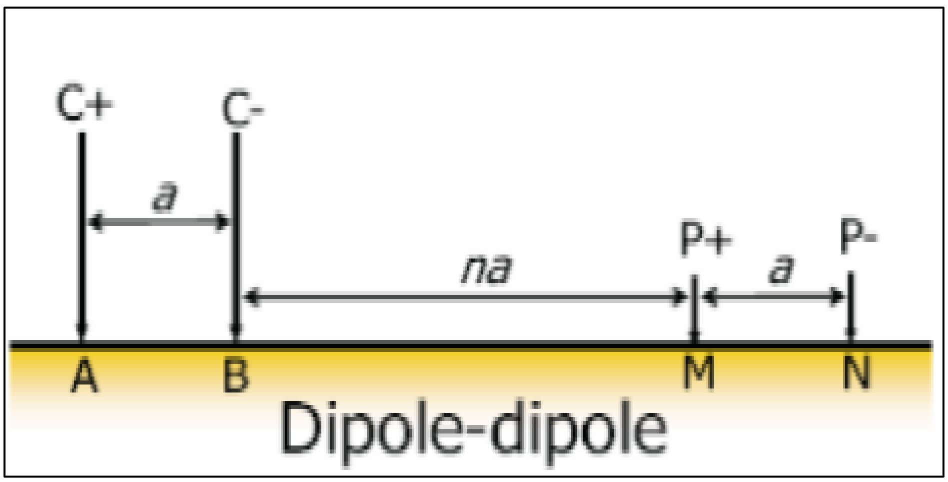

Figure 4.9. Dipole-dipole array electrode configuration

In this type of array, all four electrodes are placed along the same line, and the distance between the current electrodes A and B is equal to the distance between the potential electrodes M and N, represented by ‘a’, given by the following,

$$AB = MN = a \quad (4.16)$$

The distance between the middle points of current and the passive electrode sets is an integer multiple of a, and the factor itself is assigned to be equal to n.

The geometric factor K can be found from the following expression:

$$K_{DD} = \pi *n (n^2 -1)*a \quad (4.17)$$

The choice of the best array to use is dependent on the depth of investigation, vertical and horizontal resolution, signal strength, the type of structure being mapped, background noise level, the sensitivity of the resistivity meter and horizontal data coverage. According to M.H. Loke (2001), the Wenner array is a good choice for surveys carried out in a noisy environment because of its good signal strength. It also offers a good vertical resolution.

The Schlumberger array also has good signal strength but data acquisition time is longer when compared to the Schlumberger array. The good signal strengths in these two arrays are due to the fact that the potential measurement electrodes are located between the current injection electrodes.

The dipole-dipole array is suitable when large data coverage as well as horizontal resolution is required. A combination of Wenner and Schlumberger (the Wenner-Schlumberger array) is suitable if both good and vertical resolutions are needed, especially where good signal strength is also required. There are other arrays like the pole-pole and pole-dipole but they are not commonly used, although they have their own advantages as well.

Dipole-dipole electrode array are mostly used in the study because it has good lateral coverage, knowing that karst terrain is highly variable laterally. Typical depth of investigation is approximately 20% of the array length. In electrical resistivity tomography (ERT) survey, factors that are considered before survey are availability of space for the survey to avoid trespassing, depth of investigation and the number of electrodes available.

5. OVERVIEW OF GEOPHYSICAL TECHNIQUES USED

5.1. AUTOMATED ELECTRICAL RESISTIVITY TOMOGRAPHY (ERT)

Automated electrical resistivity tomography technique makes use of contrasting electrical properties of the earth materials to partition the earth to produce an image called tomogram. Automated multi-electrode resistivity meter known as SuperSting is used for data acquisition. After data acquisition, a 2-D cross-sectional plot of resistivity versus depth is modeled using RES2DINV software. The model can represent the geometry, lithology, hydrology and petrology of subsurface geologic formations in the area. The effectiveness of automated electrical resistivity tomography technique in mapping subsurface karst features is dependent on its sensitivity to changes in density and porosity of subsurface earth materials.

In mapping karst features, the target is usually the "Ravel zone". This zone is formed as a result of downward transportation of soil by water into voids /cavities in underlying strata, a process known as raveling. This zone can either be a high-resistivity anomaly when it is dry or a low-resistivity anomaly when it is saturated, depending on the depth to the local groundwater table in the area. Typically, deeper void space is characterized by presence of low-resistivity features indicative of carbonate materials being replaced by looser clastic sediments, or by water. An air-filled void commonly generates a high-resistivity anomaly feature which of course is not a sinkhole yet, because it has not collapsed or accepted overlying sediments.

Although there are other geophysical techniques used in mapping karst features, automated electrical resistivity tomography (ERT) has proved to be one of the most reliable techniques employed in mapping karst features, which is why it is used in combination with other techniques in almost all geophysical surveys in karst terrain. It is good in mapping sedimentary boundaries whether the material is covered or not, effective in mapping cavities, fracture zones and preferential pathways of groundwater. Multichannel analysis of surface waves (MASW) is a good complementary geophysical tool to ERT. Over all, ERT has good area coverage, and it is fast and cost-effective.

Electrical resistivity tomography has been used to map karst voids encountered during road construction in Yongweol-ri, South Korea (Muhammad Farooq et al. 2012). Ahmed M Youssef et al. (2012) used two-dimensional electrical resistivity tomography (ERT) with different electrode spacing to delineate buried sinkholes and associated subsurface cavities in Saudi Arabia. Kruse et al. (2006) successfully used a combination of ground penetrating radar (GPR) and electrical resistivity tomography (ERT) to map a large developing sinkhole in a covered karst terrain in west-central Florida (USA). Ezersky et al. (2006) combined time domain electromagnetic (TDEM), GPR, ERT and Magnetic methods to study sinkhole development in the Dead Sea area (Middle East). Turberg and Barker (1996) used a combination of ERT and radio magnetotellurics (RMT), enhanced very low frequency resistivity mode (VLF-R) to describe the near-surface epikarst zone on a test site in Switzerland. Ahmed and Carpenter (2003) combined electrical resistivity tomography and electromagnetic techniques to map high-conductivity anomalies linked to filled sinkholes in east-central Illinois (USA). Šumanovac and Weisser (2001) combined 2D ERT, seismic refraction and the high-resolution reflection seismic methods to map the vertical boundaries of a karst system in Croatia. Kaufmann and Quinif (2001) used combined two-dimensional electrical resistivity array tomography to delineate cover-collapse sinkhole-prone areas in southern Belgium. Elawadi et al. (2006) employed a combination of ERT, GPR and VLF-EM methods to delineate hazardous zones consisting of vertical and sub-vertical faults, fracture zones, and geological contacts in southern Cairo, Egypt. An integrated microgravity and ERT geophysical survey was successfully conducted by McGrath et al. (2002) to detect underground voids in south Wales (UK), and the results were integrated in groundwater vulnerability mapping. Gibson et al. (2004) used ERT to locate an unknown 210 meters (689ft.) long, 70 meters (230ft.) wide and 25meters (82ft.) deep collapse feature in eastern Ireland beneath sediments.

5.1.1. Automated Electrical Resistivity Tomography Field Equipment. Field Equipment (Figure 5.1) used for data acquisition are SuperSting, electrode cables, battery, switch box, metal stakes, rubber-band and a laptop computer.

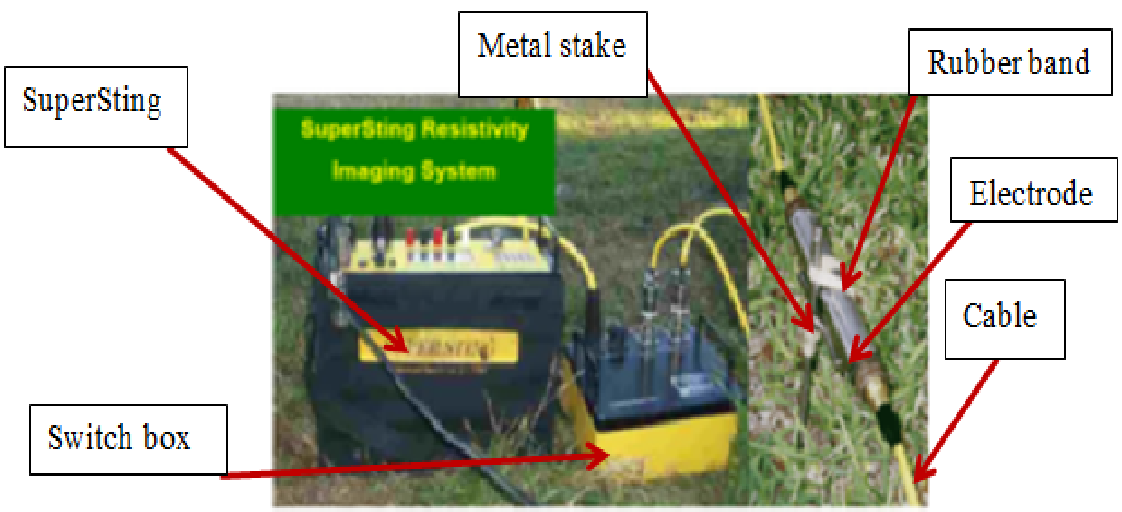

Figure 5.1. Automated electrical resistivity tomography (ERT) field-setup

5.1.2. Electrical Resistivity Tomography Data Acquisition. Data acquisition involves using the SuperSting earth resistivity meter or control unit which is powered by one or two 12-Volts battery to inject an electric current into the ground through electrodes. During the set-up, electrode cables are firmly attached to metal stakes pounded to the ground using springs or rubber-band. Switch box can also be used to connect the electrodes (passive electrodes) to the resistivity meter. A Laptop computer is used to download or upload data to the SuperSting, and may be connected to the SuperSting during data acquisition or can be used later for data transfer and processing.

At each point, normally, four electrodes are used, two current electrodes for injecting current into the ground, and two potential electrodes for measuring the resulting voltage difference. From the resulting current and voltage that are measured, the apparent resistivity value is calculated. Apparent resistivity is calculated as a weighted average of the different resistivities under the four electrodes. In a situation where the ground is homogeneous, the apparent resistivity equals the true resistivity.

In most cases, dipole-dipole array is used because it is logistically the most convenient array used in the field, especially for large scale projects. In dipole-dipole electrode array configuration, the electrodes are attached to a multi-core cable in a straight line. The cable is connected to the switching unit hardwired into the SuperSting resistivity meter. The unit controls the selection of the current (A&B) and potential (M&N) electrodes for each measurement.

It is also worthy to note that data acquisition time for a dipole-dipole array using 72 electrodes typically takes about 45minutes, and around 2hours and 3hours for 84 electrodes and 168 electrodes respectively after survey set-up. Depth of Investigation for a dipole-dipole array is about 20% -25% of the array length. Dipole-dipole electrode array (Figure 5.2) was used throughout the study.

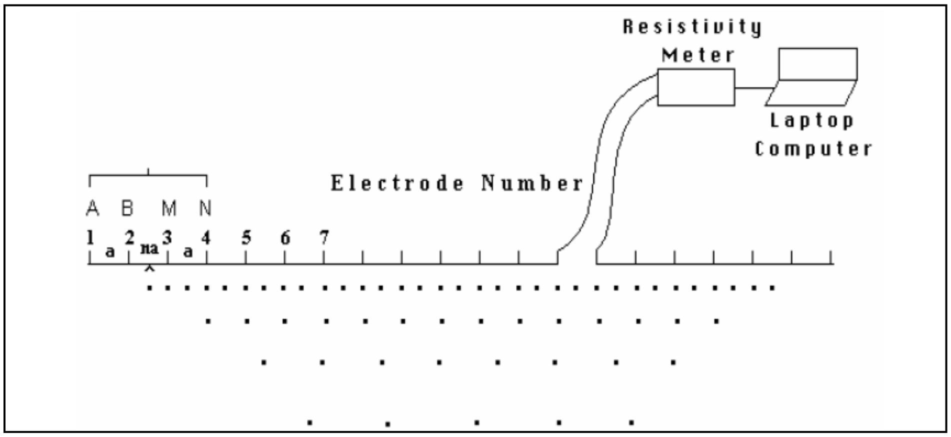

Figure 5.2. Electrical resistivity dipole-dipole array configuration used in the field

5.1.3. Electrical Resistivity Tomography Data Processing. After data acquisition, the raw data are transferred to the laptop computer for processing using RES2DINV software. The program uses "forward modeling" subroutine to specify the subsurface resistivity in order to calculate the apparent resistivity that would be measured by a survey over such a structure. In any inversion program, forward modeling is always part of it. It is used to calculate the theoretical apparent resistivity values for the model produced by the inversion routine to see whether it agrees with the measured values.

The first step in processing is the inspection of the pseudosection so as to remove 'bad data points". Bad data points can be as a result of several factors, such as failure or malfunction of equipment during survey and very poor electrode-ground contact due to dry soil or shorting across the cable due to very wet ground conditions. These points appear as stand out points of unrealistically high or low resistivity values, and are marked as red plus signs in the resistivity profile (Figure 5.3).

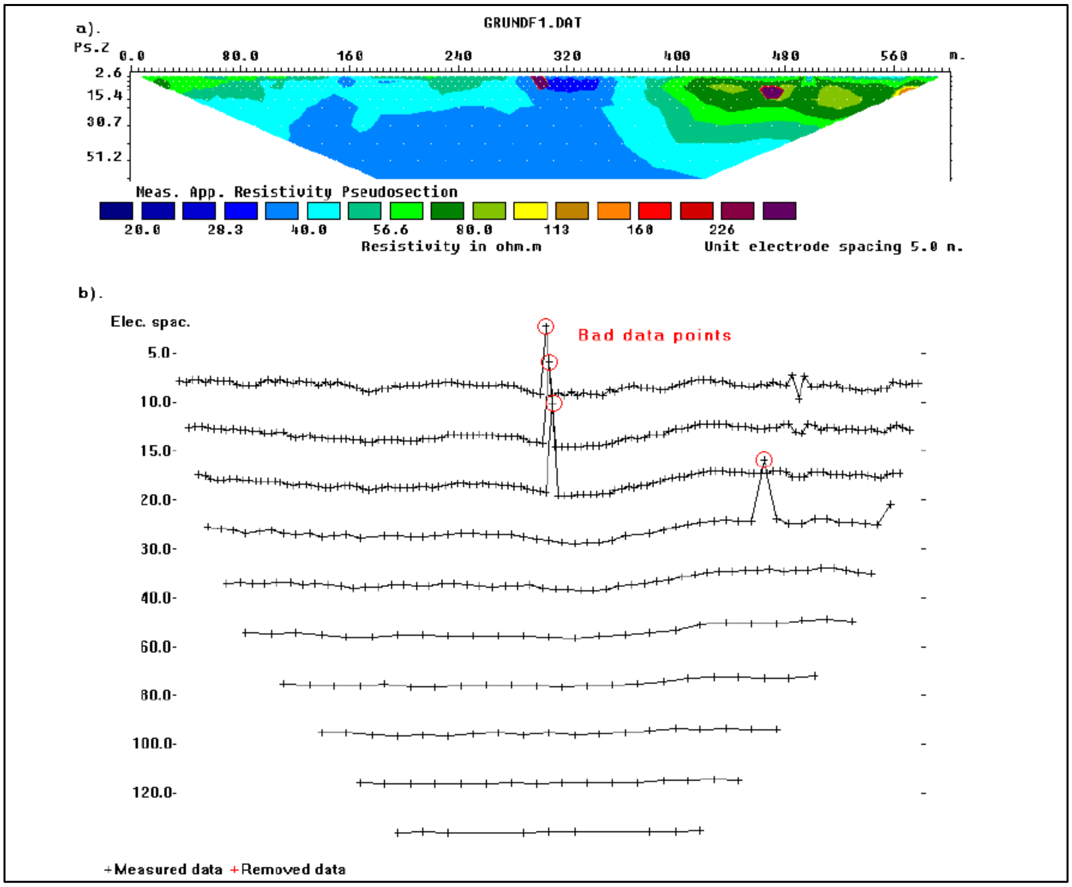

Figure 5.3. An example of a field data set with a few bad data points. The most obvious bad datum points are located below the 300 meters and 470 meters marks. The apparent resistivity data in (a) pseudosection form and in (b) profile form. (Loke, 2001)

To create a 2-D resistivity model, the RES2DINV divides the subsurface into a number of rectangular blocks (Figure 5.4). This is done with a view to determining the resistivity of the rectangular blocks that will produce an apparent resistivity pseudosection that agrees with the actual measurements. For the pole-pole, dipole-dipole and pole-dipole arrays, the thickness is set to about 0.9, 0.3 and 0.6 times the electrode spacing respectively. The thickness of each subsequent deeper layer is normally increased by 10% (or 25%).

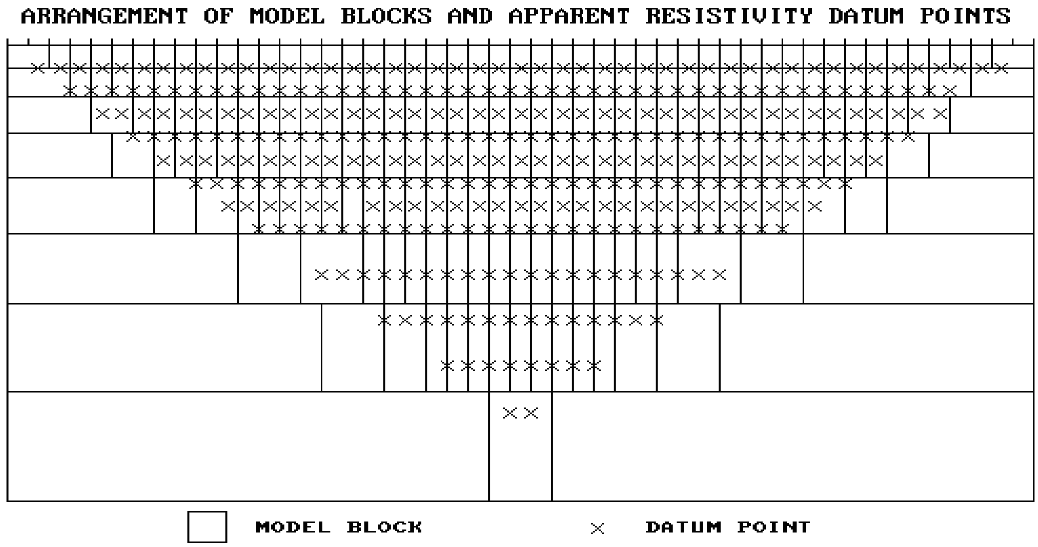

Figure 5.4. Arrangement of the blocks used in a model together with the data points (Loke, 2001)

The default optimization technique used by RES2DINV software is the Gauss-Newton method because of its fastness. What the optimization program does is to reduce the difference between the calculated and measured apparent resistivity values by adjusting the resistivity of the model blocks. The root-mean squared (RMS) error is used to measure the difference. It is worthy to note that the model with the lowest possible RMS error can sometimes show large and unrealistic variations in the model resistivity values, and might not be best model at all times when viewed from geological perspective. A careful and prudent approach is to choose the model at the iteration after which the RMS error does not change significantly. In practice, this normally occurs between 3rd and 5th iterations. Typically, RMS value of 10% or less provides a good quality control of the calculated model.

5.1.4. Electrical Resistivity Tomography Data Interpretation. Interpretation is based on the inverse model generated using the inversion software, RES2DINV. The color chart showing different colors with different ranges of resistivity is used to estimate the resistivities of the imaged subsurface earth materials.

5.1.5. Resolution of Electrical Resistivity Tomography. Resolution is a function of electrode spacing and resistivity contrast between lithologically different earth materials. The resolution of automated electrical resistivity tomography (ERT) profile defines the accuracy of interpretation of subsurface conditions. The size of a pixel is a main estimate of automated electrical resistivity (ERT) imaging resolution. This means that at this shallow depth, all objects that are less than the size of the pixel will not be easily detected. With increasing depth, the vertical dimension of the pixels becomes greater and that reduces resolution.

During data processing, the subsurface is divided into blocks. The highest achievable lateral resolution is equal to the electrode spacing; therefore, a dipole-dipole array with electrode spacing of 5 feet has a maximum lateral resolution of 5 feet. Vertical resolution is also a function of the electrode spacing. Typically the height of the shallowest block is about 0.3 of the electrode spacing. Horizontal and vertical resolutions decrease with depth. During the survey, when current is induced to flow through deeper layers, the distance between current and potential electrodes is gradually increased. This affects the sensitivity of the automated electrical resistivity tomography (ERT) method. Gradually increasing the distance between electrodes lowers the intensity of current flow, and accordingly the sensitivity of automated electrical resistivity (ERT) survey. Thus, interpretation of smaller scale objects at greater depths becomes increasingly difficult and sometimes small objects can be missed or misinterpreted.

Resistivity contrast is another parameter that defines the resolution of automated electrical resistivity tomography (ERT) profile. When lithologically different materials exhibit similar conductivity parameters, sometimes it is difficult to differentiate them simply on the basis of their resistivity parameters. For example, both intact limestone and air-filled voids typically are characterized by high resistivity values. When an air-filled void is embedded in intact limestone, it typically cannot be easily detected on resistivity profile because of low resistivity contrast.

5.1.6. General Guide to ERT Data Interpretation. Factors such as porosity, conductivity, moisture content, salinity, clay content, lithology, and temperature can affect the ability of different materials to conduct electrical current. Accordingly, materials of the same mineral content may exhibit different resistivity values (Table 5.1).

Table 5.1. Typical ranges of resistivity for some materials (Advanced Geosciences, Inc. (AGI, 2005).

Rock/material type	**Resistivity range (Ω m)**
Igneous	100-1000000
Limestone	100-10000
Sandstone	100-1000
Sand and gravel	600-10000
Clay	10-100
Unconsolidated wet clay	20
Soil	1-10
Fresh water	3-100
Drill mud, hydraul-EZ	4.5
Sea water	0.2-1
Copper (native)	0.0000002

For instance, dry soils usually have much higher resistivity than saturated soils. The same situation appears with weathered and unweathered rock. Weathered rocks are usually more porous and fractured than unweathered/intact rocks, and are more likely to be saturated with groundwater, which lowers the resistivities of the rocks. Air has an infinite resistivity (∞) or very high resistivity values above 1000 Ohm-m.

According to previous studies (Anderson et al., 2006) conducted in southwestern Missouri, typical resistivity values for the subsurface materials are characterized as follows:

- Moist clays in southwestern Missouri are normally characterized by low resistivity values (usually less than 100 ohm-m) and may vary due to different degrees of saturation, porosity, and layer thicknesses.
- Moist soils and intensively fractured rocks intermixed with clay typically have resistivity values between 100 and 400 ohm-m. Such variation is explained by different porosity, saturation, clay content, and layer thicknesses.
- Relatively intact limestone with minimal clay content is characterized by higher resistivity values, typically more than 400 Ohm-m. Resistivity values of intact limestone may vary due to varying layer thickness, moisture content, porosity, saturation, and impurities.
- Air-filled cavities usually show very high resistivity values, usually more than 1000 ohm-m, but again, are variable depending on the conductivity of the surrounding strata and depth/size/shape of void. Zones where relatively intact bedrock is surrounded by moist loose materials (such as clay), or zones where air-filled voids are embedded in relatively intact limestone, are zones of electrical resistivity contrast. These zones can be successfully detected by electrical resistivity tools.

5.2. MULTICHANNEL ANALYSIS OF SURFACE WAVES

The multichannel analysis of surface waves (MASW) geophysical technique makes use of seismic surface waves generated from different types of seismic sources to evaluate the engineering properties of subsurface materials. There are two different methods of data acquisition using surface waves; they are the active and the passive methods. The passive method utilizes surface waves generated passively by cultural activity like traffic or natural activity like thunder and tidal motion. The depth of investigation is usually shallower than 30 m with the active method, whereas it can reach a few hundred meters with the passive method. In active method, surface wave is generated through an impact source like a sledge hammer or a weight-drop.

Unlike the conventional seismic surveys (reflection and refraction) that deal with a depth range of a few tens to hundreds of meters, with frequencies above 50 Hz, the multichannel analysis of surface waves deals with surface waves in the lower frequencies (1-30 Hz) at shallower depths of few tens of meters. The sampling depth of a particular frequency component is directly proportional to its wavelength thereby making the surface wave velocity frequency dependent (dispersive).

It is widely applied in geotechnical engineering to evaluate the stiffness of subsurface materials. The propagation velocities of the surface waves generated is used to generate the shear-wave velocity (Vs) variations of the subsurface materials. Shear wave velocity can be used to measure the elastic constants of materials such as the Young's modulus (E), Poisson's ratio (n), and shear modulus (G). The general relationship between the speed of sound in a solid and its density and elastic constants is given by the following equation: $V=\sqrt{C}/\rho$, where V= speed of sound, C= the elastic constant and ρ =

the material density. The elastic constant used to calculate the shear wave velocity depends on the type of wave in propagation. When calculating the velocity of a longitudinal wave, Young's Modulus and Poisson's Ratio are commonly used. When calculating the velocity of a shear wave, the shear modulus is used.

Factors affecting shear wave velocity (Vs) are fracture spacing (increases with increased Vs), fracture density (decreases Vs when high), hardness (increases with increased Vs) and weathering (decreases Vs when high).

The main target of multichannel analysis of surface waves (MASW) in imaging karst features is the “ravel zone”, just like the automated electrical resistivity tomography (ERT). This zone forms as a result of downward transportation of soil into voids/cavities in underlying strata by surface water, and is characterized by increased porosity and reduced percentage of fines. The relatively weak nature of the sediments in this zone (low strength) compared to adjacent, undisturbed soil is a good contrast (velocity contrast) needed by MASW to give a better result. The zone is marked by reduced seismic velocities when imaged using the technique.

5.2.1. Multichannel Analysis of Surface Waves Field Equipment. For data acquisition using the Multichannel analysis of surface waves technique, the equipment used are seismograph, sledge hammer, geophones, battery, impact plate or base plate, cables, connectors and a computer laptop (Figures 5.5 and 5.6)

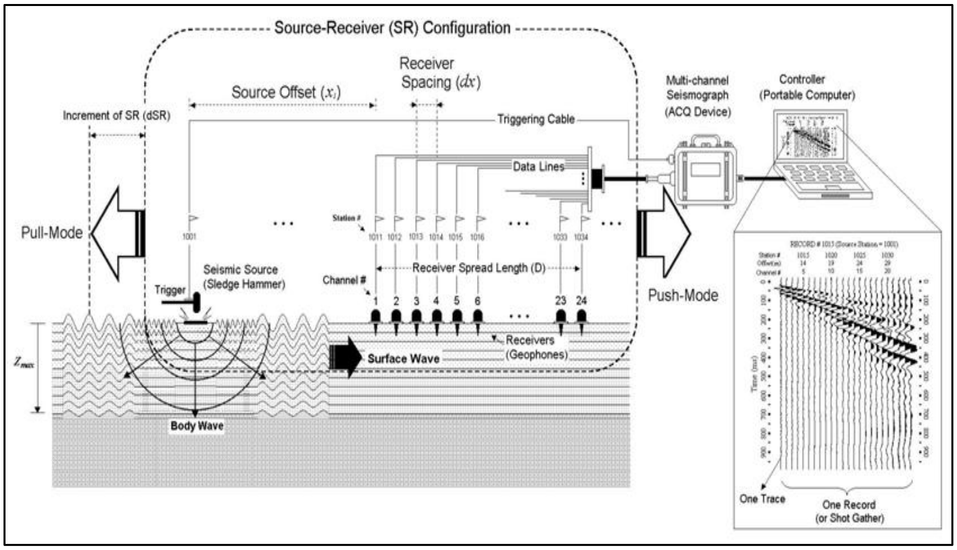

Figure 5.5. MASW field set-up (http://www.masw.com/DataAcquisition.html)

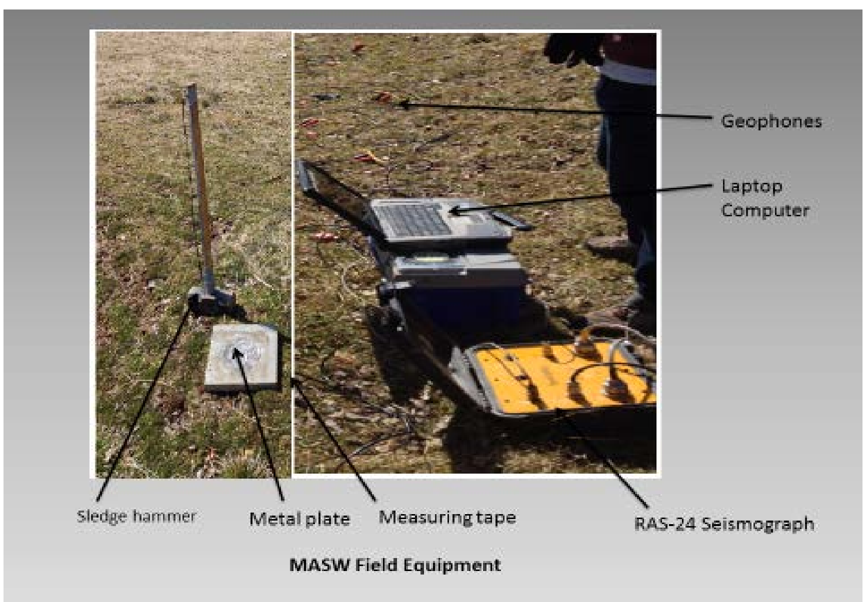

Figure 5.6. MASW field equipment

5.2.2. Multichannel Analysis of Surface Waves Data Acquisition. The procedure for Multichannel analysis of surface waves (MASW) data acquisition consists of discharging an acoustic source at the earth's surface and recording the resultant Rayleigh wave energy (Figure 5.7) by sensors placed at multiple locations.

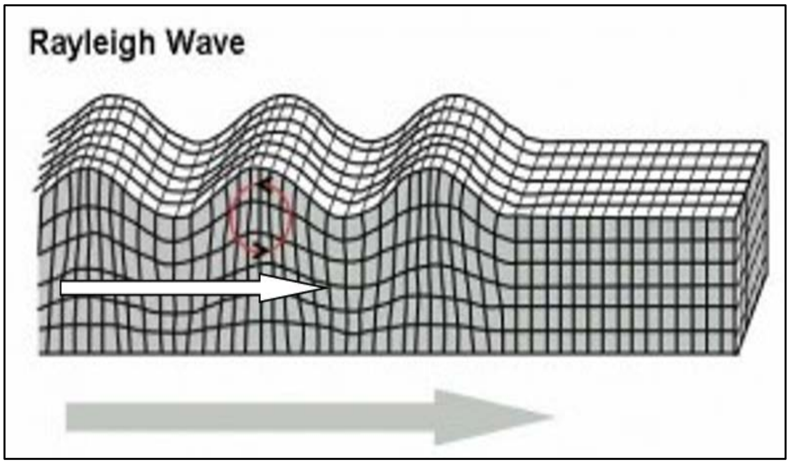

Figure 5.7. Example of Rayleigh wave particle motion

The equipment used for the study are, a 20-Lb sledge hammer as acoustic source, impact plate (also called base plate) which helps the source impact point become less intrusive into soil, RAS 24 channel seismograph, geophones, a 12-volts battery and a computer laptop. After striking the hammer three or five times (stacking), the recorded data on the seismograph is saved in a laptop computer for processing.

5.2.3. Multichannel Analysis of Surface Waves Data Processing. After data acquisition, field data are analyzed using software (Surfseis is used in this case). Data processing involves two steps, first step involves extracting the fundamental-mode dispersion curves called overtone (one from each record), and then inverting these curves to generate 1-D (depth) shear wave velocity profile (Figure 5.8). This shows depth vs shear wave velocity relationship in linear form.

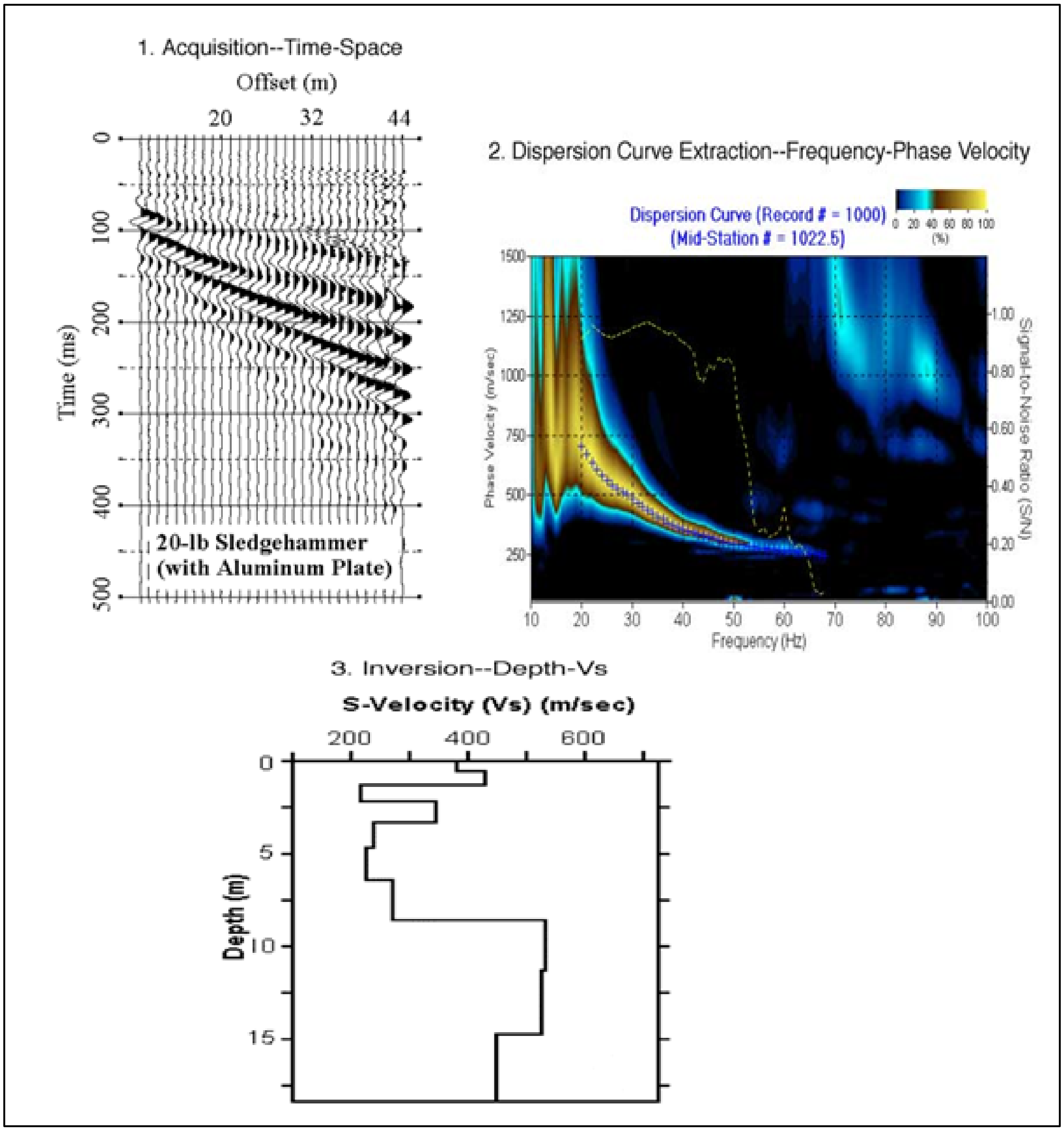

Figure 5.8. MASW processing step 1 (http://www.kgs.ku.edu/software/surfseis/masw.html)

The second step involves appropriate interpolation of the 1-D (depth) shear wave velocity profiles generated from all the records to construct a 2-D shear wave velocity profile (Figure 5.9).

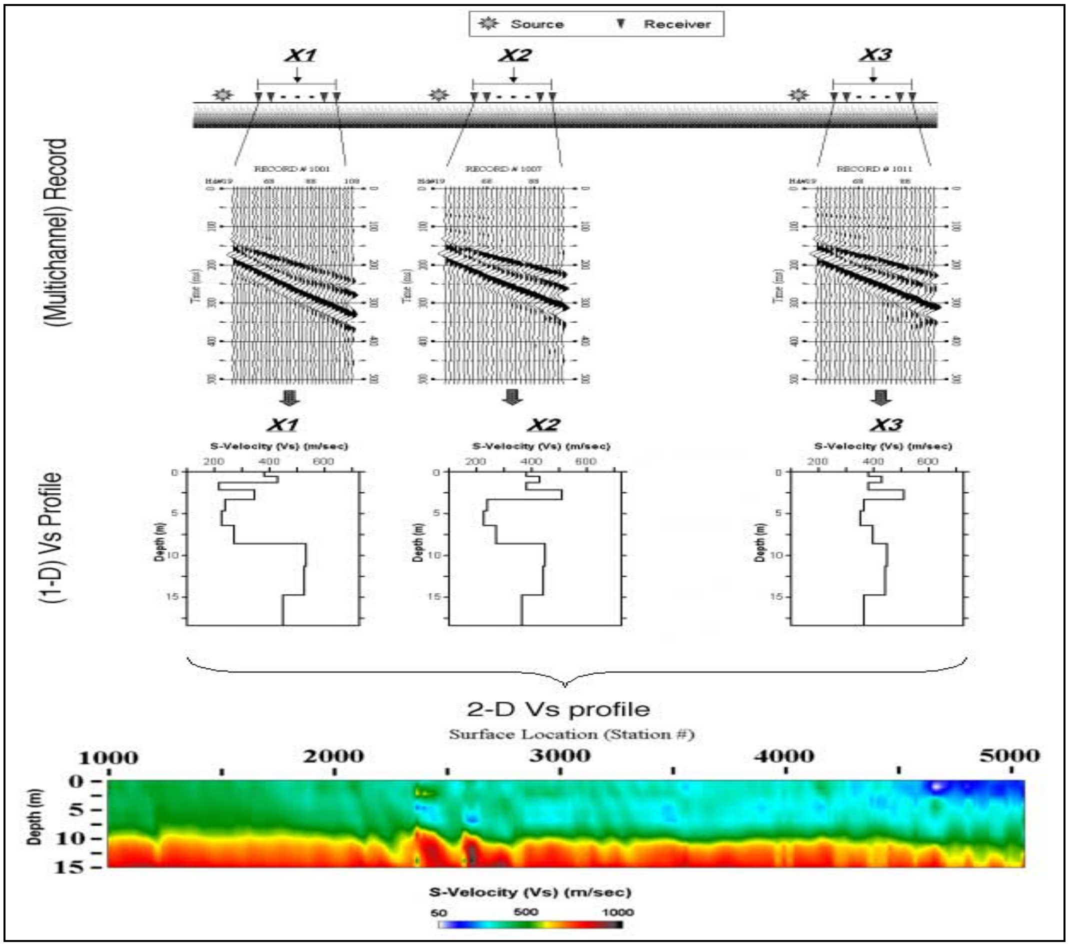

Figure 5.9. MASW processing step 2 (http://www.kgs.ku.edu/software/ surfseis/gifs/masw_3.jpg)

5.2.4. Multichannel Analysis of Surface Waves Data Interpretation. Data interpretation of MASW involves using the generated model to determine the variations of the shear wave velocities of the investigated area with depth using the color chart. The depth to top of bedrock can also be determined. In Missouri for example, the shear wave velocity value used to determine the depth to top of bedrock is mostly 1000ft/sec. but can vary. Again, highly stiff earth materials have relatively high shear wave velocities compared to fractured or weak earth materials (Table 5.2).

Table 5.2. Shear wave velocity (Vs) of some earth materials (National earthquake hazards reduction program)

Earth Material	**Shear wave velocity at 30 meters depth(V_{s30})**
Hard rock	>5000ft/sec. (>1500 m/sec.)
Rock	2500-5000ft/sec. (760-1500 m/sec.)
Very dense soil and soft rock	1200-2500ft/sec. (360-760 m/sec.)
Stiff soil	600-1200ft/sec. (180-360 m/sec.)
Soft soil	<600ft/sec. (<180 m/sec.)

5.2.5. Resolution of Multichannel Analysis of Surface Waves. Resolution is a function of the receiver (geophone) spacing, and the receiver spacing is related to shortest wavelength and therefore determines the shallowest resolvable depth of investigation. The length of the array or the receiver spread is directly related to the longest wavelength that can be analyzed, which in turn determines the maximum depth of investigation. In practice however, the maximum depth of investigation is limited by the seismic source as it is the most governing factor. It is less than 100 feet in most cases. The source offset distance controls the degree of contamination by the near-field effects. Common practice is to use about 20% of the maximum depth of investigation. Low-frequency (e.g., 4.5 Hz) geophones are always recommended and vertical instead of horizontal geophones are effective. Vertical stacking with multiple impacts can suppress ambient noise significantly, giving a high signal to noise ratio (S/N). This is good in surveys in urban areas. Three to five vertical stacks are recommended during survey.

6. NIXA CASE STUDY

6.1. ABSTRACT

Four Automated electrical resistivity tomography (ERT) profiles were acquired to map solution-widened joints and top of bedrock in proximity to a collapsed sinkhole in Nixa, Christian county, Missouri. The collapse occurred after a major storm event that caused massive flooding in the area, and exposure of limestone bedrock.

The result of the interpreted ERT data acquired showed that two sets of solution-widened joints trending approximately S-N and NW- SE directions. Further extrapolation of these joints showed that the point of interception of the joints was where the sinkhole collapse occurred. Top of bedrock varies between 5 feet to 30 feet. The orientation of known faults in the area corresponds with the orientation (NW-SE) of one of the sets of solution-widened joints mapped in the area. The observed pattern of the images of the joint sets showed uniformity in width of the joints even at greater depths, and are mostly infilled with clay, characterized by low resistivity values (high conductivities).

6.2. INTRODUCTION

A major storm event occurred in the city of Nixa in Christian County of Missouri. The storm event caused massive flooding allowing a large quantity of soil and surficial materials to be eroded thereby leading to sinkhole collapse in the area. Limestone bedrock and cavities were exposed in the collapsed area. The sinkhole was about 37 feet deep with length and width of over 30 feet and 20 feet respectively. Although no immediate damage was caused to lives and properties, the collapse may pose a long-term risk to the residents in the area. Because of this, sinkhole collapse evaluation was initiated to know the possible remediation method to use to stabilize the ground around the area. Automated Electrical Resistivity Tomography (ERT) geophysical method supported by boring information was used to characterize the site.

6.3. SITE GEOLOGY AND DESCRIPTION

Nixa is a city in Christian County Southwest Missouri. It is part of the Springfield Missouri Metropolitan (Figure 6.1). Karst density in the area is among Missouri's highest, and one of the most notable sinkhole collapses in the US occurred in this area in 2006 where a car and a garage were swallowed when a 75-foot deep sinkhole that collapsed.

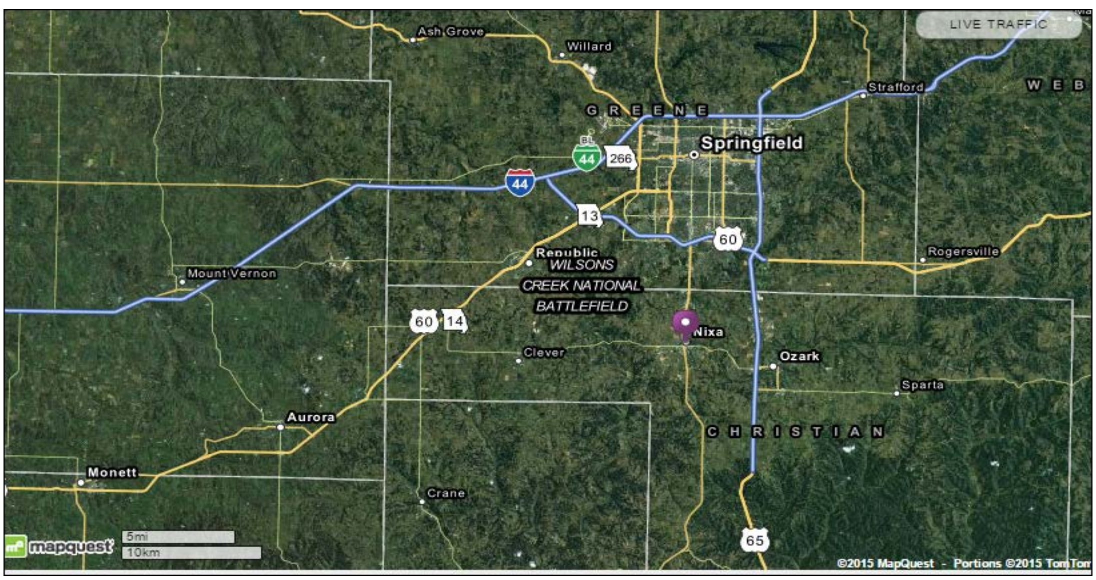

Figure 6.1. Map of Missouri showing Nixa in Christian County

The site consists mainly of limestone and siltstone. The primary rock unit was the Burlington-Keokuk limestone. The project site was an open land covered by grasses and unconsolidated surface materials, and looks like a sports field (Figure 6.2).

Figure 6.2. Sinkhole in the project site covered with barrier for safety purpose

Surficial materials in the area are mainly clay, silty clay and cherty clay. The collapse exposed the Burlington-Keokuk limestone bedrock (Figure 6.3) in the area which was covered by unconsolidated soil and surficial materials.

Figure 6.3. Exposed limestone bedrock (Looking East) in the project area

The geologic unit in the area belongs to the Osagean Series (Table 6.1). Other secondary rock types found in the area are chert, shale, sandstone and dolostone.

Table 6.1. Geologic and stratigraphic units in Nixa area (adopted from USGS)

System	**Series**	**Group**	**Formation**	**Maximum Thickness (ft.)**
Mississippian	Osagean		Keokuk Limestone	100
			Burlington Limestone	70
			Elsey Formation or Grands Falls Formation	100
			Reeds Spring Formation	225
			Pierson Limestone	60
			Fern Glen Formation	45

6.4. DATA ACQUISITION

Four automated electrical resistivity tomography (ERT) profiles were acquired using dipole-dipole electrode configuration with sixty four (64) electrodes at four feet spacing. Two of the four profiles were acquired parallel to each other (Figure 6.4), and thirteen feet apart. The length of each profile was 252 feet. The estimated depth of investigation was about fifty feet. Multichannel analysis of surface waves (MASW) data was also acquired along the profiles but the data was of poor quality (noisy) and could not be used, so boring information obtained from borehole logs in the area was used for ground truth.

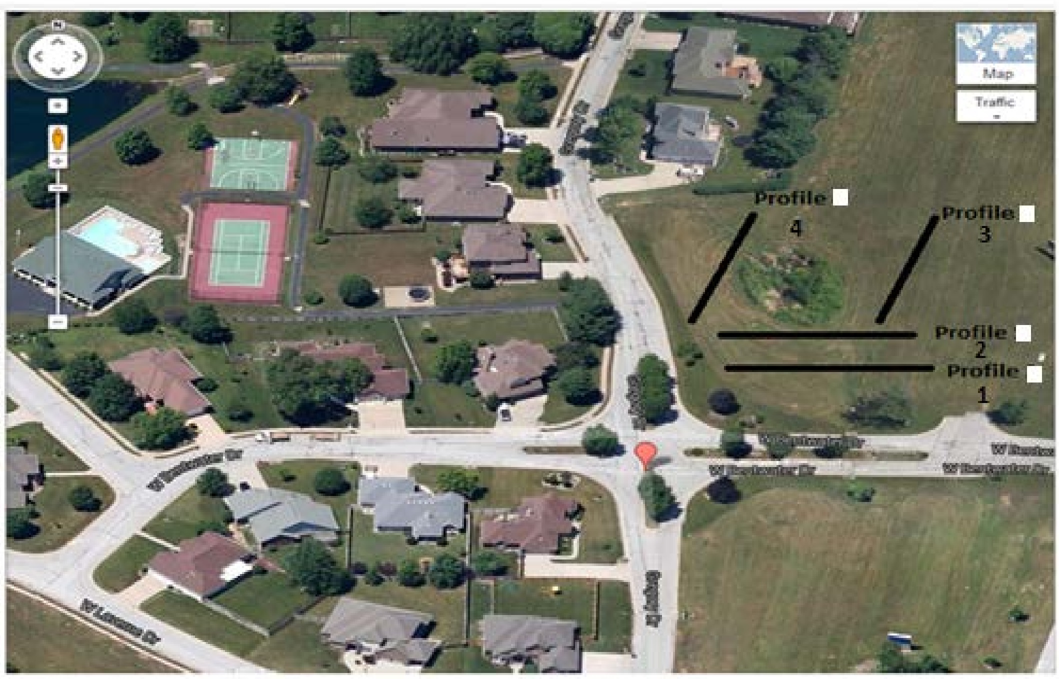

Figure 6.4. Map of the project site from Google. Four automated electrical resistivity tomography (ERT) profiles are shown as black lines. The sinkhole is shown at the center of the profiles, and appears as a circular figure when viewed from Google map as shown. The lines were not drawn to scale but represent the orientation of the four ERT profiles during data acquisition.

The distance between profiles 1 and 2 was 13 feet (Figure 6.5) and they were parallel to each other as seen from the sketch. For safety reasons the survey was carried out some distance away from the sinkhole because the ground around the area was not that stable.

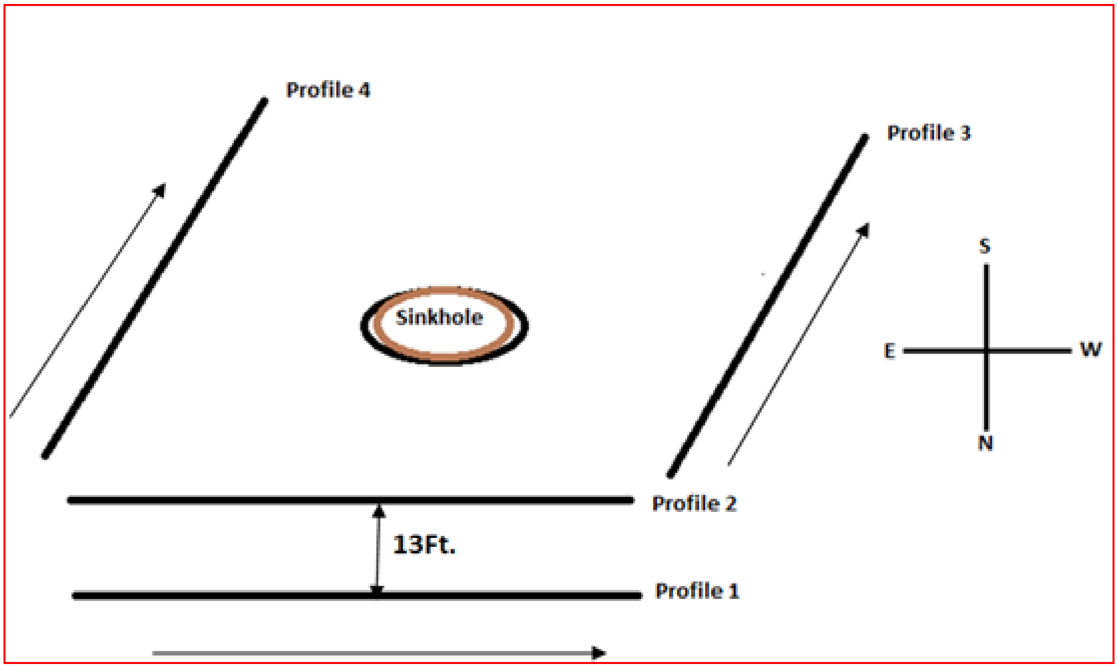

Figure 6.5. A sketch of the four automated electrical resistivity tomography (ERT) profiles

6.5. DATA PROCESSING

The electrical resistivity tomography (ERT) data acquired along four profiles were processed using RES2DINV software to generate a 2D resistivity model of the subsurface materials in the project site. The generated model is represented as uninterpreted profiles (Figures 6.6-6.9). There was no topography data available, so a flat topography was assumed. During processing, five iterations were used to generate the resistivity model. Even when the number of iterations was increased the resistivity model did not change. The quality of the model was also affected by noise which is one of the problems usually encountered as a result of cultural features like electric poles; also the ground was a bit dry as can be seen from the low resistivity spot on the ERT images generated from the four profiles.

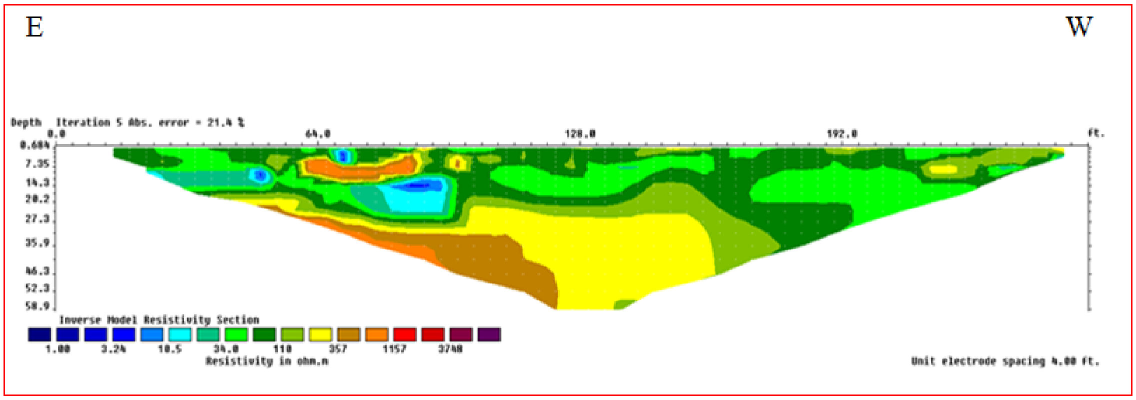

Figure 6.6. Uninterpreted ERT Profile 1

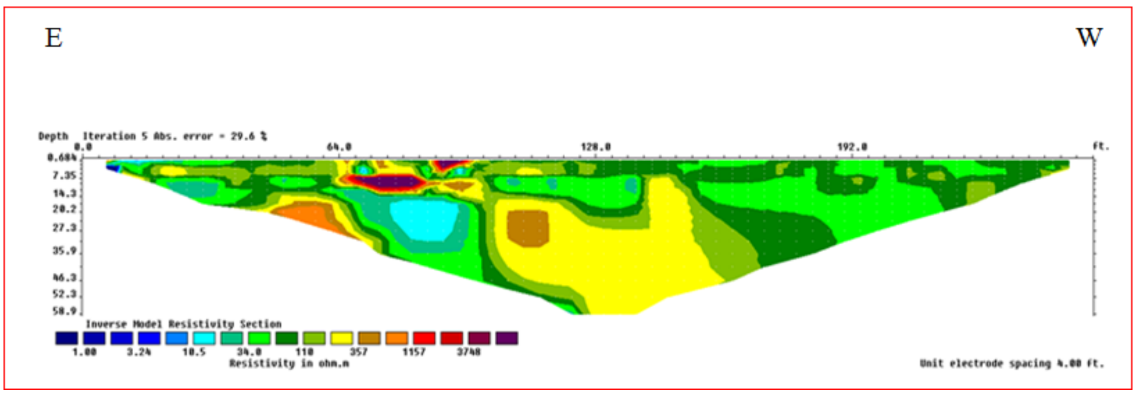

Figure 6.7. Uninterpreted ERT Profile 2

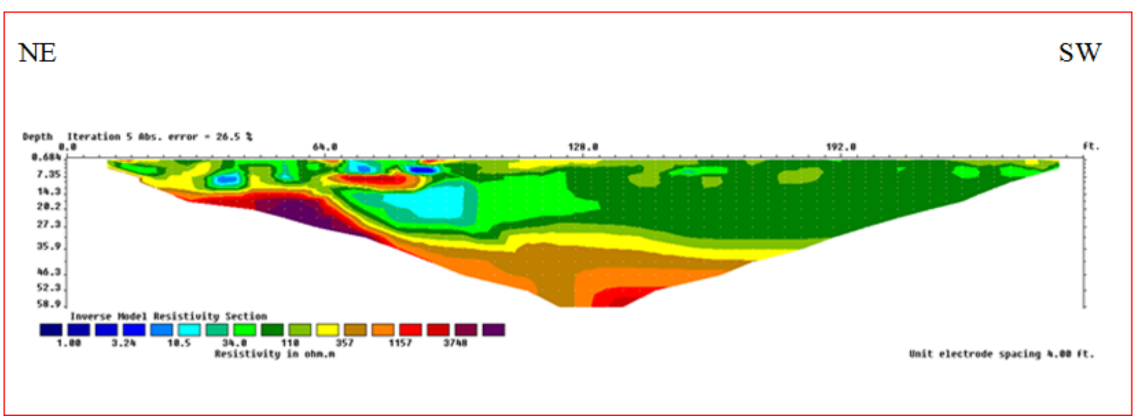

Figure 6.8. Uninterpreted ERT Profile 3

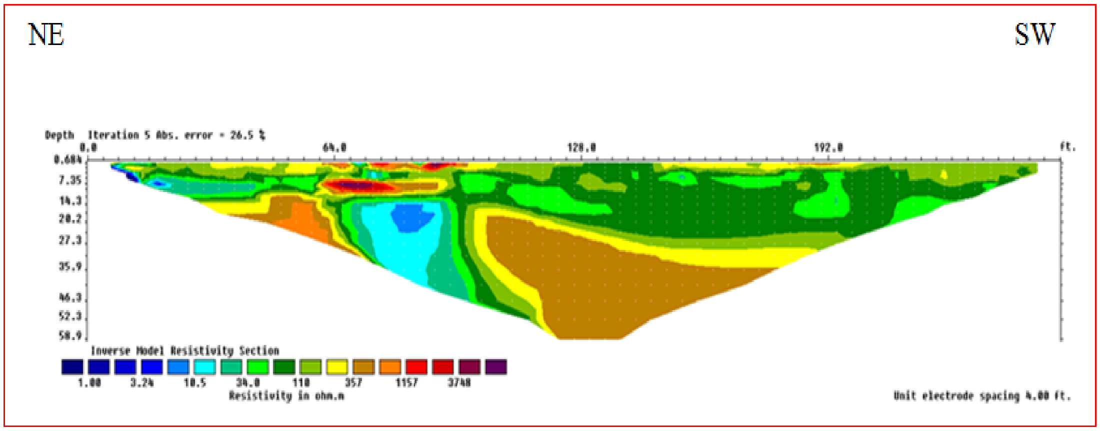

Figure 6.9. Uninterpreted ERT Profile 4

6.6. DATA INTERPRETATION

The processed electrical resistivity tomography (ERT) data were interpreted (Figures 6.10 and 6.11) using two borehole logs in immediate proximity to the area for ground truth. The borehole logs were obtained from Missouri Department of Natural Resources. The depth to top of bedrock from ERT images (110 ohm-m contour intervals) varies from 7 feet to around 45 feet, and was 30 feet from the boring logs (Figure 6.12). Some high resistivity values recorded at shallow depth was interpreted as dry soil or loose rock materials.

The low resistivity fracture zone (around 10.5 Ohm-m contour interval) was interpreted as solution-widened joint. This is the channel through which acidic surface water percolates into the subsurface and further enlarges the bedrock fractures. The channels are mostly filled with low resistivity clay-sized materials/ sediments. This process can cause ground subsidence to occur, and is basically how sinkhole collapse occurs.

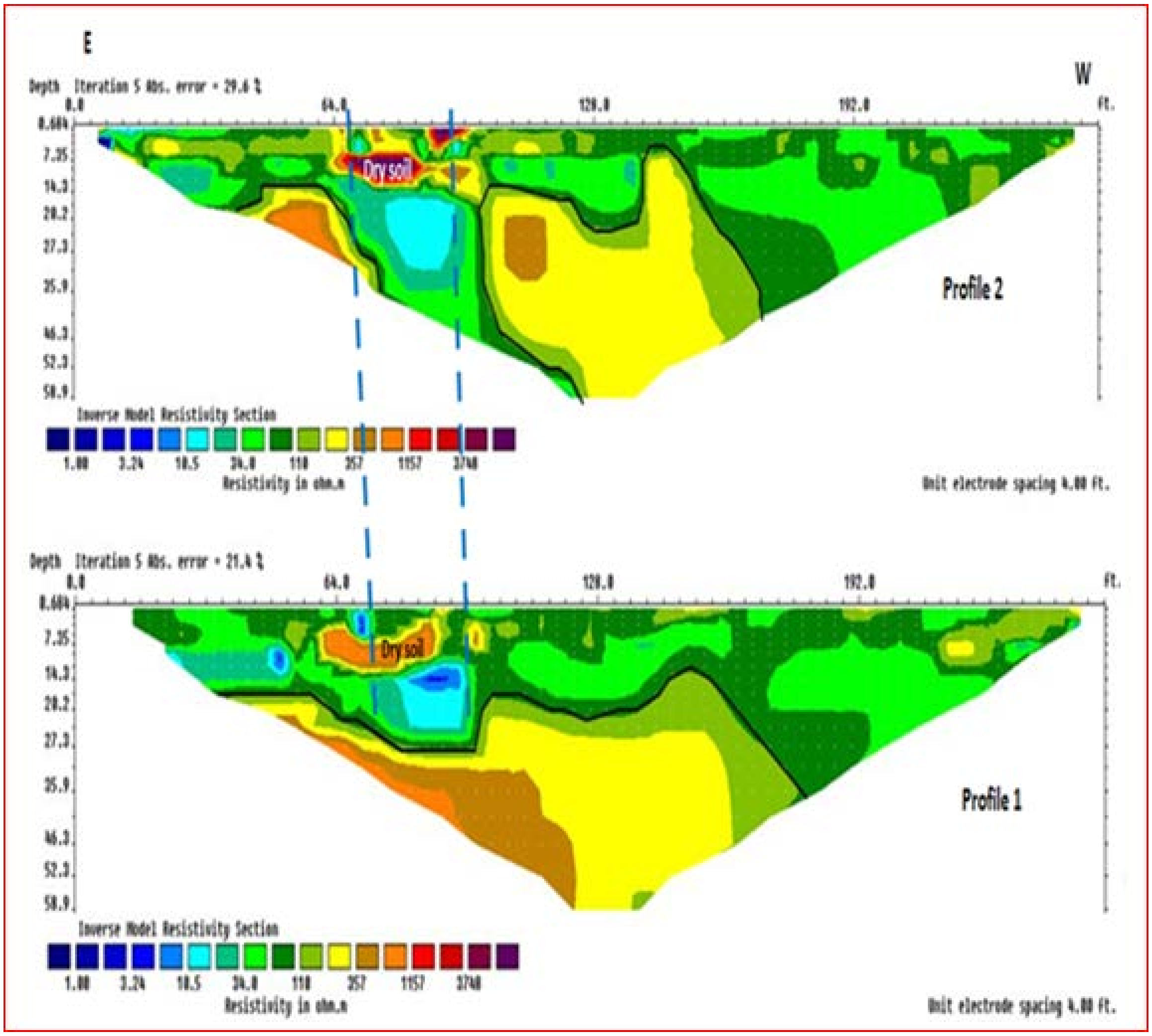

Figure 6.10. Interpreted ERT profiles 1 and 2. The black lines represent the mapped top of bedrock in the area. Top of bedrock varies from around 7 feet to 30 feet in the area. The dotted blue lines represent a set of near vertical solution-widened joints (trending S-N) indicating areas of anomalously low resistivity values of around 10.5 Ohm-m that was mapped.

The joint was mostly infilled with piped clay and low resistivity fine-grained materials. The low resistivity clay/sediment-filled zone interpreted as a set of solution-widened joints showed that moisture content was not high since the data was acquired when the ground was not wet enough. Based on the ERT images obtained, the width of the interpreted set of solution-widened joints was around 30 feet as shown.

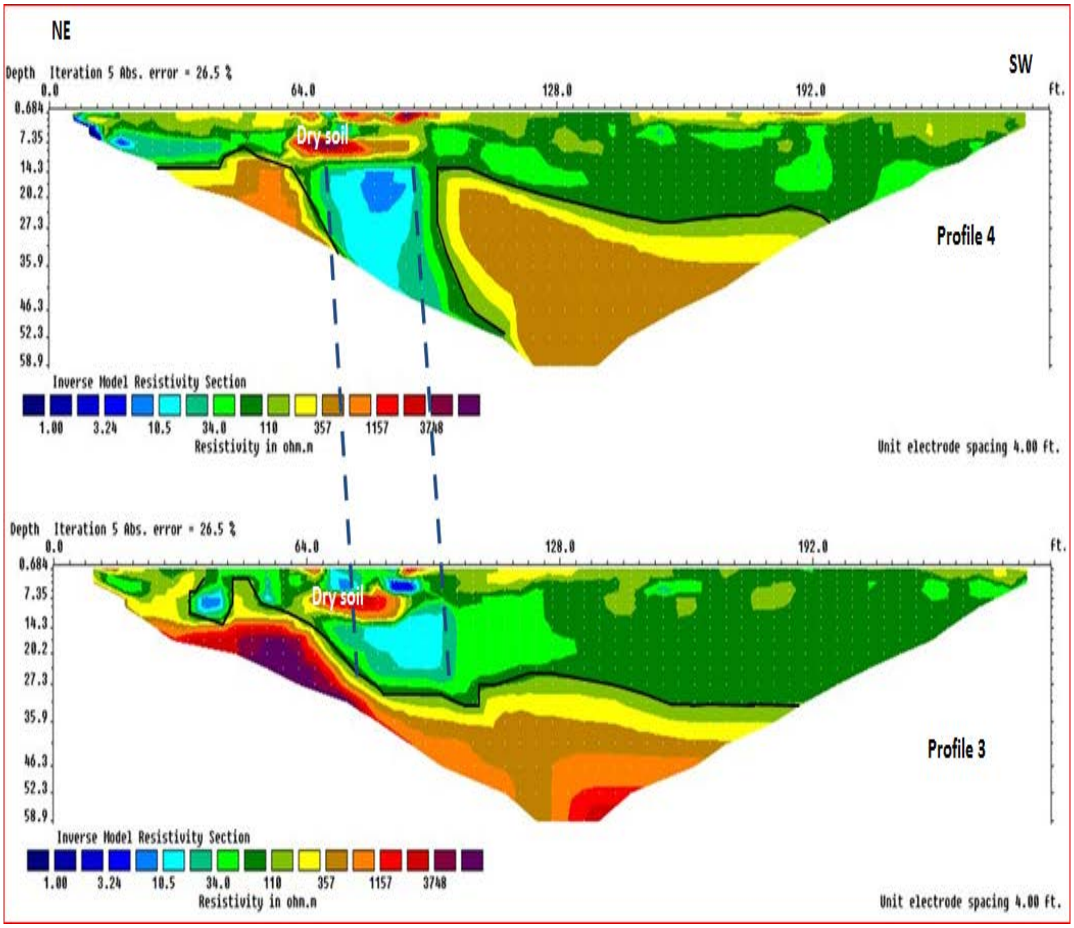

Figure 6.11. Interpreted ERT profiles 3 and 4. The black lines represent the mapped top of bedrock in the area. Top of bedrock varies from around 10 to 30 feet in the area. The dotted blue lines represent a set of solution-widened joints (trending NW-SE) indicating areas of anomalously low resistivity values of around 10.5 Ohm-m that was mapped. The joint set was mostly infilled with piped clay and low resistivity fine-grained materials.

The placements/orientations of the two sets of solution-widened joints were S-N and NW-SE. The orientation of known faults (Figure 6.13) in the area corresponds with the orientation (NW-SE) of one of the sets of solution-widened joints meaning that surface water seepage and groundwater pathways are preferentially controlled by these joints. There was a pattern observed from ERT images which showed that bedrock is shallower on the eastern part where these joints are prominent than on the western part.

This supports the fact that dissolution of carbonate rock is fast in areas where the rocks are exposed at land surface or are covered by thin layers of soil and permeable sand (solution sinkhole).

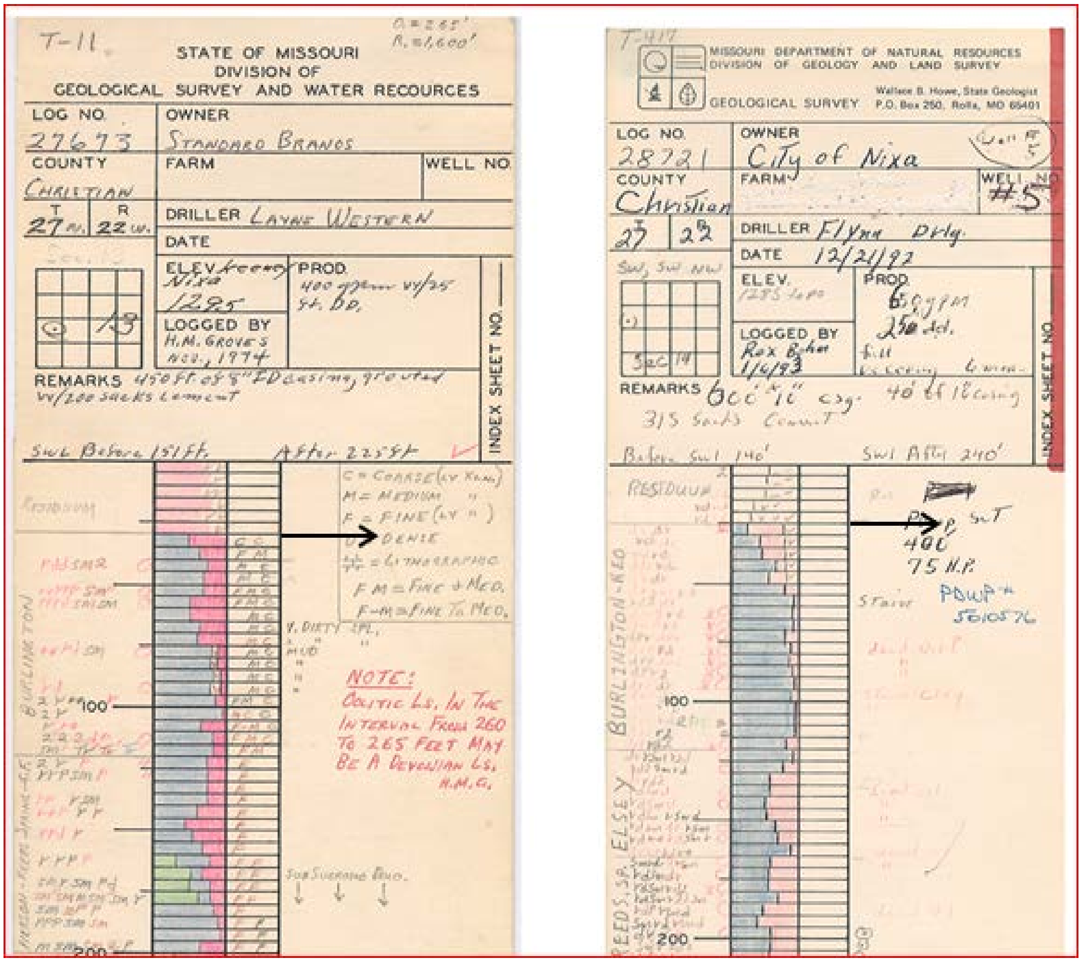

Figure 6.12. Well logs 027673 and 028721from Missouri department of natural resources (http://dnr.mo.gov/env/wrc/logmain/index.html)

Also, the images of the joint sets showed uniformity in width even at greater depths, and are characterized by low resistivity values (high conductivities). These showed that surface-run-off in the area is not constrained; hence rainwater seeps more or less uniformly into the soil and the underlying rock.

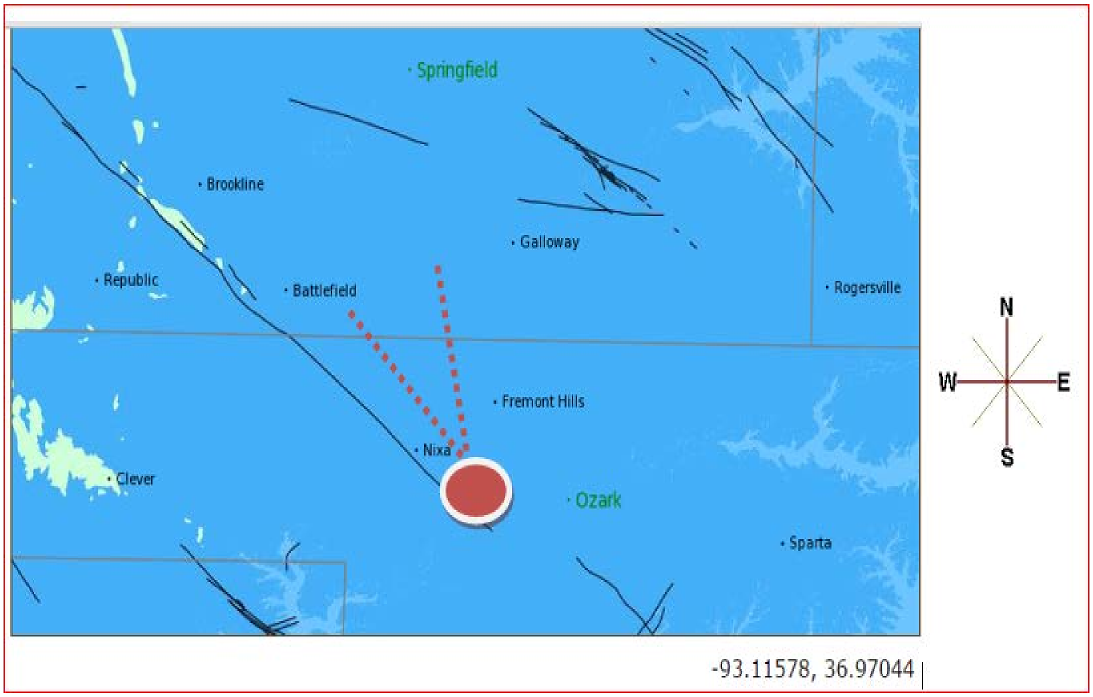

Figure 6.13. Solution-widened joints superposed on a map of known structural lineaments in Nixa (http://mrdata.usgs.gov/sgmc/mo.html).The black lines represent faults in the area. The dotted brown lines (not drawn to scale) represent the orientation of solution widened joints in the area. The circular feature represents the sinkhole. The joints trend S-N and NW-SE, and known faults in the study area trend mostly NW-SE. dened joints

6.7. CONCLUSION

Interpreted result of the study showed that the two sets of joints trending S-N and NW-SE were mapped in the area. The storm event increased surface run-off which are controlled by these joints. As a result, weak surficial materials are eroded and transported down the subsurface through these joints, resulting in cover- subsidence sinkhole. The point where these joints intersect was where the sinkhole was located. If no immediate remedial measure is taken, the sinkhole will enlarge further and become a major threat to lives and properties in the area.

7. GASCONADE RIVER CASE STUDY

7.1. ABSTRACT

Five automated electrical resistivity tomography (ERT) profiles were acquired to map solution-widened joints, voids and top of bedrock in proximity to a bridge foundation. This was necessary after a void was detected near the bridge pier during the construction of a drilled shaft.

The result of the interpreted data showed that a set of solution-widened joints trending NE-SW and E-W were mapped, the first one was orthogonal to known structural lineaments (trending NW-SE) in the area. The joints set were mostly filled by low resistivity wet sand and silt materials that are washed down to occupy the space vacated by the dissolved dolomite bedrock. Low resistivity materials which are possible karst in-fill /clay-in-fill are mostly found in the south eastern part of the profile where the bedrock is shallow indicating a possible formation of a less prominent set of solution-widened joints. The voids encountered were not massive enough to threaten the structural integrity of the bridge foundation. Depth to top of bedrock varies between 18 to 35 feet, as per driller's log.

7.2. INTRODUCTION

A structural support was needed to strengthen the load-bearing capacity of a bridge foundation located in Laclede County in South-Central Missouri. Background Information showed that the bridge was constructed in 1955 and traffic volume on the bridge was increasing. During the construction of a drilled shaft for the substructure, a few feet north of the footing of the pier 6, voids were noted beneath a roughly 2-foot-thick cap of dolomite. To characterize the site by mapping karst features like solution-widened joints, and the voids detected (vertical and lateral extent), automated electrical resistivity tomography (ERT) geophysical technique was used, supported with boring data acquired on the site. Top of bedrock and was also mapped.

7.3. SITE GEOLOGY AND DESCRIPTION

The site is located in Lebanon area in Laclede County, Missouri (Figures 7.1 and 7.2). The main geologic Formation in the site was the Roubidoux Formation which consists of sandstone, chert and some interbedded cherty dolostone (dolomite), and belongs to the Early Ordovician-Ibexian series.

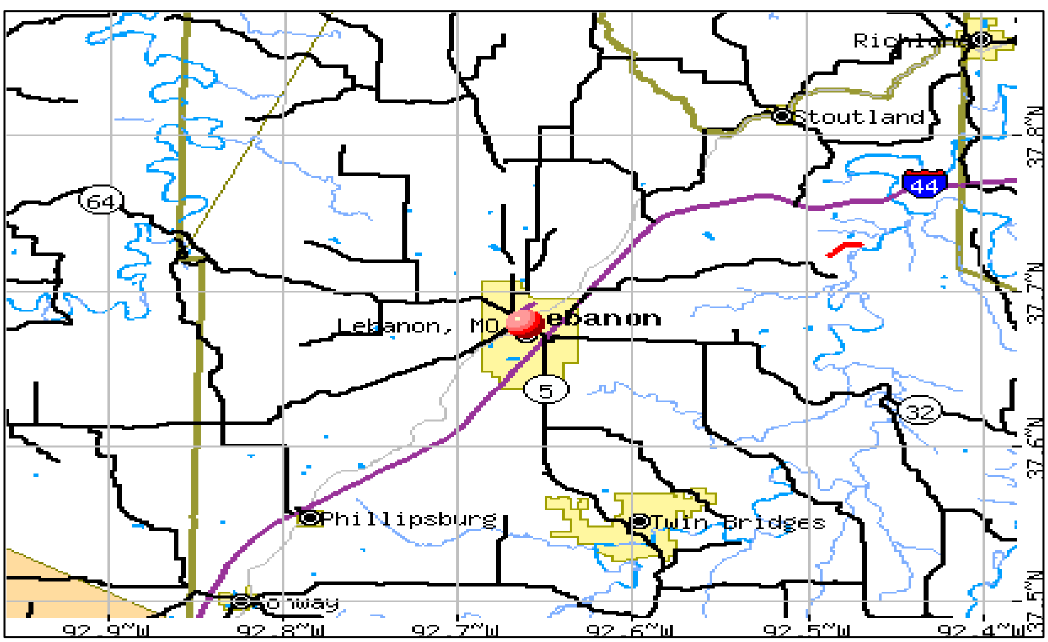

Figure 7.1. Map of the Gasconade bridge project site. The red circle marks the location of the site

Figure 7.2. Aerial photo of the project site (Google map)

The project site has an undulating topography with majority of the sloped areas covered with grasses, shrubs and trees. The area is covered mostly by alluvium; weathered or eroded particles of minerals which are transported by a river and deposited usually temporarily at points along the flood plain of a river. The alluvium consists of chert gravels and cobbles interbedded with clay, silt, and sand. The cherty residuum is developed from weathering of dolomite, chert and sandstone.

7.4. DATA ACQUISITION

Five automated electrical resistivity tomography profiles were acquired using a SuperSting R8 resistivity unit with 72 electrodes spaced at 2.5 feet (0.76m) each for a total array length of about 177.5 feet (54.1m) and depth of investigation of around 36 feet (11m). Dipole-dipole electrode array configuration was used, and the data was processed using RES2DINV software. Profiles 1, 2, 3 and 4 were acquired parallel to the bridge bents and were spaced 5 feet each, while profile 5 was acquired; crossing profiles 1, 2, 3 and 4 (Figure 7.3). Nine borings (logged) drilled at the site were used for ground-truth table (7.1).

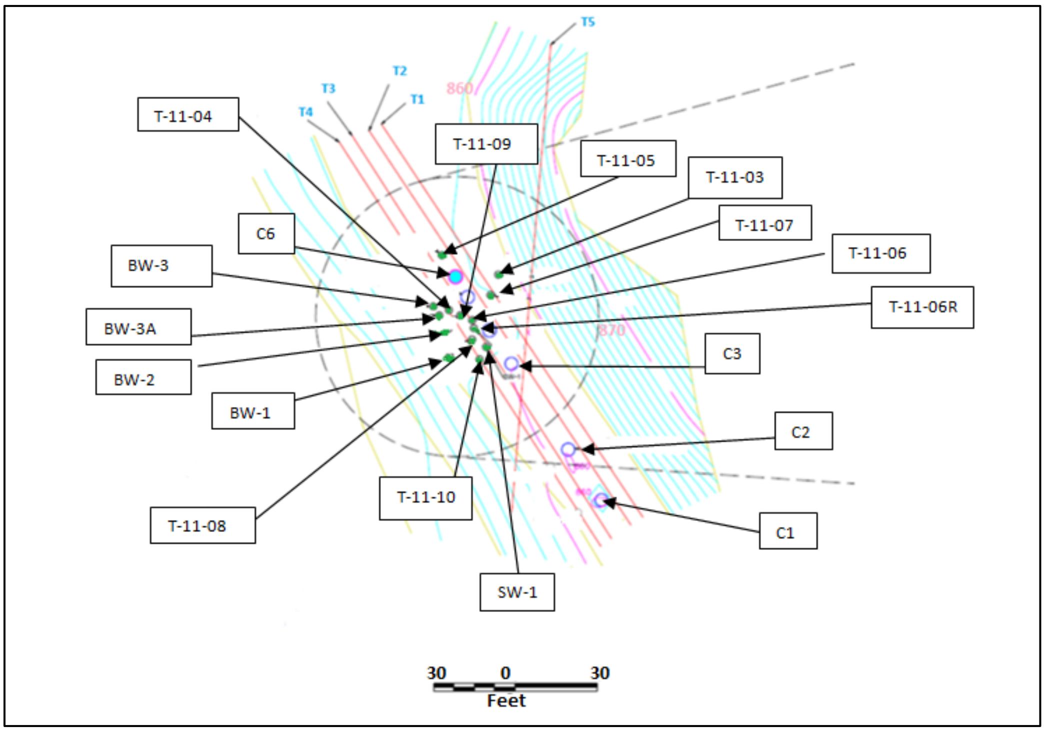

Figure 7.3. General site plan showing boring locations and ERT profiles. The green dots represent boring locations. Borings SW-1, BW-1, BW-2, BW-3 and BW- 3A are not logged. Borings T-11-03 to T-11-11 are logged. The columns (C1-C6) are represented as circles and the five profiles are represented as (T1-T5). C6 is the primary target.

The electrical resistivity tomography (ERT) survey lines were set up in such a way that the bridge columns were covered by the ERT traverses (Figure 7.4) . Also the borehles were drilled on or between the ERT traverses to give a good correlation between ERT results and the boring data which serves as a groud truth. The boring log (Table 7.1) was used to constrain the ERT interpretations.

Figure 7.4. Data acquisition under the bridge at the project site

Table 7.1. Summary of the results of the logged boreholes at the project site (from driller's log)

Borings								
T-11-03 Depth (ft.)	T-11-04 Depth (ft.)	T-11-05 Depth (ft.)	T-11-06 Depth (ft.)	T-11-07 Depth (ft.)	T-11-08 Depth (ft.)	T-11-09 Depth (ft.)	T-11-10 Depth (ft.)	T-11-11 Depth (ft.)
0-20.5 Soil	0-20.6 Soil	0-18.5 Soil	0-18.5 Soil	0-19.2 Soil	0-22.3 Soil	0-20.5 Soil	0-23.0 Soil	0-20.8 Soil
20.5-21.3 Weathered rock	20.6-21.2 Weathered rock	18.5-28 Vuggy rock	18.5-19.0 Weathered rock	19.2-28.4 Vuggy rock	22.3-22.9 Weathered rock	20.5-22.0 Weathered rock	23.0-25.2 Weathered rock	20.8-31.6 Vuggy rock
21.3-33.0 Hard rock	21.2-27.7 Void		19.0-20.7 Vuggy rock		22.9-27.4 Void	22.0-27.4 Void	25.2-34.2 Vuggy rock	
	28.0-28.5 Rock		20.7-20.9 Void		27.4-34.0 Vuggy rock	27.4-34.2 Vuggy rock		
			20.9-23.4 Vuggy rock					
			23.4-27.0 Void					
			27.0-34.2 Vuggy rock					

7.5. DATA PROCESSING

The ERT data acquired along four profiles were processed using RES2DINV software to generate a 2D resistivity model of the subsurface materials in the project site. Elevation data was not available, so a flat topography was assumed during data processing. The five ERT images generated (Figures 7.5-7.9) are shown as uninterpreted ERT profiles since no interpretation has been done.

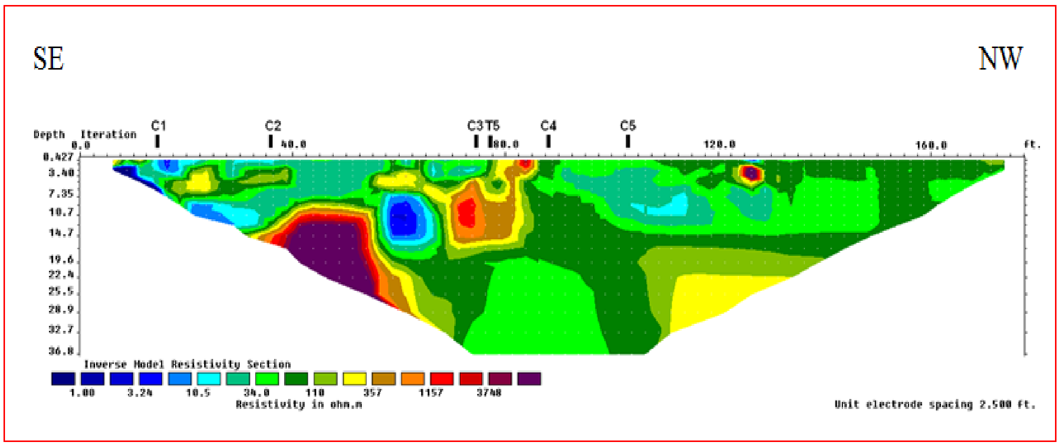

Figure 7.5. Uninterpreted ERT profile 1

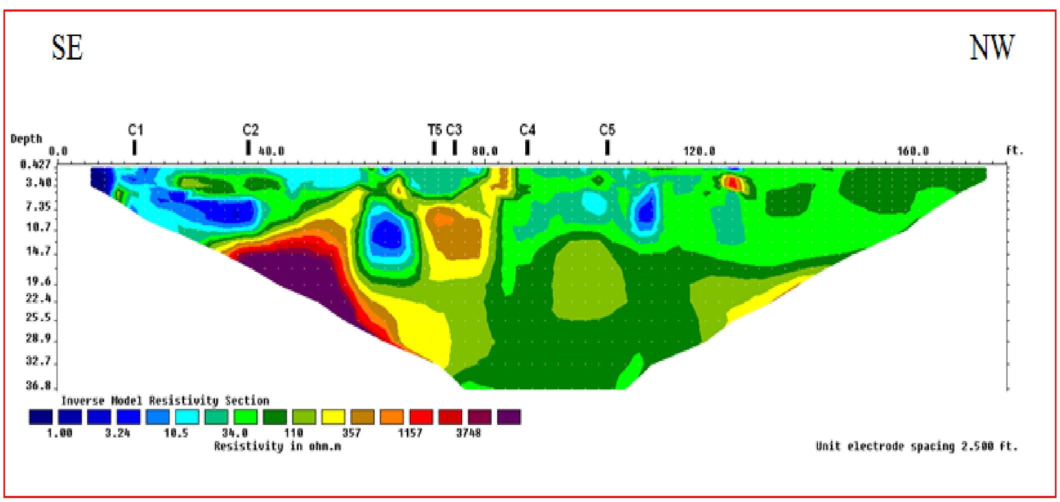

Figure 7.6. Uninterpreted ERT profile 2

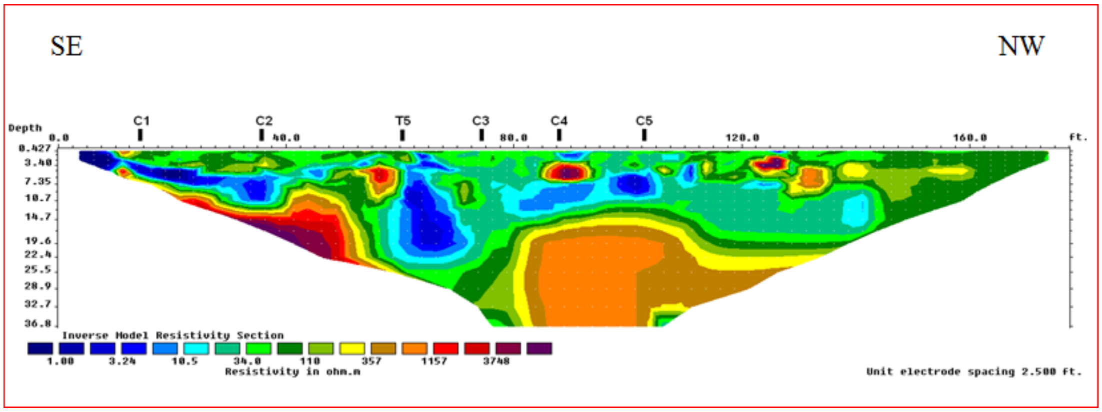

Figure 7.7. Uninterpreted ERT profile 3

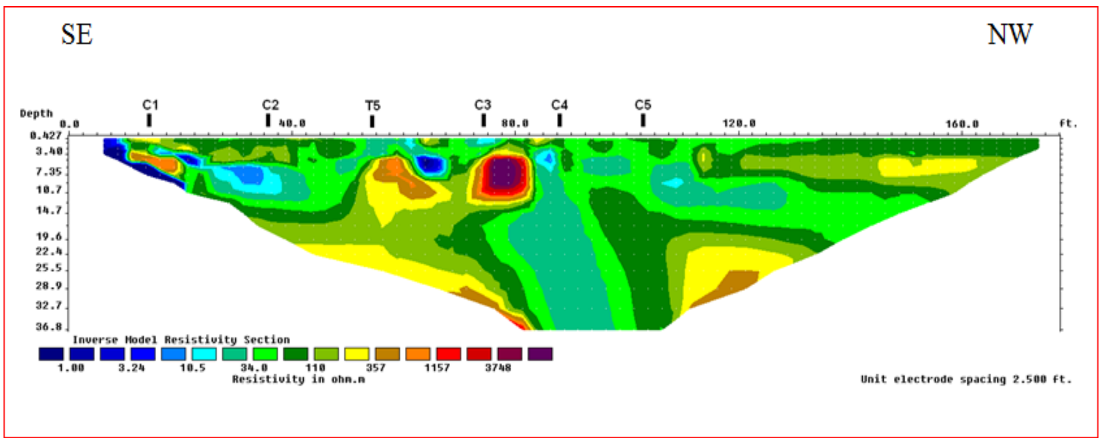

Figure 7.8. Uninterpreted ERT profile 4

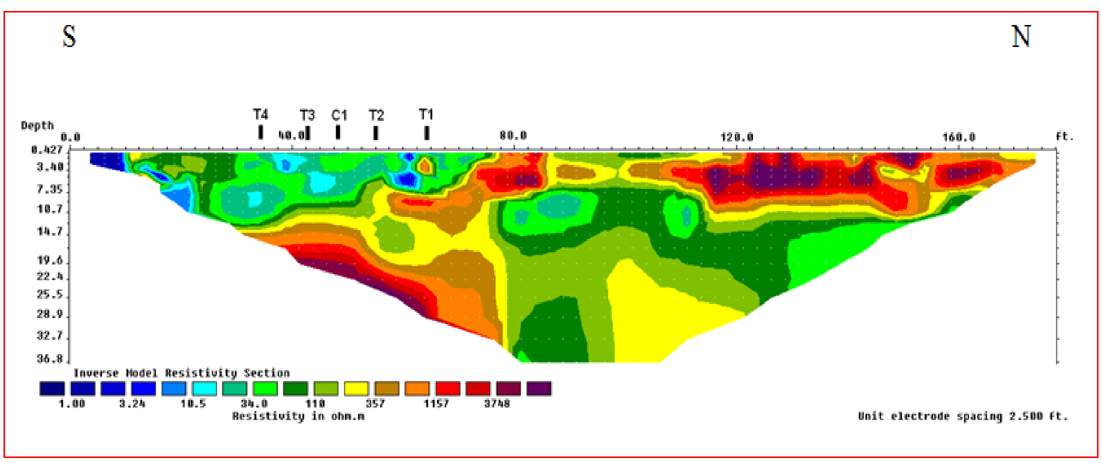

Figure 7.9. Uninterpreted ERT profile 5

7.6. DATA INTERPRETATION

Data interpretation was based on inverse model resistivity model generated (Figures 7.10 - 7.14) supported with boring log for ground truth.

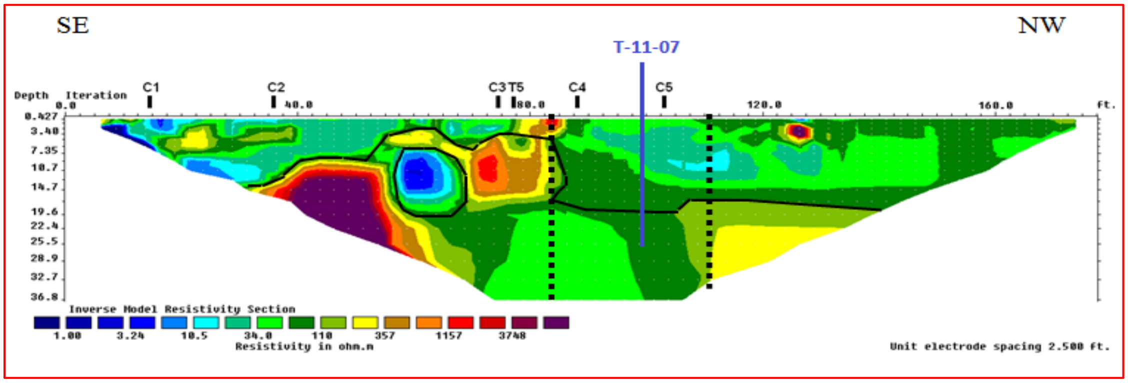

Figure 7.10. Interpreted ERT profile 1.Solid black line represents interpreted top of bedrock, dashed vertical black lines represent a lineament interpreted as solution-widened joint. T5 is the point where the profile crosses profile 5. Vuggy rock was encountered between 19.2-28.8 feet depth in boring T-11-07 represented by vertical blue line. The low resistivity (<5 Ohm-m) area in blue is interpreted as sediment/clay infill.

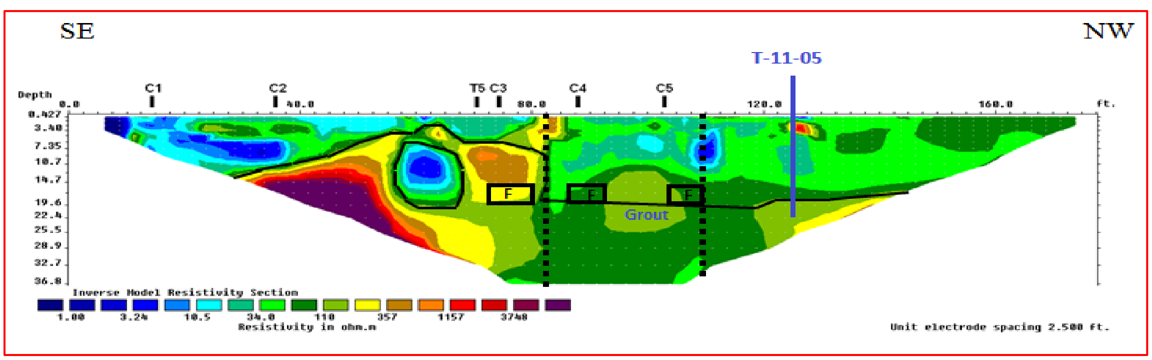

Figure 7.11. Interpreted ERT profile 2. Solid black line represents interpreted top of bedrock, dashed vertical black lines represent a lineament interpreted as solution-widened joint. T5 is the point where the profile crosses profile 5. C1, C2, C3, C4 and C5 represent the Columns. The rectangles represent the footings. The high resistivity area is interpreted as grout placed long time ago. Vuggy rock was encountered between 18.5-28 feet in boring T-11-05 represented by blue vertical line. The low resistivity (<5 Ohm-m) area shown as blue color is interpreted as sediment/clay infill.

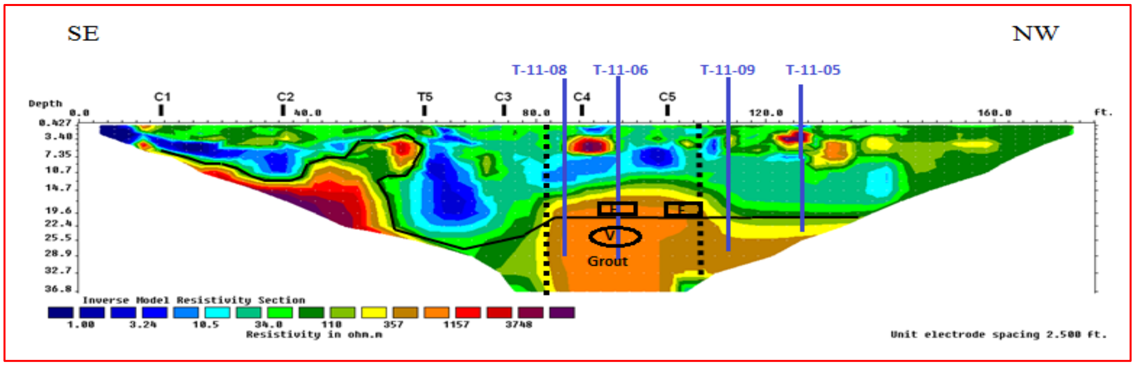

Figure 7.12. Interpreted ERT profile 3. Solid black line represents interpreted top of bedrock, dashed vertical black lines represent a structural lineament interpreted as solution widened joint. T5 is the point where the profile crosses profile 5. C1-C5 represents the Columns. Weathered rock was encountered in boring T-11-05 at a depth of about18.5feet. Voids were encountered in borings T-11-06, T-11-08 and T-11-09 at a depth of about 20.5 feet. The high resistivity zone represents grout possibly used to stabilize the voids in the past. The low resistivity (<5 Ohm-m) area shown as blue color is interpreted as sediment/clay infill.

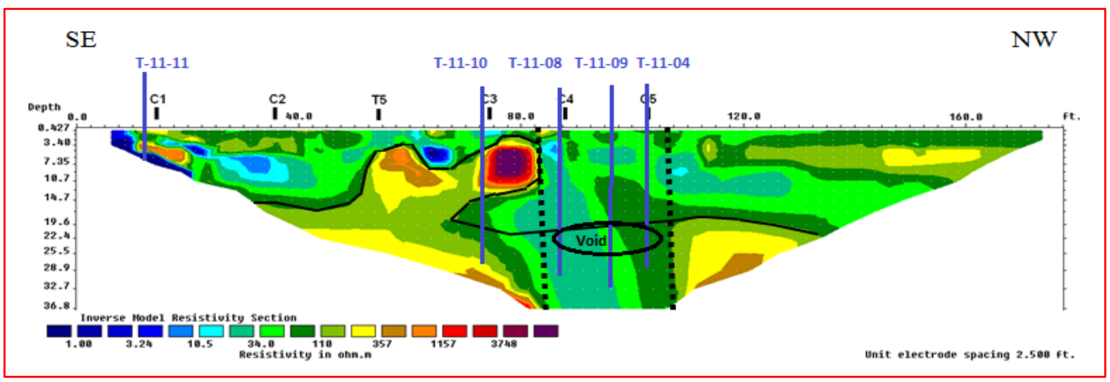

Figure 7.13. Interpreted ERT profile 4. Solid black line represents interpreted top of bedrock, dashed vertical black lines represent a structural lineament interpreted as solution widened joint. T5 is the point where the profile crosses profile 5. C1-C5 represents the Columns. Vuggy rock was encountered at about 20.8 feet in boring T-11-11; weathered rock was encountered in boring T-11-10 at a depth of about 23 feet. The oval shaped figure represents the approximate location of void encountered. Borings T-11-04, T-11-08 and T-11-09 encountered voids that are more than 5feet deep. The low resistivity (<5 Ohm-m) shown as blue color is interpreted as sediment/clay infill. The high resistivity (>3500 Ohm-m) portion around 80ft. mark is interpreted as gravel.

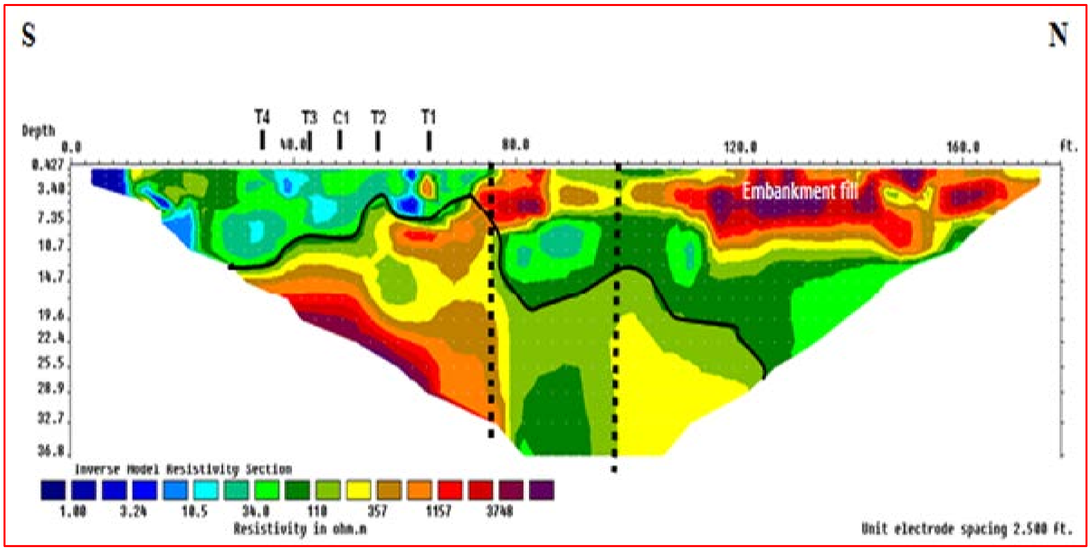

Figure 7.14. Interpreted ERT profile 5. The Profile cuts the other four profiles obliquely; T1, T2, T3 and T4 are marked as those points. The solid black line represents interpreted top of bedrock, the vertical dashed black lines represent a linear feature interpreted as solution widened joint trending W-E. Interpreted embankment fill (shown at the top right corner with high resistivity value) was encountered. Resistivity values were low at the center of the profile compared to the surrounding rocks.

The width of the interpreted set of solution-widened joint in this profile is approximately 23 feet. Depth to top of bedrock was shallow on the southern side of the ERT profile compared to the northern side, with lower resistivity clay/sediment infill. On the northern side of the profile at shallow depth was a high resistivity area which was interpreted as embankment fill based on the information from the boring logs.

To show how the lineament, interpreted as solution-widened joints, the profiles 1-4 were placed side by side (Figure 7.15). The black dotted parallel lines are interpreted as a set of solution-widened joints which are areas marked by anomalously low resistivity values. The solution-widened joints were also superposed on the location map (Figure 7.16) and known structural lineaments in the area (Figure 7.17) to show the orientation of the joints in relation to the boring locations and known faults in the area.

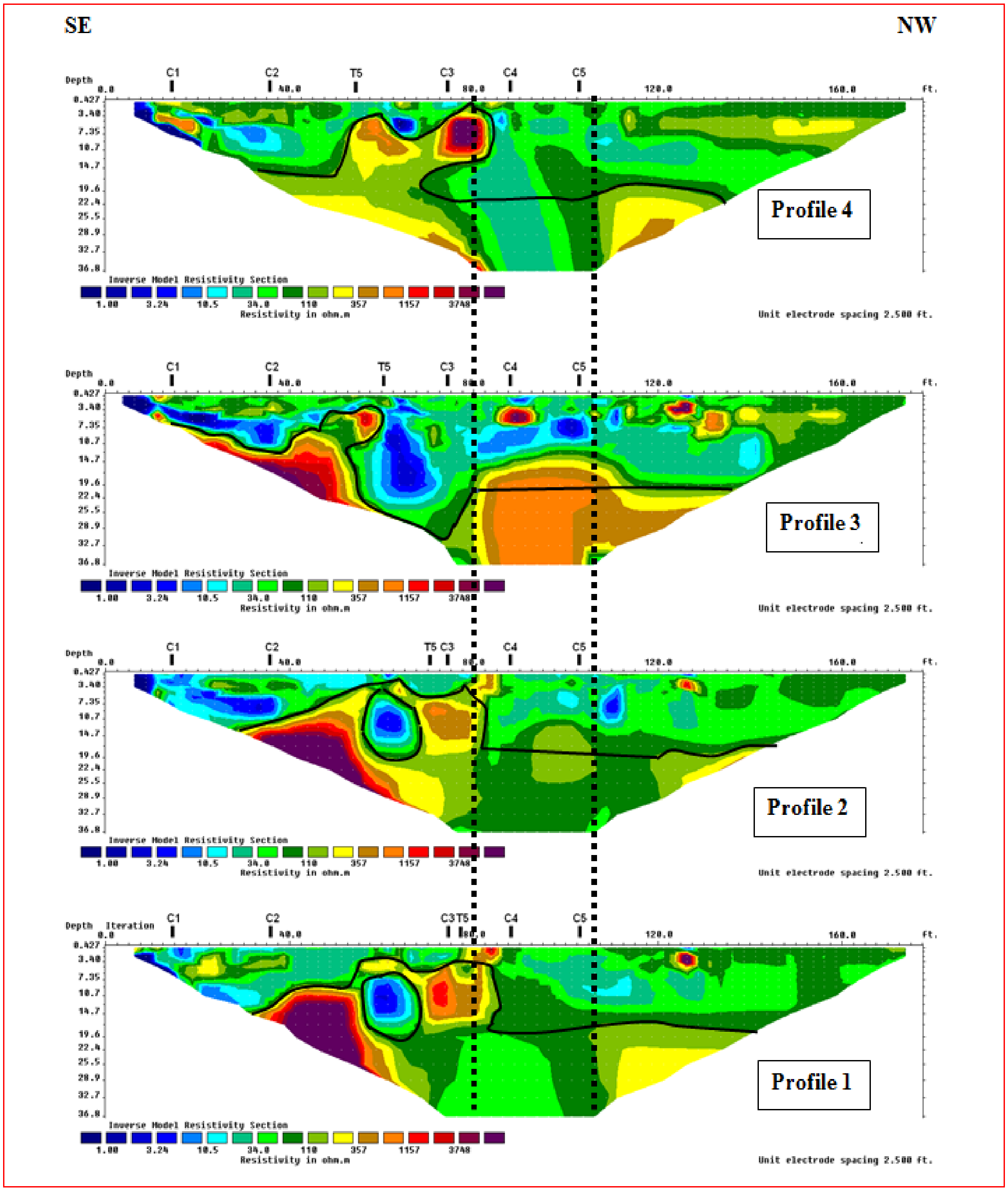

Figure 7.15. Side by side comparison of ERT profiles 1-4 showing a linear geological feature. The black dotted parallel lines are interpreted as a set of solution-widened joints which are areas marked by anomalously low resistivity values with possible sediment/clay infill. The boundary is between 85 feet and 105 feet mark. Depth to top of bedrock marked as black line is greater on the NW side of the profiles than on the SE side (bedrock dips steeply from East to West). The solution widened joint is trending SW-NE.

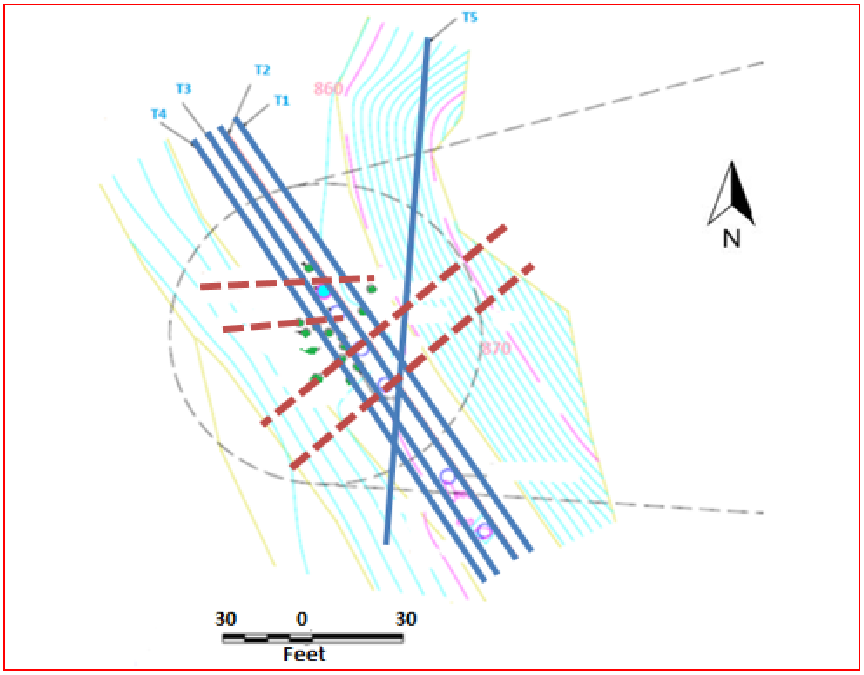

Figure 7.16. Interpreted set of solution-widened joints superposed on the automated ERT profiles with boreholes locations map. The dotted brown lines show the orientation of the mapped zone of solution-widened joints, trending SW-NE, and E-W, and the blue lines show the five ERT profiles. The green dots represent the boreholes and the circles represent the bridge foundation (Columns).

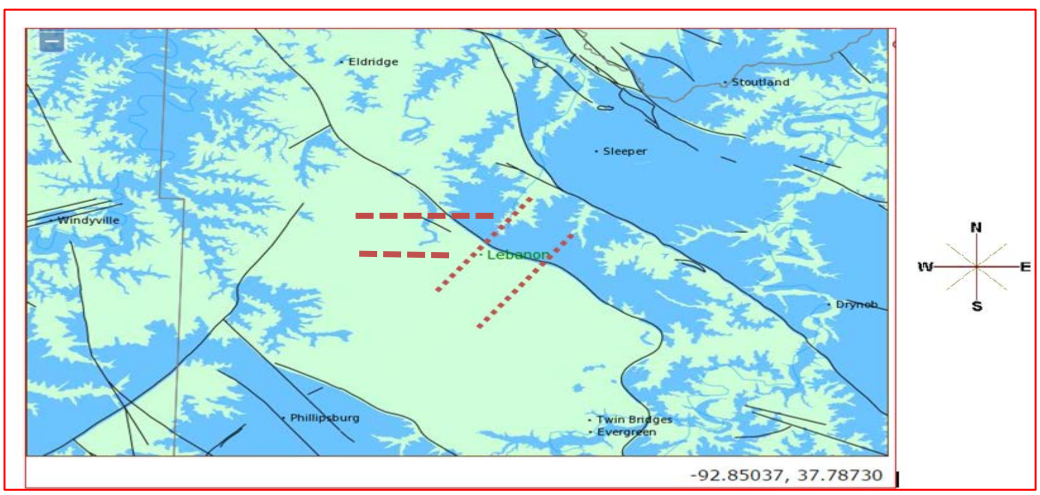

Figure 7.17. Solution-widened joints superposed on a map of known structural features in the study area (http://mrdata.usgs.gov/sgmc/mo.html). The dotted brown lines represent the solution- widened joints trending NE-SW and E-W (not drawn to scale). The black lines represent faults in the area, which are mostly trending NW-SE, though a few of them trend in other directions.

7.7. CONCLUSION

Interpreted result of automated electrical resistivity tomography (ERT) data with borehole control suggested that the orientation of the sets of solution-widened joints (NE-SW) and E-W encountered in the project site.

Known faults/ lineaments in the study area trend NW-SE. The joints are mostly filled by low resistivity wet sand and silt that are washed down to occupy the space vacated by the dissolved bedrock. The mapped joints developed most probably along horizontal bedding planes rather than vertical bedrock joints and control surface water flow direction in the area. The resistivity of rocks encountered was around 110 Ohm-m contour interval, and the low resistivity zone was interpreted as clay with resistivity value of less than 5 Ohm-m. The low resistivity materials which are possible karst in-fill are mostly found in the south eastern part of the profile where the bedrock was shallow which indicated a possible formation of a less prominent solution-widened joint set in the area. Based on the driller's log from the site, the void encountered was up to 6 feet high and up to 30 feet wide based on the ERT images. The anomalously high resistivity zone of more than 350 Ohm-m encountered on ERT profile 3 was due to the grout material placed in the area in the past, and was confirmed when the area was drilled. Also, the voids encountered were not massive enough to threaten the structural integrity of the bridge foundation, and information obtained from the drilling crew in that site revealed that only about 22124 cubic feet (81.94 cubic yards) of grout was used to stabilize the ground around the structure. This also indicated that the encountered voids/rock openings were not that large based on the volume of grout used to stabilize the ground around the structure.

8. AURORA CASE STUDY

8.1. ABSTRACT

Six automated electrical resistivity tomography (ERT) profiles supported with multichannel analysis of surface waves (MASW) data were acquired to map an area where sinkhole developed in a parking lot. Sixty eight (68) electrodes and dipole-dipole array were used for ERT data acquisition with electrode spacings varying from 3, 4 and 5 feet. Multichannel analysis of surface waves (MASW) data were acquired with geophone spacing of 2.5 feet and 20Lb sledge hammer.

Interpreted data showed that the sinkhole formed as a result of preferential dissolution of the limestone bedrock along joints and bedding planes. Known structural lineaments around the area trend W-E and NW-SE, and conform with the trends of two of the three interpreted solution-widened joints from ERT. It was possible that past activities near the site such as the abandoned Zin mine and the removal of a large sycamore tree during the construction of the parking lot contributed to the development of the sinkhole. There was a pattern observed where low resistivity clay-filled voids are mostly circular in shape. This type of circular pattern is mostly linked to cover-collapse sinkhole.

8.2. INTRODUCTION

A sinkhole developed in a motor pool parking lot in Aurora Missouri, and there was need to remediate the sinkhole to avoid further development. Prior to the construction of the park, the area was covered with grasses. Close observation of the sinkhole showed that under a space of 2 days, the width has increased from 2 feet to 8 feet with a depth of around 10 feet, and was filled with water up to 3 feet down the hole. Initial site assessment and background information showed that part of the project site was a Zinc mine in the past (1950's). Also a large Sycamore tree was removed from this area the construction of the parking lot. Geophysical investigation was needed to locate the voids and map the fractures (joints) controlling the development of the sinkhole so that suitable remediation measure would be taken.

8.3. SITE GEOLOGY AND DESCRIPTION

The project site is located in Aurora (Figure 8.1), Lawrence County Missouri. The geologic unit in the area belongs to the Osagean Series and Mississippian System, and consists mainly of Keokuk limestone with chert and clay. Other rock Formations in the area are Burlington Limestone, Elsey Formation or Grands Falls Formation, Reeds Spring Formation, Pierson Limestone and Fern Glen Formation. The sinkhole that was assessed (Figure 8.2), developed on this formation.

Figure 8.1. Map of the project area from Google; the site is shown as a red figure in the center

Figure 8.2. Mapped Sinkhole in the parking lot

8.4. DATA ACQUISITION

Six automated electrical resistivity tomography (ERT) and two multichannel analysis of surface waves (MASW) profiles (Figure 8.3) were acquired to cover the area where the sinkhole was located. Sixty eight (68) electrodes and dipole-dipole array were used for data acquisition with electrode spacings varying from 3, 4 and 5 feet. Also, multichannel analysis of surface waves (MASW) data with electrode spacing of 2.5 feet were also acquired to supplement the ERT data (Figure 8.4).

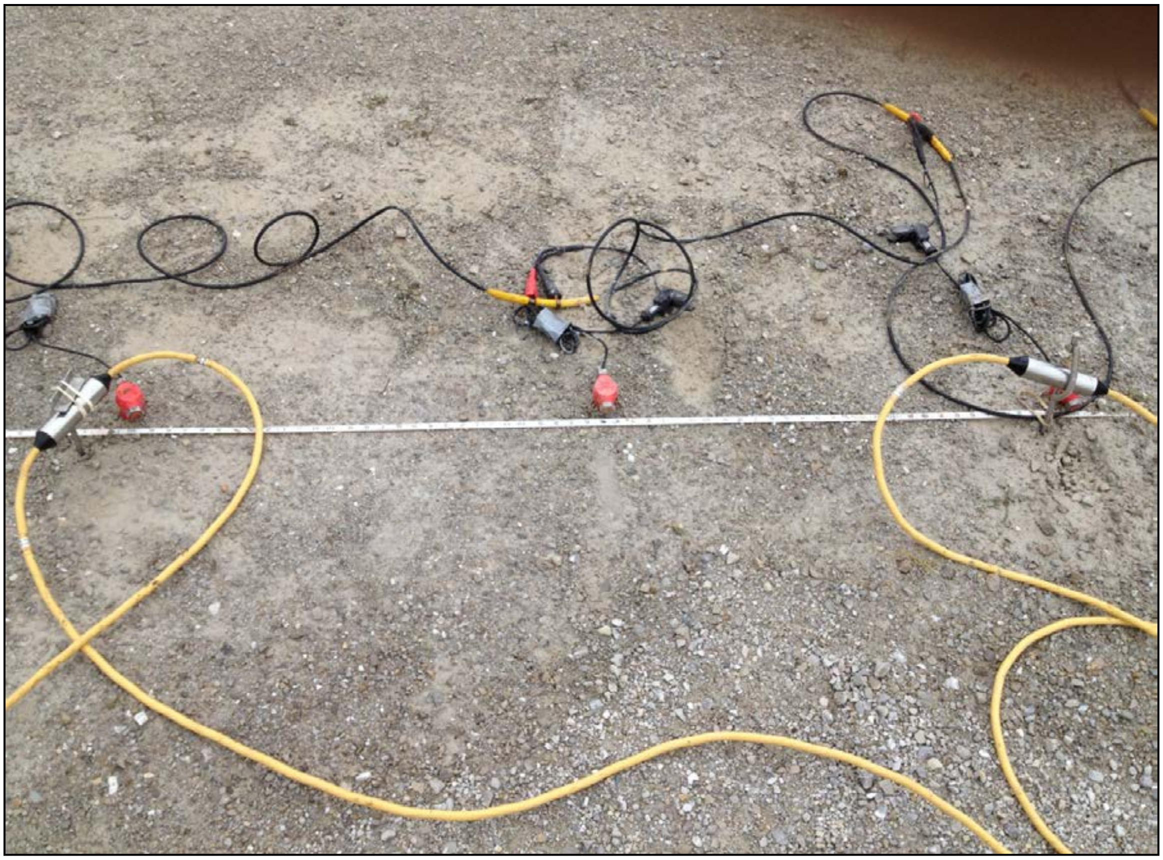

Figure 8.3. ERT and MASW field layout during data acquisition

It was difficult to pound in the metal stakes for automated electrical resistivity tomography (ERT) due to the nature of the terrain (parking lot). Also water were poured sufficiently to the ground to ensure a good electrode contact between the ground and the metal stakes. Geophones used for multichannel analysis of surface waves (MASW) data acquisition were relatively easy to insert into the ground.

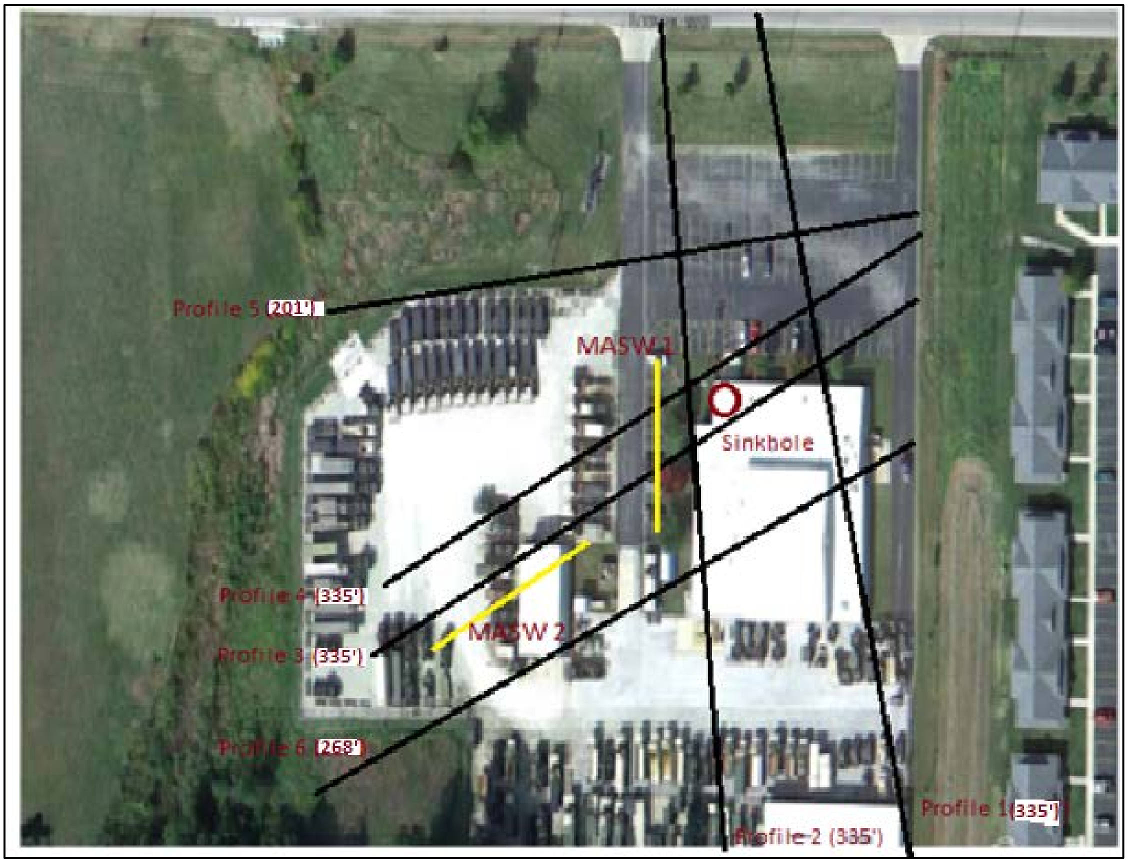

Figure 8.4. Map of the compound (Google Earth) showing the locations of the ERT profiles

8.5. DATA PROCESSING

The automated electrical resistivity (ERT) data acquired were processed using RES2DINV software to generate resistivity models of the subsurface at the location. Six ERT models (Figure 8.5) were generated. Also, multichannel analysis of surface waves (MASW) data acquired were processed using SurfSeis3 software to generate 1-D shear wave velocity profiles of subsurface materials (Figures 8.6 and 8.7) at the location to supplement ERT data.

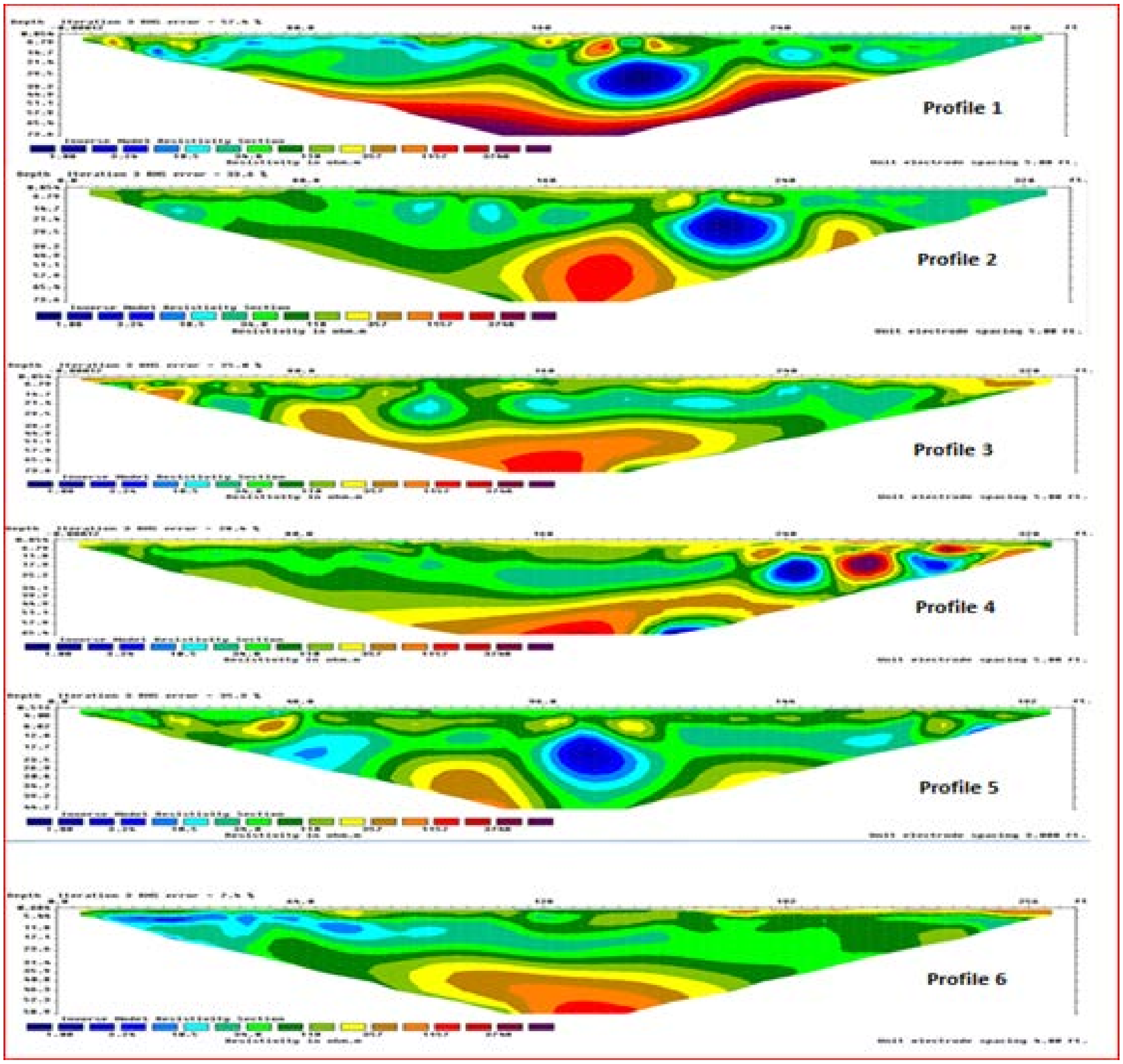

Figure 8.5. Uninterpreted ERT profiles 1-6

The automated electrical resistivity tomography (ERT) profiles shown do not mean that they were all oriented in the same direction. Profiles 1 and 2 were oriented S-N, profiles 3, 4 and 6 were oriented SW-NE while profile 5 was oriented W-E. Profiles 1 and 2 show a very similar resistivity model. The resistivity models remained unchanged after 3 to seven iterations were tested. So, all of the six automated electrical resistivity tomography (ERT) profiles were generated at 3 iterations to save processing time.

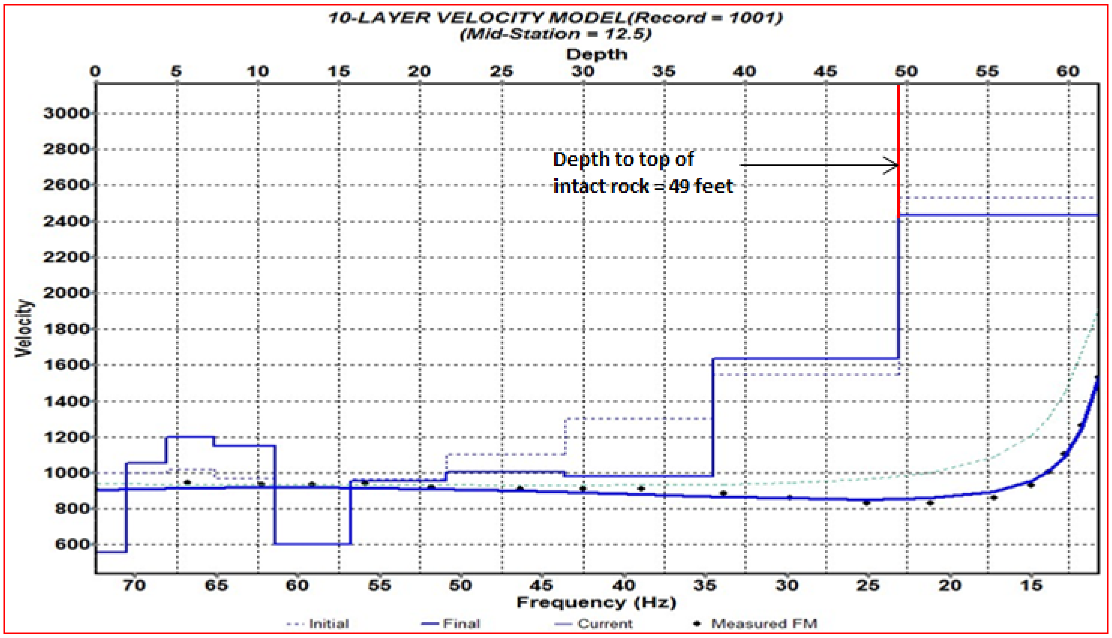

Figure 8.6. 1-D shear wave velocity model generated (MASW 1). Data were acquired at station 150 on ERT profile 2. Depth to top of intact bedrock was 49feet

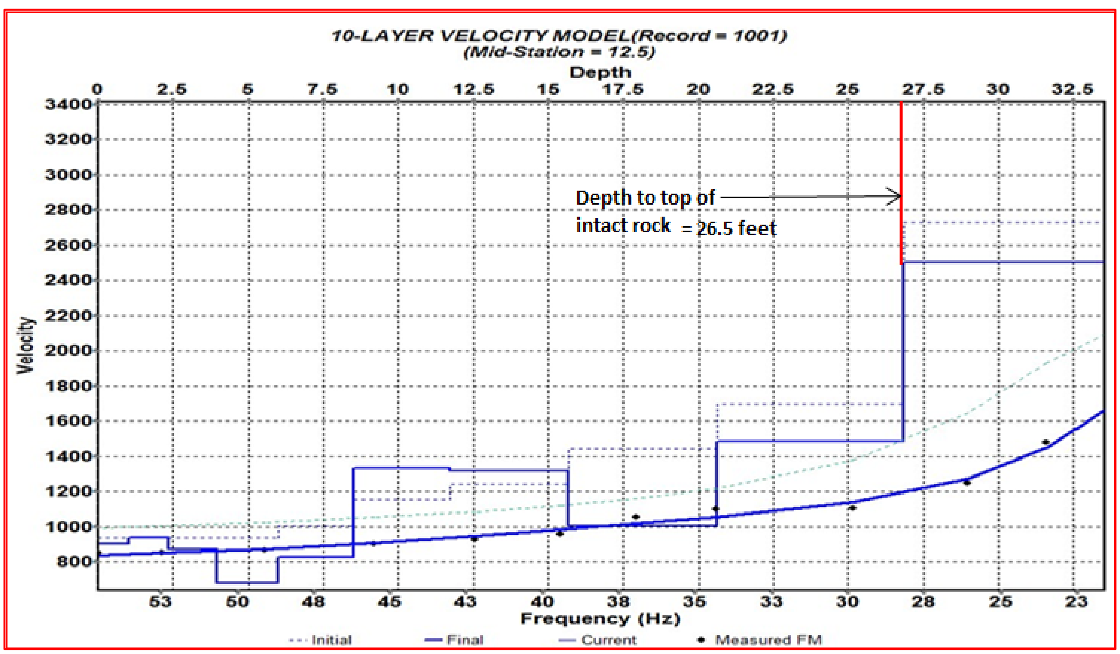

Figure 8.7. 1-D shear wave velocity model generated (MASW 2). Data were acquired at station 100 on ERT profile 3. Depth to top of intact bedrock was 26.5 feet

8.6. DATA INTERPRETATION

From the generated ERT and MASW profiles, top of bedrock, solution-widened joints and clay were mapped and interpreted (Figures 8.8, 8.9 and 8.10). Vertical lines represent interpreted solution-widened joints; black lines represent top of bedrock and the low resistivity blue spots represent clay/sediment infill.

The mapped solution-widened joints were superposed on a map of known structural lineaments in the area (Figure 8.11) to show the orientation of the mapped features in relation to the lineaments. Known structural lineaments around the area trend W-E and NW-SE, and conform with two of the three interpreted solution-widened joints from the ERT profiles.

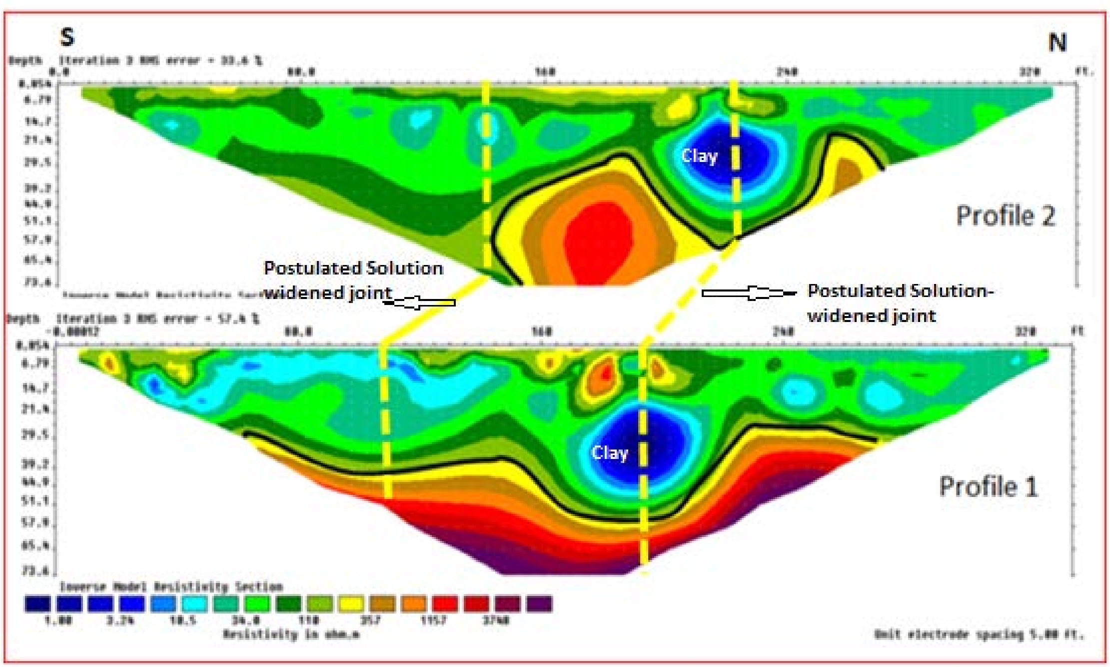

Figure 8.8. Interpreted ERT profiles 1 and 2. The dotted yellow lines represent solution-widened joints trending W-E, and the blue spots represent low resistivity clay-filled openings. MASW data acquired (MASW1) at station 150 on ERT profile 2 showed interpreted top of intact bedrock at a depth of around 49 feet, and around 45 feet on ERT profile 2.

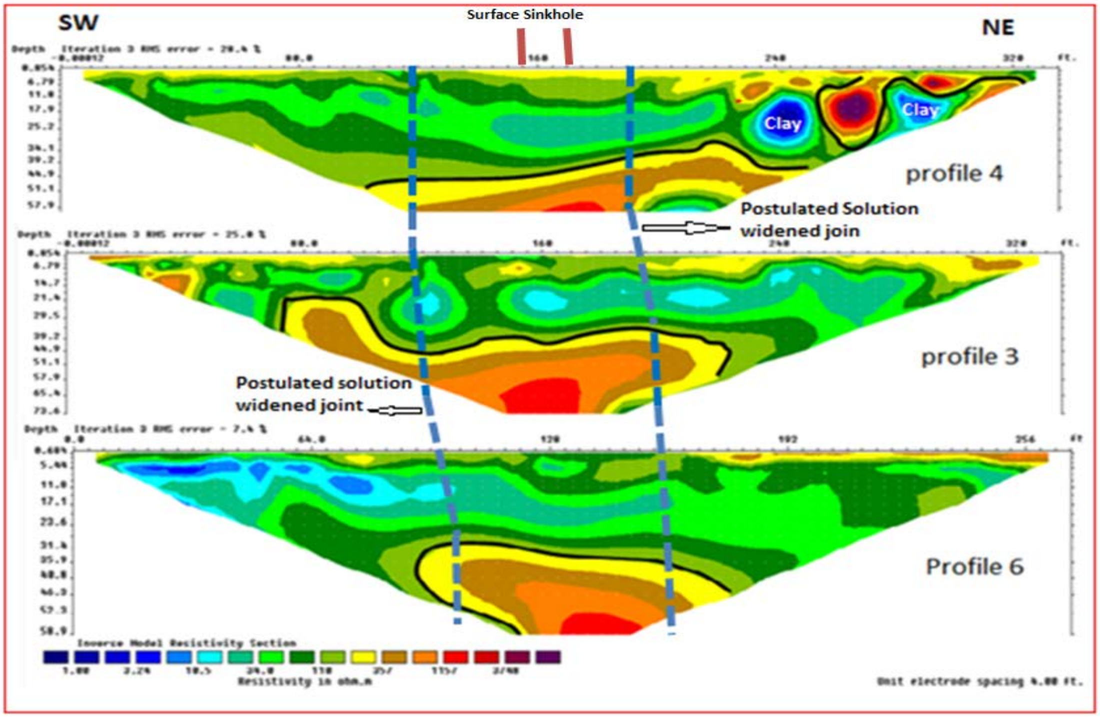

Figure 8.9. Interpreted ERT profiles 3, 4 and 6 nearly parallel to one another. The dotted blue lines represent a set of solution-widened joints trending NW- SE, and the blue spots represent low resistivity clay-filled openings. The two vertical brown lines represent the position of the sinkhole. MASW data acquired (MASW 2) at station 100 on ERT profile 3 showed interpreted top of intact bedrock at a depth of around 26.5 feet, and around 28 feet on ERT profile 3.

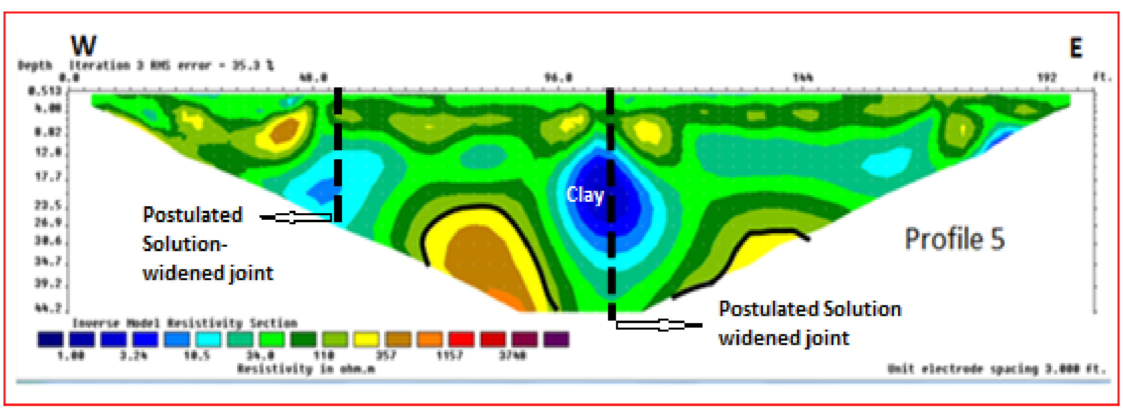

Figure 8.10. Interpreted ERT profile 5. The thick dotted black lines represent a near-vertical solution-widened joints trending N-S, black lines represent top of bedrock and the blue spots represent low resistivity clay-filled openings.

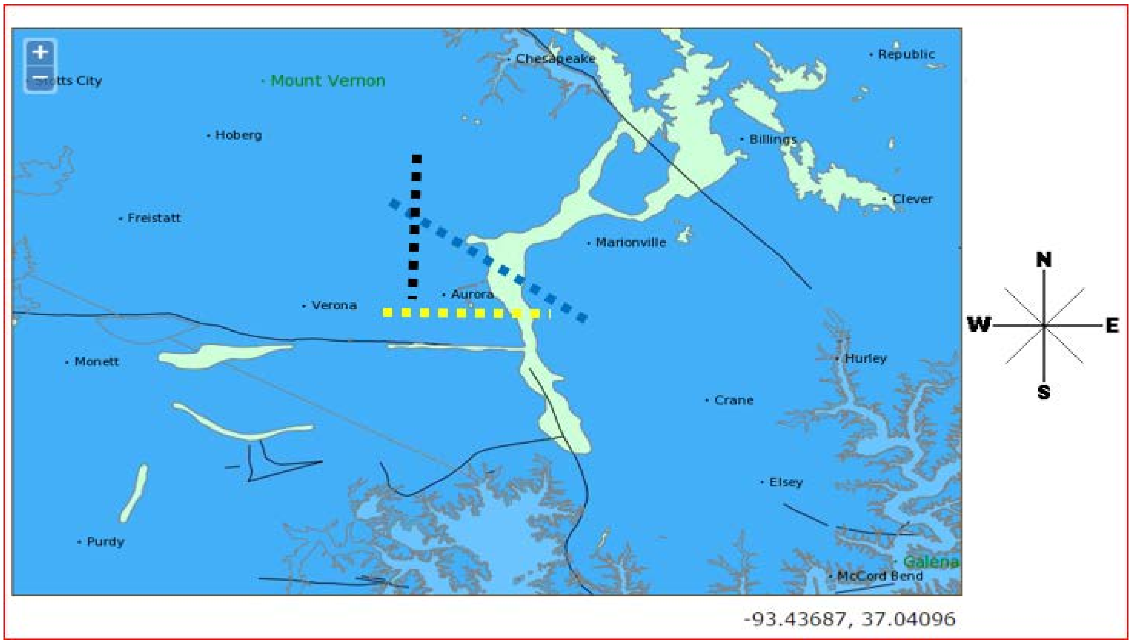

Figure 8.11. Mapped solution-widened joints superposed on a map of known structural lineaments in the project area (USGS). The lineaments are not localized in the project area. The joints are shown as dotted lines (yellow, black and blue). Known structural lineaments around the area trend W-E and NW-SE, and they conform with two of the three interpreted solution-widened joints from ERT.

8.7. CONCLUSION

Interpreted data showed that the sinkhole formed as a result of preferential dissolution of the limestone bedrock along joints and bedding planes. Known structural lineaments around the area trend W-E and NW-SE, and they conform with two of the three interpreted solution-widened joints from ERT. It is possible that past activities near the site such as the abandoned Zinc mine and the removal of a large sycamore tree during the construction of the parking lot contributed to the development of the sinkhole. There was a pattern observed where low resistivity clay-filled voids are mostly circular in shape. This type of circular pattern is mostly linked to cover-collapse sinkhole.

9. PROTEM CASE STUDY

9.1. ABSTRACT

Four automated electrical resistivity tomography (ERT) profiles were acquired parallel to one another and about 40 feet apart to map subsurface fractures in the site. The site would be used for building construction in future. Interestingly, there was a sinkhole around the area that gets filled with water during rainfall but drains immediately after rainfall.

Interpreted ERT results showed a set of solution-widened joints trending NE-SW direction which was interpreted as a stream channel through which the nearby sinkhole recharges a creek in the area. The joints are in-filled with low resistivity loose soil and rock materials. There was no structural lineaments shown in immediate proximity to the area from USGS data to know whether the solution-widened joints follow the trend of the lineaments or not. So, bedrrock dissolution was controlled by these joints and depth to top of rock was between 10-20 feet. The presence of the stream channel would be a concern and needs more detailed geotechnical investigations.

9.2. INTRODUCTION

The aim of the study was to map karst features in the project site and determine the orientation of fractures that control surface and groundwater flow in the site using automated electrical resistivity tomography (ERT) technique and boring control. An interesting feature around the project area was the presence of a sinkhole which holds water immediately after rainfall but does not hold it for a long time.

9.3. SITE GEOLOGY AND DESCRIPTION

The study site is located in Protem, Taney County in Missouri; about ten miles north of the Arkansas state line (Figure 9.1). The area is a flat field covered by grasses and shrubs. There are a lot of trees surrounding the creek near the site (Figure 9.2). The primary bedrock in the area is Smithville dolomite of Early Ordovician with thin beds of sandstone and shale. There was a sinkhole up to 5 feet deep and 6 feet wide around the project area.

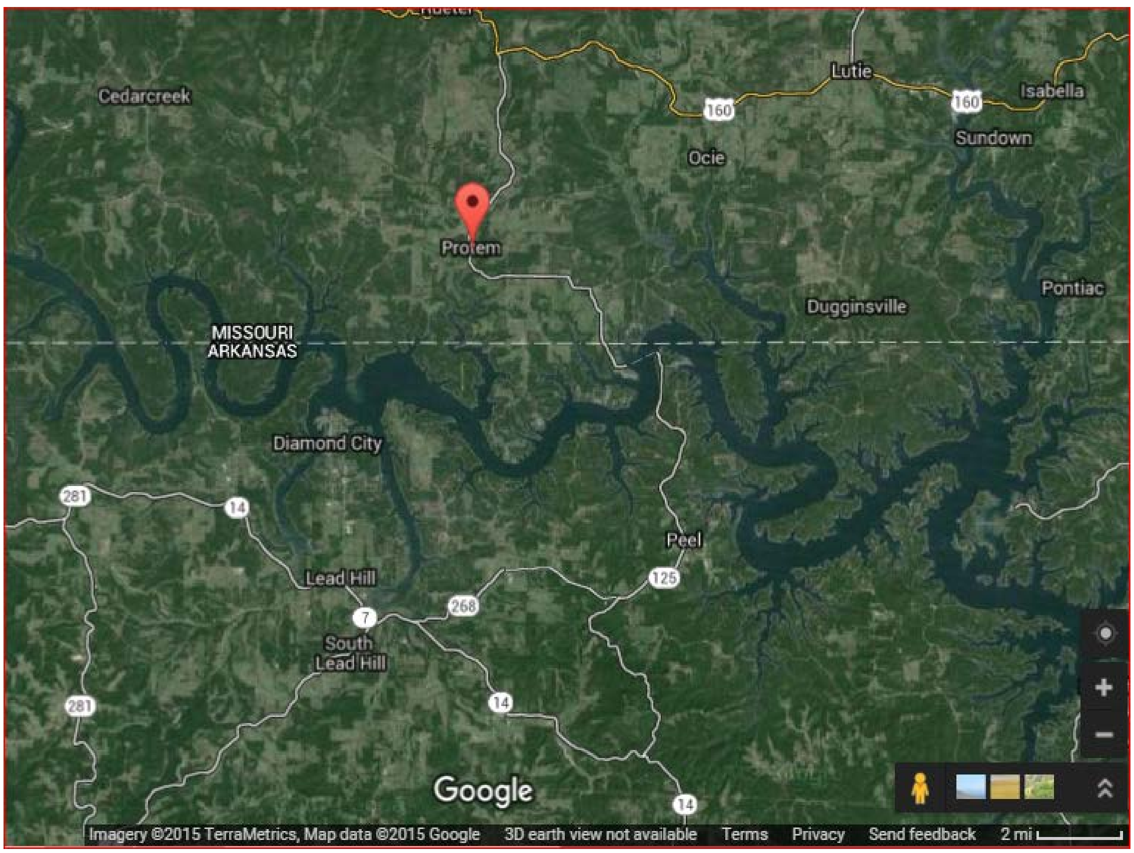

Figure 9.1. Study site location. The site is represented by the red object, and was very close to Missouri-Arkansas boarder.

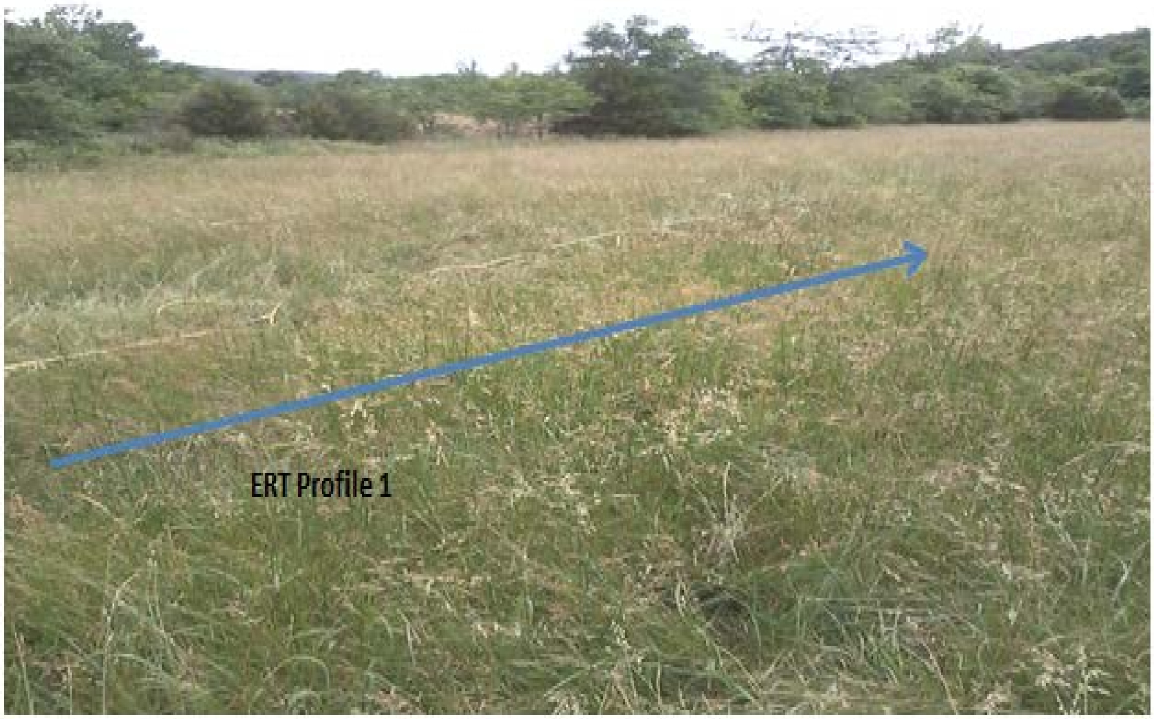

Figure 9.2. The study site showing electrode cables used for ERT data acquisition

9.4. DATA ACQUISITION

Four automated electrical resistivity tomography (ERT) profiles were acquired parallel to one another and about 40 feet apart. Eighty four electrodes were used, and spaced at 5 feet intervals to give a profile length of 435 feet each. Dipole-dipole electrode configuration was used.The orientation of the profiles was NW-SE.

9.5. DATA PROCESSING

The acquired data were processed using RES2DINV software to generate a 2-D resistivity model that represents the geology of subsurface materials in that particular area. The data were of good quality with minimal RMS error (Figures 9.3-9.6). There was no elevation data, so the topography was assumed to be flat. But generally, it was a flat farmer's field.

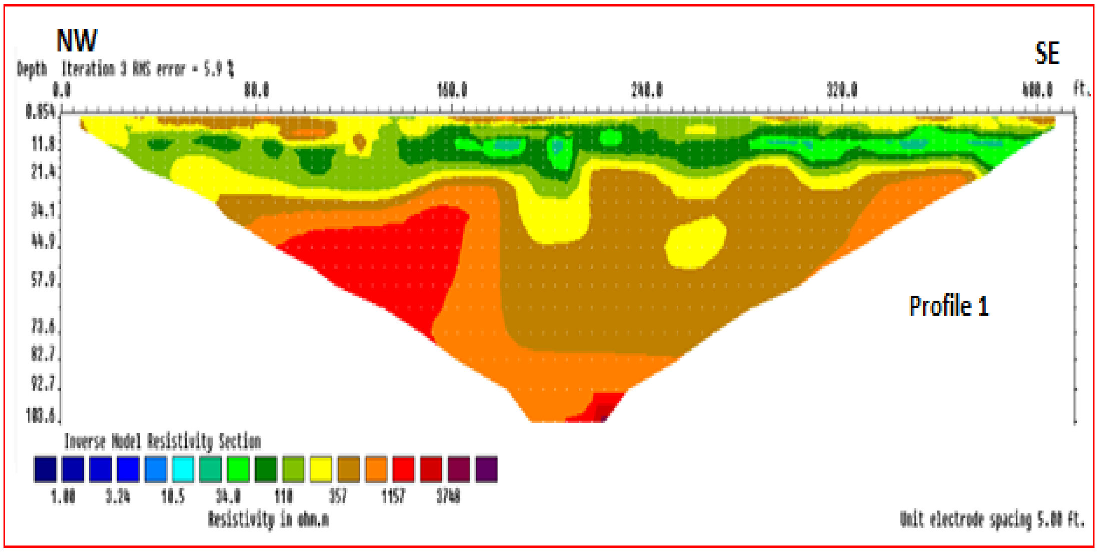

Figure 9.3. Uninterpreted ERT profile 1

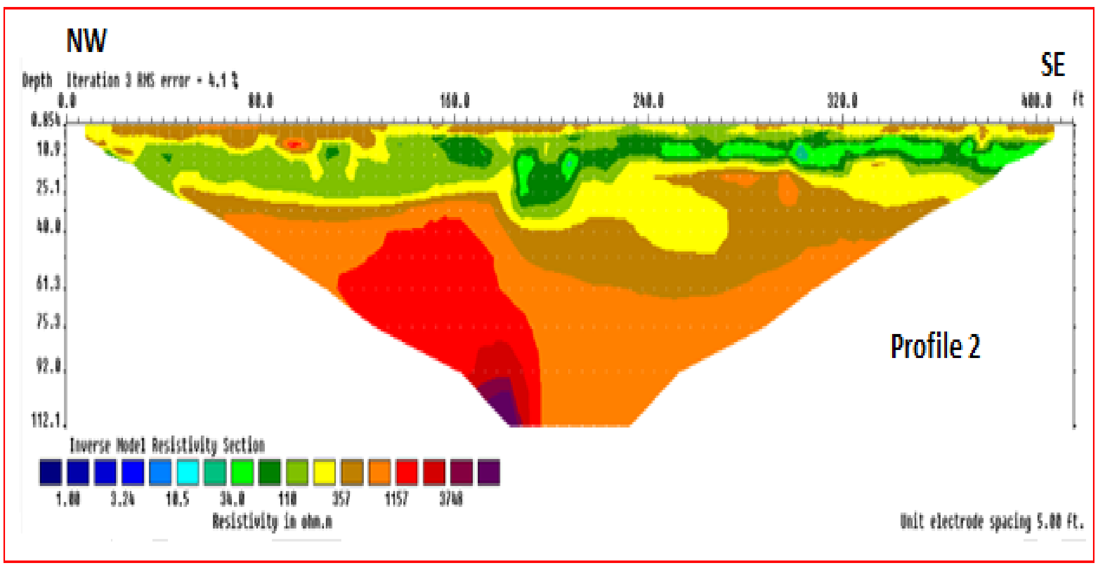

Figure 9.4. Uninterpreted ERT profile 2

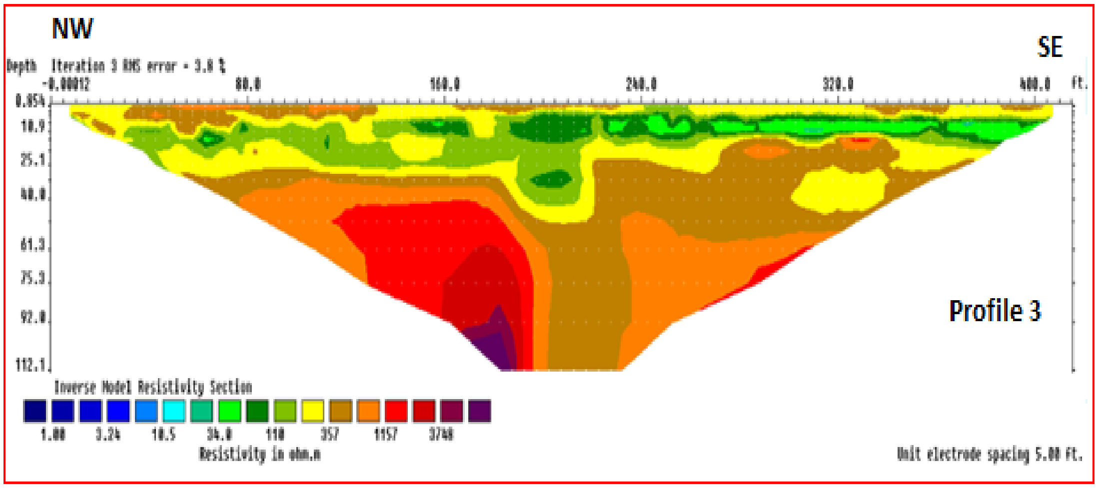

Figure 9.5. Uninterpreted ERT profile 3

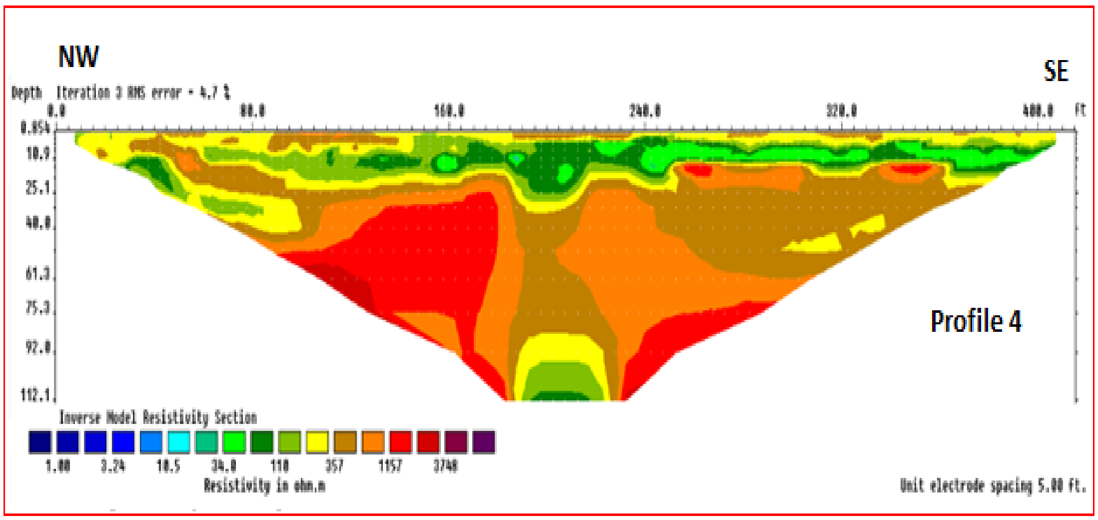

Figure 9.6. Uninterpreted ERT profile 4

9.6. DATA INTERPRETATION

Interpreted data from automated electrical resistivity data with boring control showed that the depth to top of bedrock was between 10 and 25 feet in ERT profiles (Figure 9.7) and 20 feet in borehole data (Figure 9.8). A set of solution-widened joints trending NE-SW was mapped.

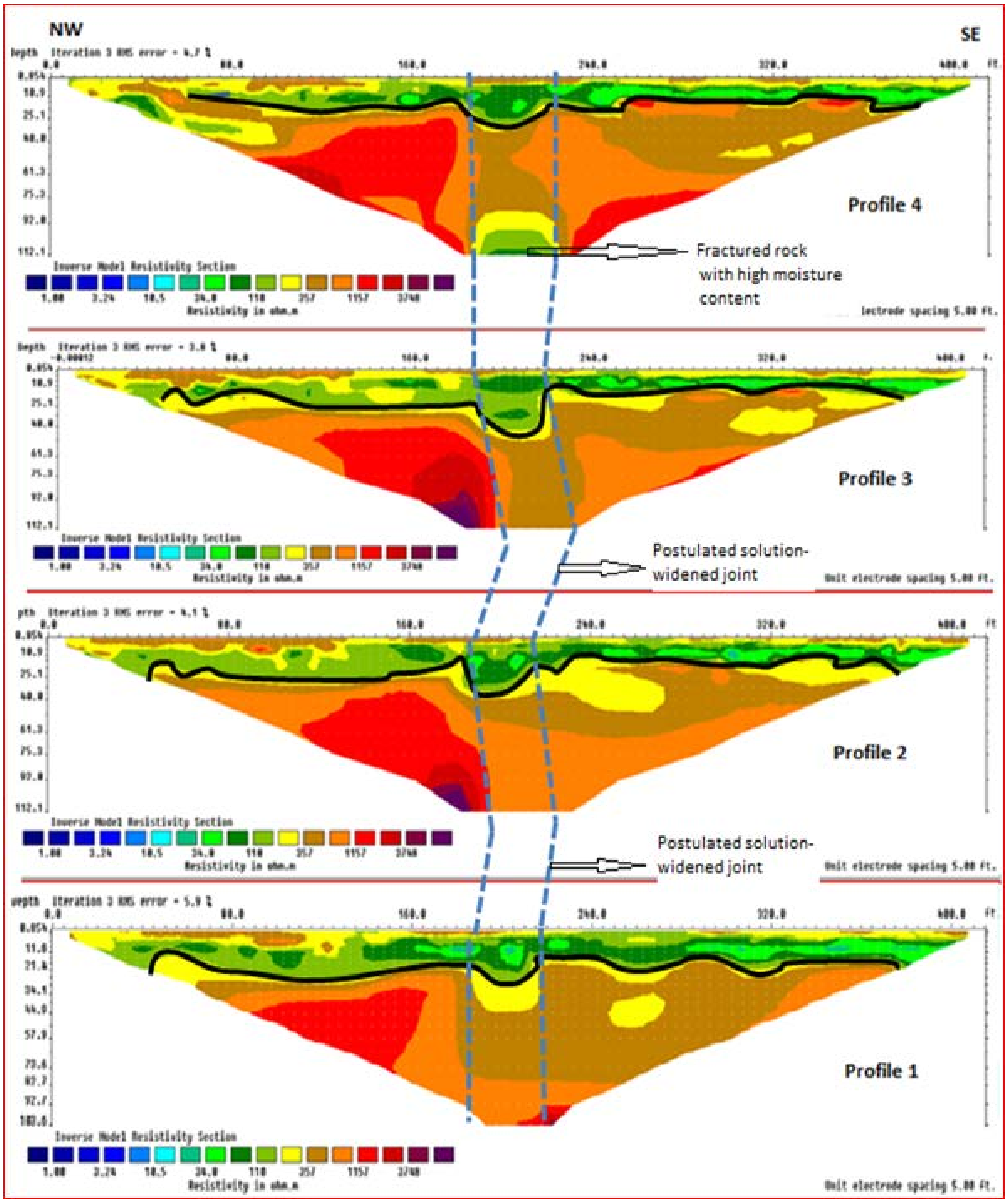

Figure 9.7. Interpreted ERT profiles. The black lines represent mapped top of rock, and the dotted blue lines represent a set of solution-widened joints trending NE-SW. Top 10 feet is mainly covered by dry soil and clay. The set of joints are interpreted as possible stream channel which could be an avenue through which a nearby sinkhole around the site recharges a nearby creek in the area.

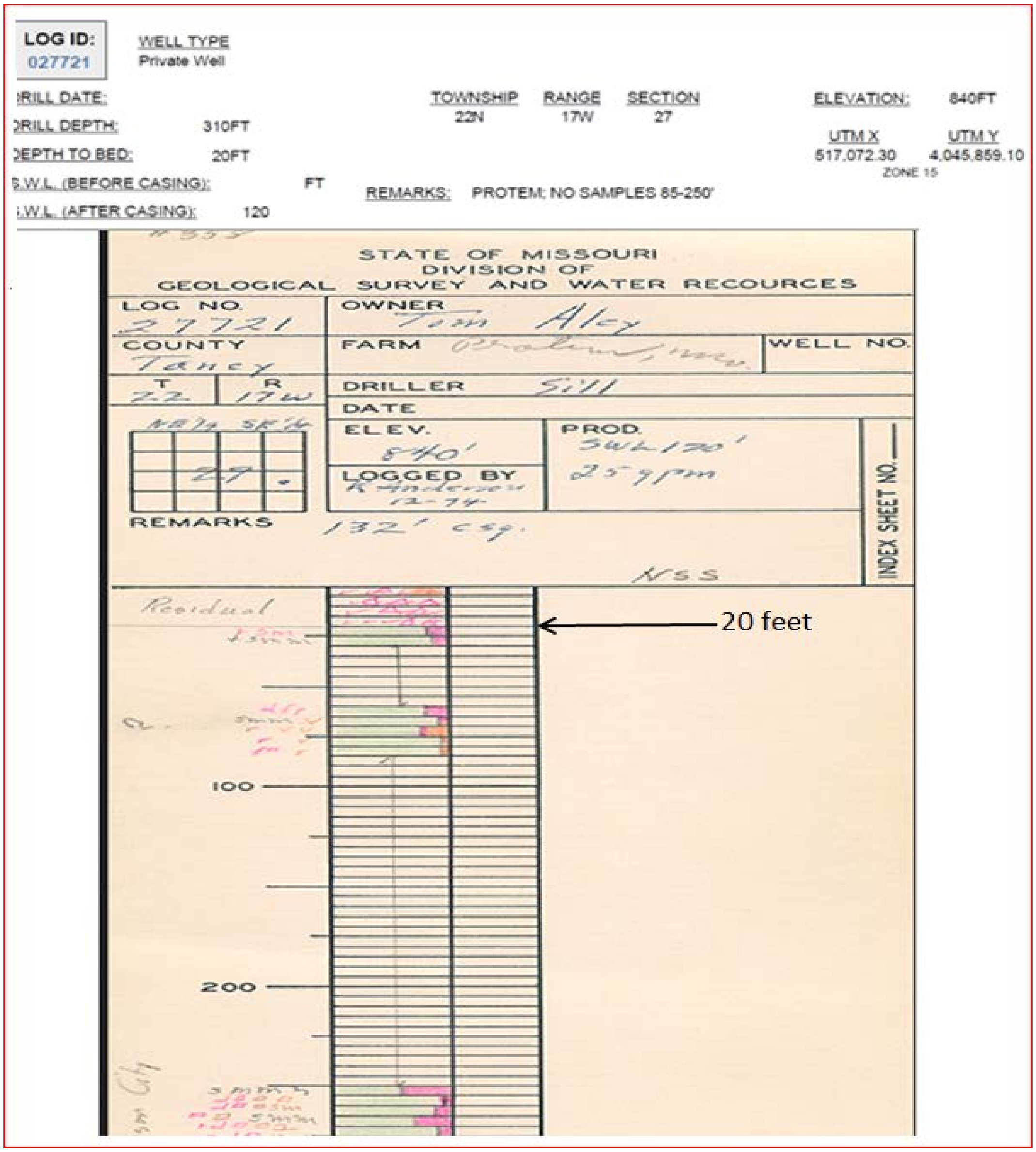

Figure 9.8. Borehole log from a nearby well in the area. The log was obtained from Missouri department of natural resources (MDNR). Depth to top of dolomite bedrock is 20 feet (shown by the arrow).

The interpreted set of solution-widened joints was superposed on a map of known structural lineaments in the area (Figure 9.9) to show the orientation of the joints in relation to the known lineaments in the area.

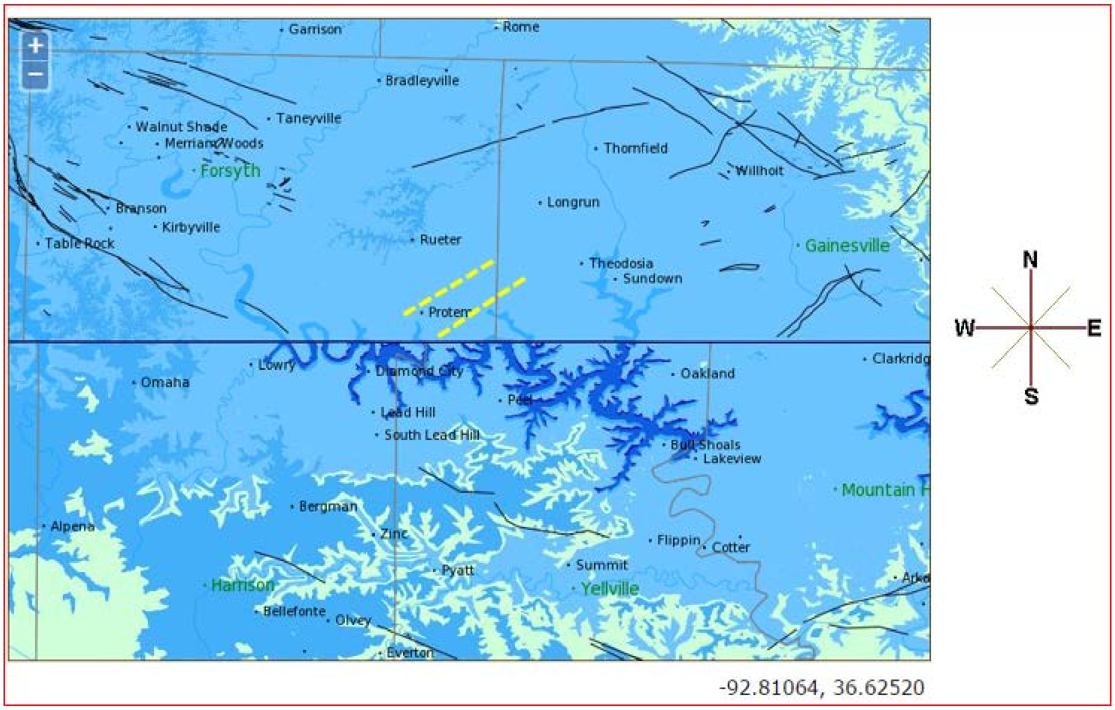

Figure 9.9. Interpreted set of solution-widened joints trending NE-SW. The joints are shown as dotted yellow lines superposed on a map of known structural lineaments around the project area (http://mrdata.usgs.gov/sgmc/mo.html)

9.7. CONCLUSION

Interpreted ERT results showed a set of solution-widened joints trending NE-SW direction which was interpreted as a stream channel through which the nearby sinkhole recharges a creek in the area. The joints are in-filled with low resistivity loose soil and rock materials. There was no structural lineaments shown in immediate proximity to the area from USGS data to know whether the solution-widened joints follow the trend of the lineaments or not. So, bedrrock dissolution was controlled by these joints and depth to top of rock was between 10-20 feet. The presence of the stream channel would be a concern and needs more detailed geotechnical investigations.

10. BATTLEFIELD CASE STUDY

10.1. ABSTRACT

Four automated electrical resistivity tomography (ERT) profiles, supported with multichannel analysis of surface waves and borehole data were used to map karst features in a proposed landfill in Battlefield Missouri. The suitability of the site for such project was assessed by mapping fractures in the bedrock like solution widened joints and underground openings through which groundwater in the area could be contaminated by the landfill**.**

Interpreted result of the survey showed that near vertical N-S and approximately W-E trending solution-widened joint sets are dominant in the area, and are mostly associated wih man-made features including roads, ponds and drainage ditches. The joint sets occur at least every 400 feet and in some cases every 150 feet (density of the joints), and are infilled with low resistivity (high conductivity) piped clays. A pattern where the joint sets often broaden with depth with lower resistivity values at greater depths was observed in the ERT images. This could be as a result of higher moisture concentrations at depth and the broadening of vertical seepage pathways through fractured rock. Cutter and pinnacle type of karst is most likely in the area especially around the E-W oriented ERT profiles.

10.2. INTRODUCTION

Automated electrical resistivity tomography (ERT), supported with multichannel analysis of surface waves and borehole data was used to map karst features in a proposed landfill in Battlefield Missouri. The suitability of the site for such project was assessed by mapping fractures in the bedrock like solution widened joints and underground openings through which groundwater in the area could be contaminated by the landfill. Depth to top of bedrock was also determined.

10.3. SITE GEOLOGY AND DESCRIPTION

The site was located in Battlefield in Greene County Missouri (Figure 10.1). The primary rock unit in the area is Burlington-Keokuk limestone of early Mississippian age (Table 10.1).

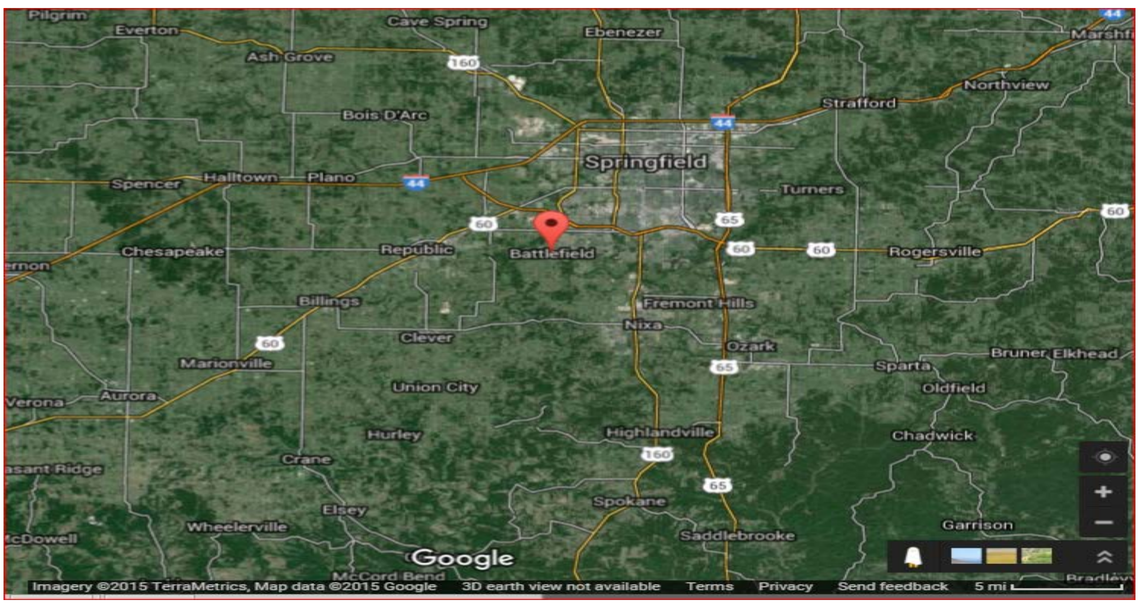

Figure 10.1. Study site location. The red object shows the location of the site

The limestone is mostly red in color and intermixed with chert and shale. Most karst features in Southwestern Missouri are developed in this formation. Solution sinkholes both formed and forming (Figure 10.2) were scattered around the area including ponded bodies of water. The site was more of a pasture land and crop land.

Figure 10.2. Sinkhole development in the area starting with soil depression

Table 10.1. Geologic and stratigraphic units in Battlefield project area (USGS)

System	Series	Group	Formation	Maximum Thickness (ft.)
Mississippian	Osagean		Keokuk Limestone	100
			Burlington Limestone	70
			Elsey Formation or Grands Falls Formation	100
			Reeds Spring Formation	225
			Pierson Limestone	60
			Fern Glen Formation	45

The limestone is mostly red in color and intermixed with chert and shale. Most karst features in Southwestern Missouri are developed in this formation. Solution sinkholes both formed and forming are scattered around the area including ponded bodies of water. The site was more of a pasture land and crop land.

10.4. DATA ACQUISITION

Four automated electrical resistivity tomography (ERT) profiles were acquired with 168 electrodes and electrode spacing of 5 feet. To get a better coverage of the karst features in the area, two profiles were acquired along E-W direction and another two along N-S direction. Due to the length of the project area to be covered, a roll-along survey method was used. This method is usually applied when the survey line is longer than the available electrode spread or when an obstacle could not allow the survey line to continue. After the initial data acquisition using 168 electrodes, the next data set was acquired by moving half of the electrode cable section, in this case 84 electrodes were moved forward in a leap-frog way. At the end of the survey line, data for each roll were added to form one profile data.

Also, multichannel analysis of surface waves (MASW) data were acquired parallel to ERT profiles (Figure 10.3) at selected locations more or less every 400 feet to detrmine the shear wave velocities/engineering properties of subsurface materials along the profiles as well as costrain ERT results with respect to depth to top of bedrock and thickness of overburden materials. Twenty four channels seismograph with geophone spacings of 2.5 feet and 5 feet were used for MASW data acquisition. Boring data (Figure 10.4) were also obtained from boreholes drilled in close proximity to MASW and ERT profiles for ground-truth.

Figure 10.3. Data acquisition at the project site. A: ERT, B: MASW, C: Drilling rig for borehole data

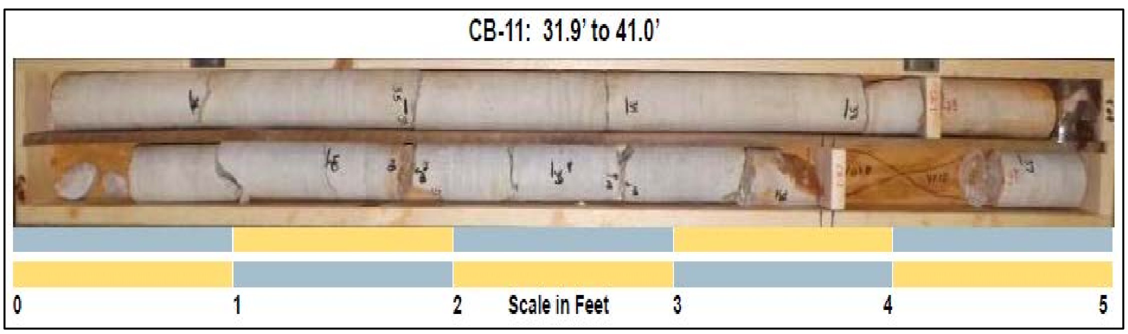

Figure 10.4. Limestone recovered from boring CB-11. Depth to top of bedrock was 31.9 feet

10.5. DATA PROCESSING

Automated ERT data with elevation data were processed using RES2DINV software to generate 2D ERT model (Figures 10.5-10.9) described as uninterpreted ERT profiles. Data from each roll were stitched together to form a single profile, a process known concatenation. MASW data were processed using SurfSeis3 software to generate

1-D shear wave velocity profiles of the subsurface materials along the ERT profile locations.

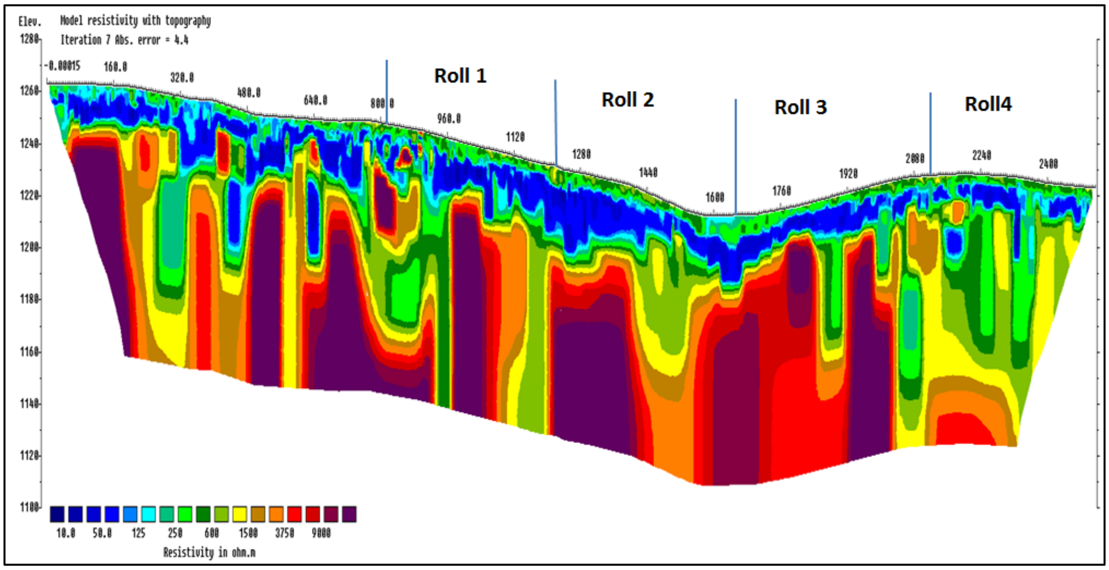

Figure 10.5. Processed/Uninterpreted ERT profile showing Roll-along survey lines. The lines are represented by the vertical blue lines as represented by the vertical blue lines

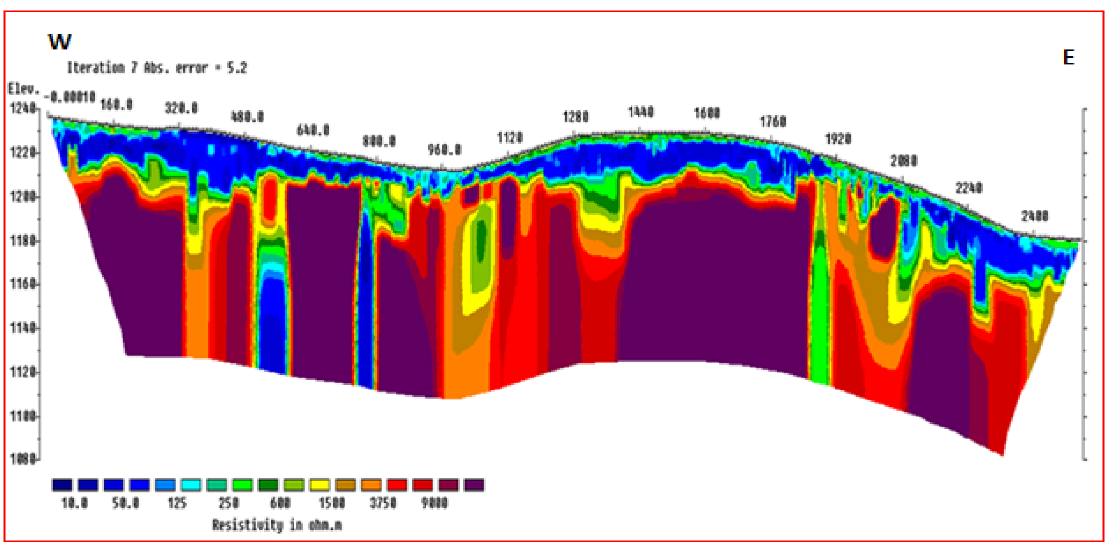

Figure 10.6. Uninterpreted ERT profile 1

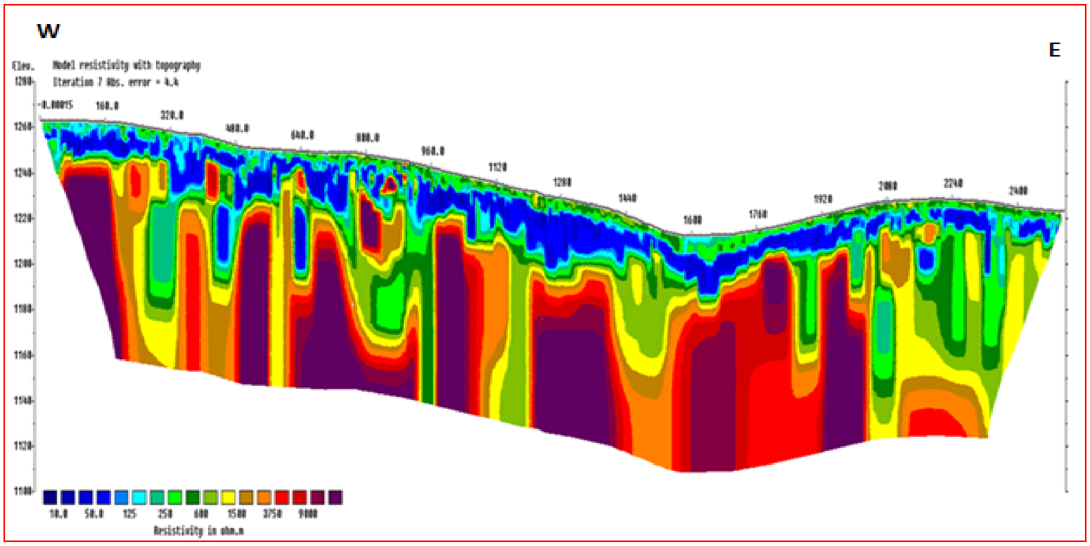

Figure 10.7. Uninterpreted ERT profile 2

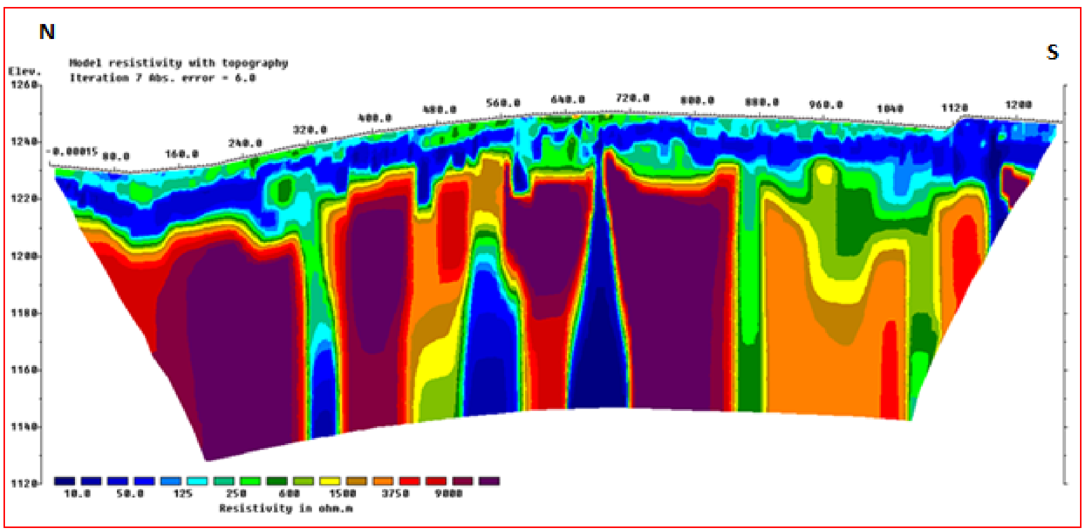

Figure 10.8. Uninterpreted ERT profile 3

The length of the automated electrical resistivity tomography (ERT) profiles generated varies as a result of different data acquisition spaces available on the site or obstacles such as fences and property boundaries. The generated profiles that are not too long shows a clearer ERT images as can be seen.

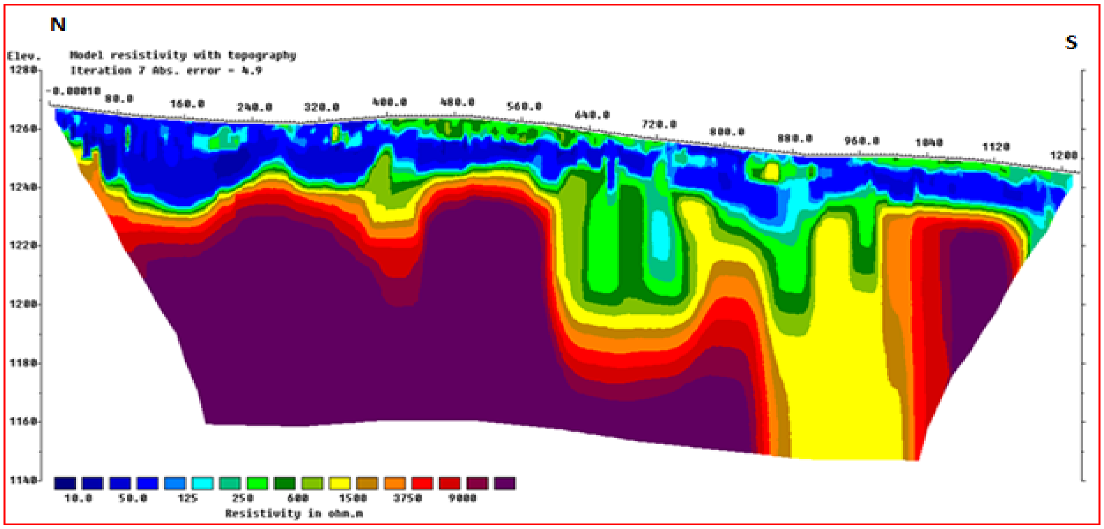

Figure 10.9. Uninterpreted ERT profile 4

10.6. DATA INTERPRETATION

Interpreted features mapped in the site were solution-widened joints with clay-infill, top of bedrock and thickness of overburden materials. Some of the features mapped have developed a pattern that characterized both surface and subsurface geological activities around the project area. The interpreted ERT and MASW profiles (Figures 10.10- 10.18) showed that depth to top of bedrock varies along the profiles, and a near vertical set of solution widened joints with clay-infill were mapped.

A Section of ERT profile 3 showed the image of a visually prominent solution-widened joint with a pattern showing that the joint broaden with depth (Figure 10.17) with lower resistivity values at greater depths. The interpreted solution-widened joints were superposed on a map of known structural lineaments in the area (Figure 10.19) to show the orientation of the joints in relation to known structural lineaments in the area. The joints were trending N-S and W-E.

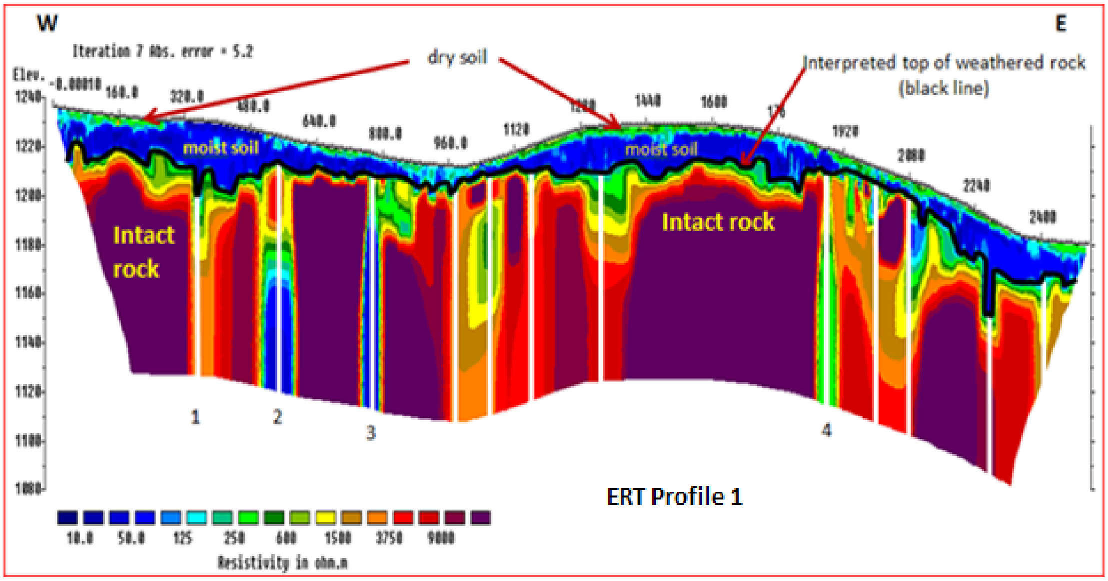

Figure 10.10. Interpreted ERT profile 1. Depth to top of bedrock is around 20 feet and corresponds to the 125 ohm-m contour interval. The vertical white lines represent interpreted N-S trending joint sets. The prominent joint sets (1, 2, 3, and 4) are characterized by lowest resistivity values.

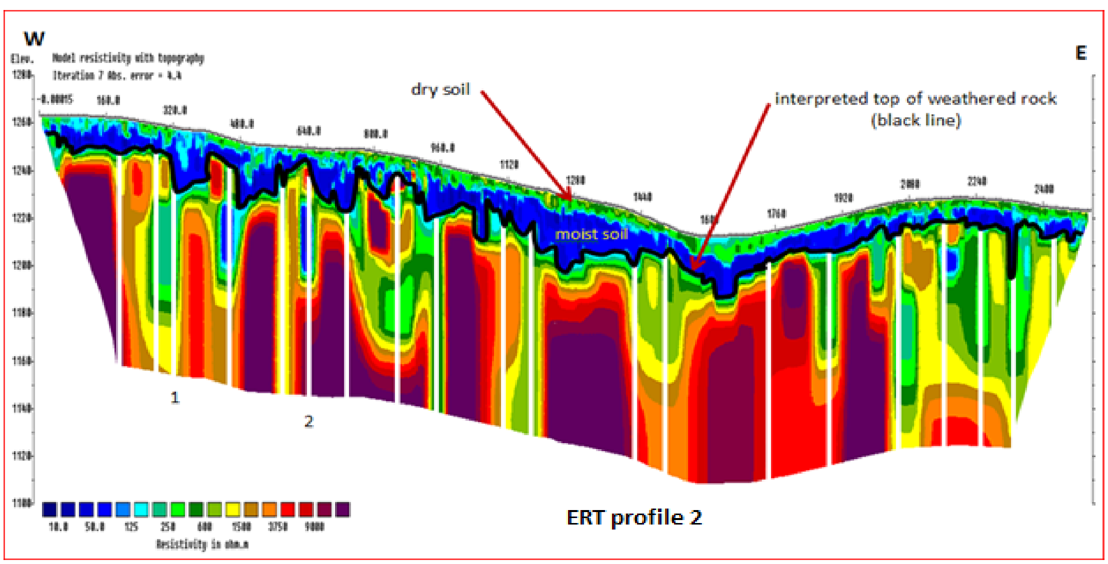

Figure 10.11. Interpreted ERT profile 2. Depth to top of bedrock varies from 10-30 feet and corresponds to the 125 ohm-m contour interval. The vertical white lines represent interpreted N-S trending joint sets. Joint sets 1and 2 have sinkholes located around the area, about 100 feet to the north of the joint sets.

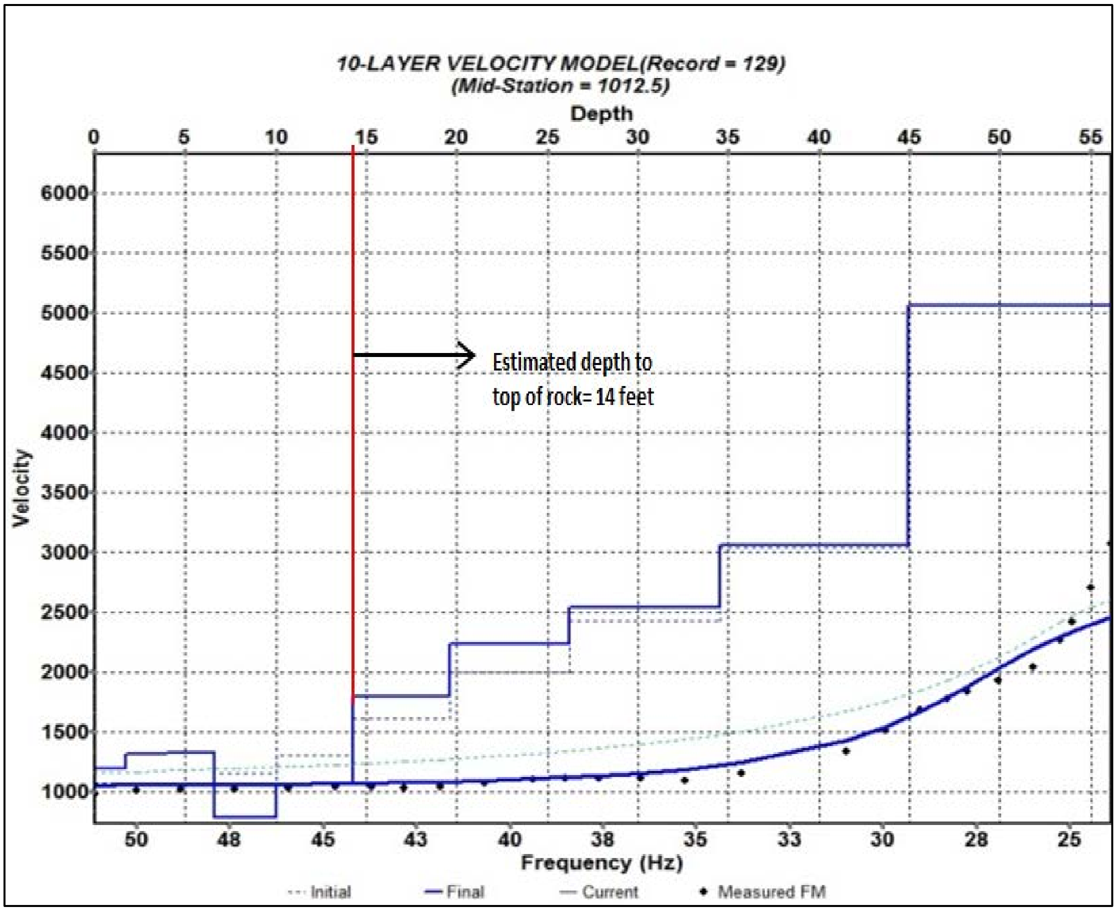

Figure 10.12. 1-D shear wave velocity profile centered at 900 feet mark on ERT profile 2. Interpreted depth to top of rock was 14 feet and around 12 feet on ERT profile which was a good correlation.

There was a good correlation between the mapped depths to top of bedrock in electrical resistivity tomography (ERT) profiles and multichannel analysis of surface waves 1-D shear wave velocity profiles acquired along the same line (parallel). The shear wave velocity value used to map top of bedrock was between 1600 and 1700 ft./sec. Mapped depth to top of bedrock using ERT was determined using 125 Ohm-m contour interval.

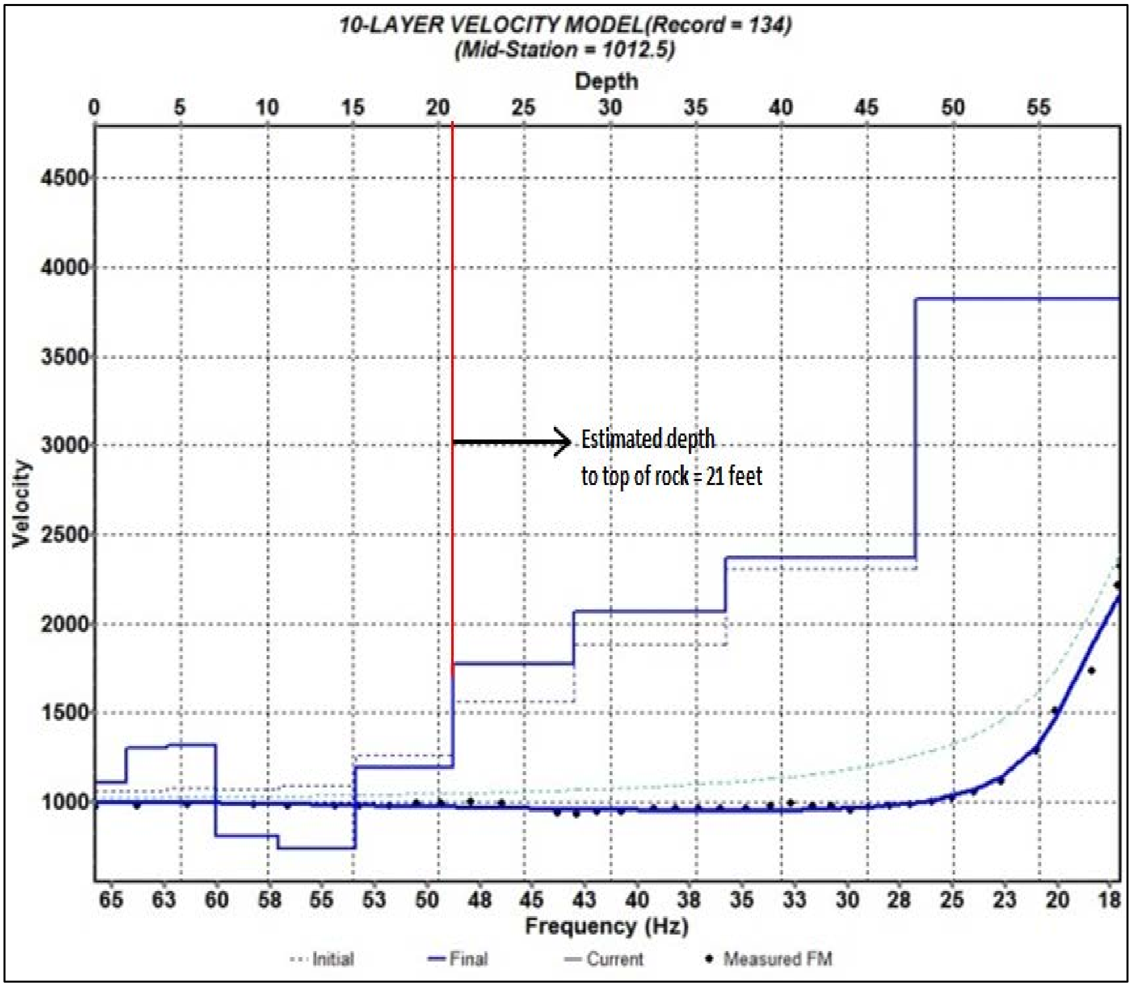

Figure 10.13. 1-D shear wave velocity profile centered at 1300 feet mark on ERT profile 2. Interpreted depth to top of rock was 21 feet and around 23 feet on ERT profile which was a good correlation.

There was a good correlation between the mapped depths to top of bedrock in electrical resistivity tomography (ERT) profiles and multichannel analysis of surface waves 1-D shear wave velocity profiles acquired along the same line (parallel). The shear wave velocity value used to map top of bedrock was between 1600 and 1700 ft./sec. Mapped depth to top of bedrock using ERT was determined using 125 Ohm-m contour interval.

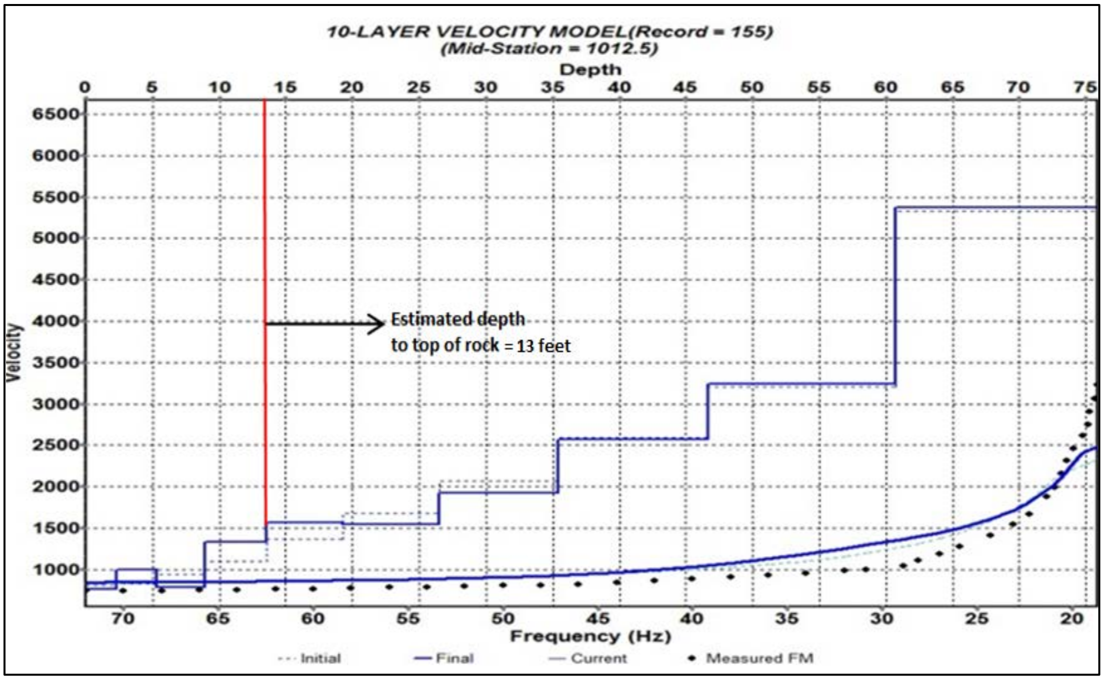

Figure 10.14. 1-D shear wave velocity profile centered at1700 feet mark on ERT profile 2. Interpreted depth to top of rock was 13 feet and around 12 feet on ERT profile which was a very good correlation

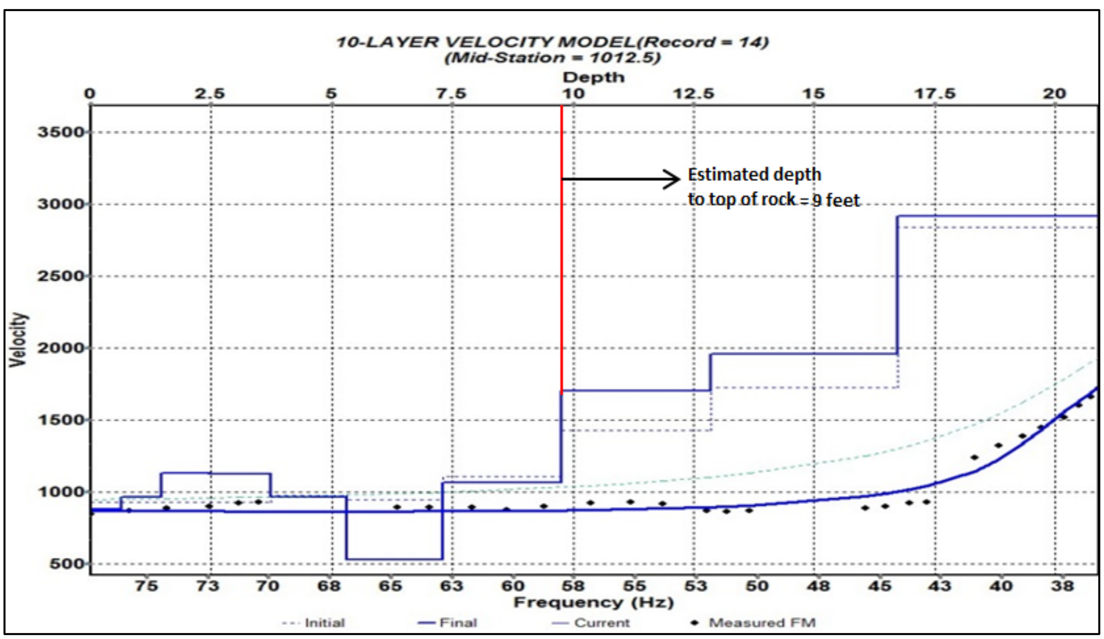

Figure 10.15. 1-D shear wave velocity profile centered at 2100 feet mark on ERT profile 2. Interpreted depth to top of rock was 9 feet and around 11feet on ERT profile 2, and that was a good correlation.

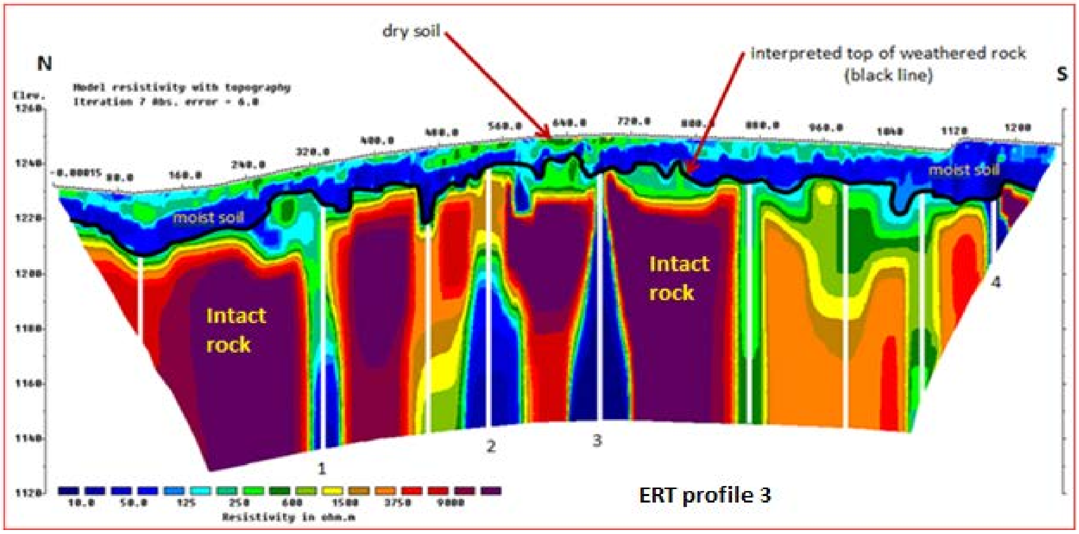

Figure 10.16. Interpreted ERT profile 3. Depth to top of rock varies from 8-30 feet and corresponds to the 125 ohm-m contour interval. The vertical white lines represent interpreted W-E trending joint sets. The most prominent joint sets, characterized by lowest resistivity values are labeled 1, 2 and 3.

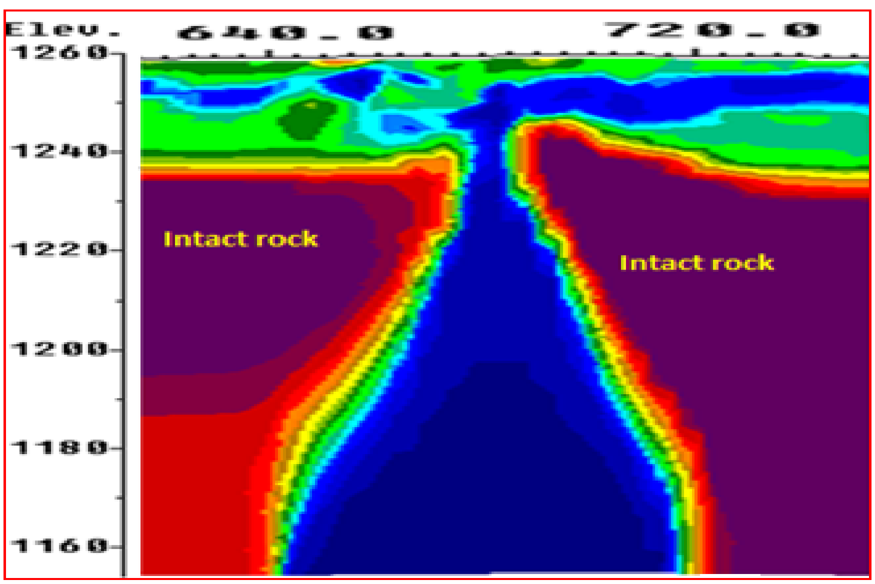

Figure 10.17. Section of ERT profile 3 showing images of visually prominent solution-widened joint. The joint is characterized by anomalously lower resistivity values. There is a pattern that developed here which shows that the joint broaden with depth with lower resistivity values at greater depths.

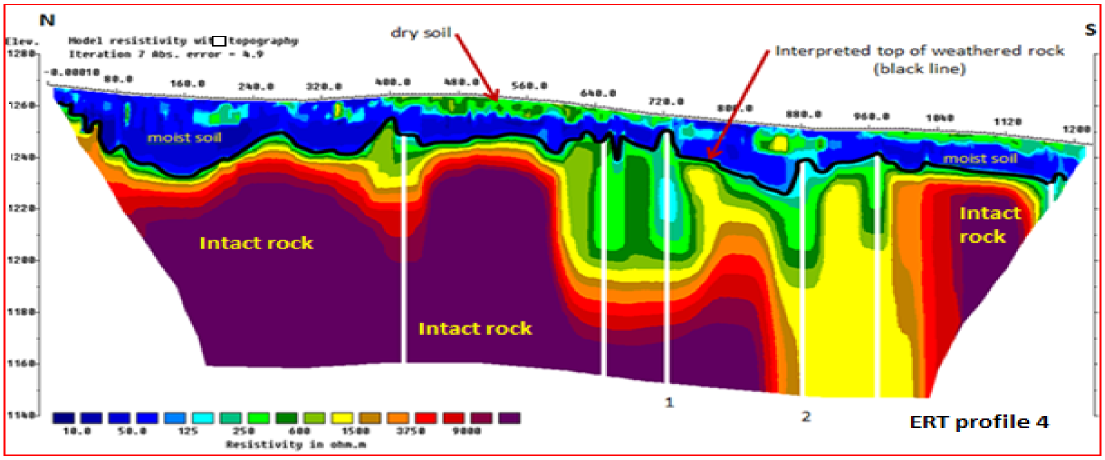

Figure 10.18. Interpreted ERT profile 4. Depth to top of rock varies from 10-40 feet and corresponds to the 125 ohm-m contour interval. The vertical white lines represent interpreted W-E trending joint sets. Sinkholes are located adjacent to joint sets 1and 2.

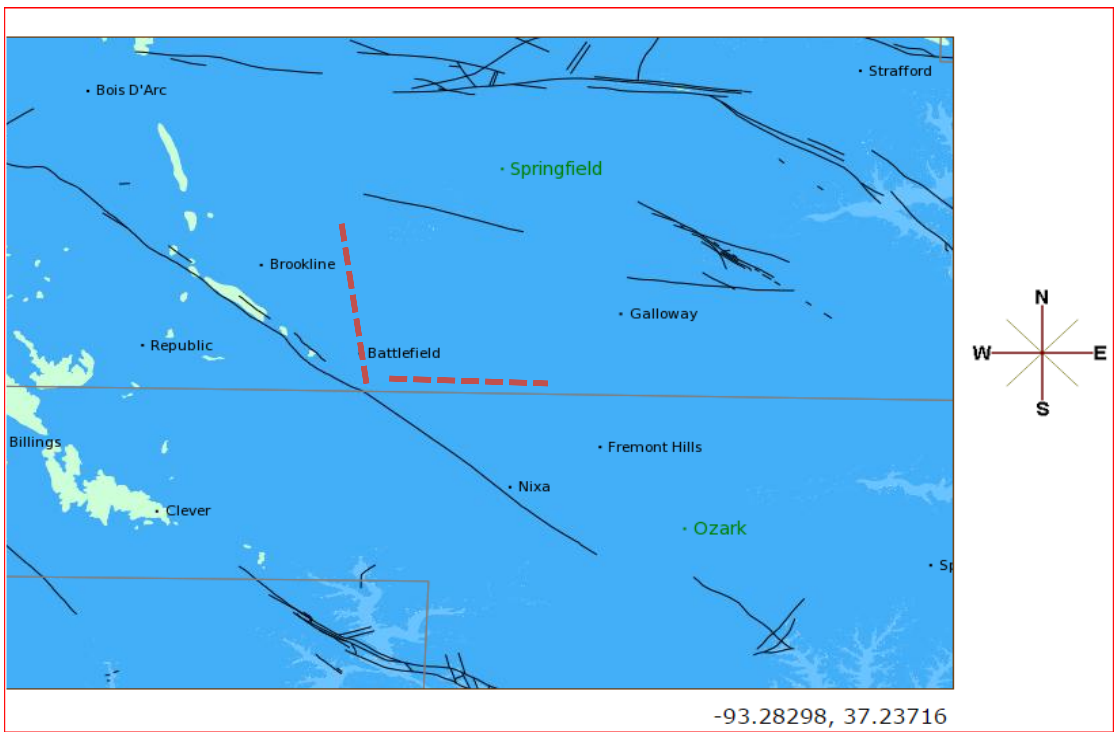

Figure 10.19. Interpreted sets of solution-widened joints trending N-S and W-E superposed on a map of known structural lineaments in the area. The sets of joints are represented by dotted brown lines. The joint sets control movement of surface and groundwater during the dissolution of limestone bedrock in the area.

10.7. CONCLUSION

Interpreted result of the survey showed that near vertical N-S and approximately W-E trending solution-widened joint sets are dominant in the area, and are mostly associated with man-made features including roads, ponds and drainage ditches. The joint sets occur at least every 400 feet and in some cases every 150 feet (density of the joints), and are infilled with low resistivity (high conductivity) piped clays. The joints control the direction of flow of both surface and groundwater. As observed from the ERT images, some joints have low resistivity values and others have high resistivity values. A possible explanation to this could be that groudwater flows laterally in specific joints and changes direction in others since there are a lot of fractures in the bedrock.

A pattern where the joint sets often broaden with depth with lower resistivity values at greater depths was observed in the ERT images. This could be as a result of higher moisture concentrations at depth and the broadening of vertical seepage pathways through fractured rock.

Also, the pattern could also be as a result of more extensive solution-widening of fractures at depth (more moisture content) and increased concentrations of piped low resistivity clays/sediments at greater depth.

Another observed pattern was that the ERT images of many of the interpreted joint sets extend to subsurface depths in excess of 100 feet.

Cutter and pinnacle type of karst is most likely in the area especially around the E-W oriented ERT profiles. In cutter-and-pinnacle karst, the contact between bedrock and soil overburden is very irregular, and water preferentially dissolves bedrock along some planar features, such as bedding, joints, or fractures.

11. RICHLAND CASE STUDY

11.1. ABSTRACT

Three automated electrical resistivity tomography (ERT) profiles were acquired parallel to multichannel analysis of surface waves (MASW) profiles to map karst features on a private property for residential building. Sixty electrodes with electrode spacing of five feet and dipole-dipole electrode array configuration were used, giving an array length of two hundred and ninety five feet and approximate depth of fifty nine feet. Borehole data from Missouri department of natural resources (MDNR) was used for ground-truth. Interpreted results of the study showed that a near-vertical solution-widened joint was mapped in the area, and dissolution of the dolomite bedrock is controlled by this joint, in line with structural lineaments in the area. The joint is filled with low resistivity (moderately conductive soils) materials which are possible karst infills. The property was underlain by up to 50 feet of either fractured /weathered rock or competent soil or a combination of both. The joint cut across a surface depression at 150 feet mark around ERT profile 2, and was interpreted as a possible channel through which surface water percolates into the subsurface.

11.2. INTRODUCTION

The Richland study site involved property evaluation for karst features to determine its suitability for construction of residential building. Automated electrical resistivity tomography (ERT) technique and multichannel analysis of surface waves were used to map the area. Features mapped were solution-widened joints and bedrock in the area since they play a major role in the development of caves and sinkholes.

11.3. SITE GEOLOGY AND DESCRIPTION

The site is located in Richland, Pulaski County in Missouri (Figure 11.1). The site was covered by trees, shrubs and grasses, and loose rock materials (Figure 11.2). The primary rock unit in the area is Jefferson City dolomite intermixed with sandstone and chert.

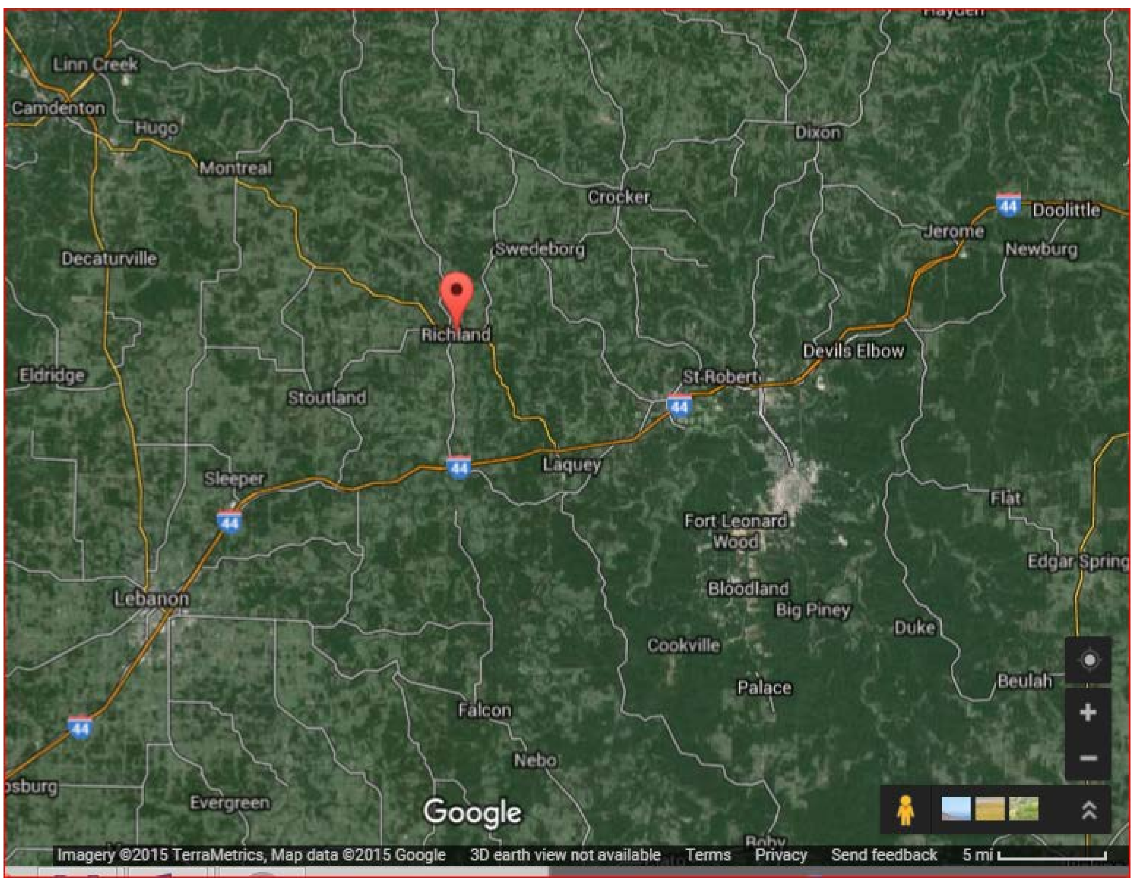

Figure 11.1. Study site location (Google map). The site is represented by the red object.

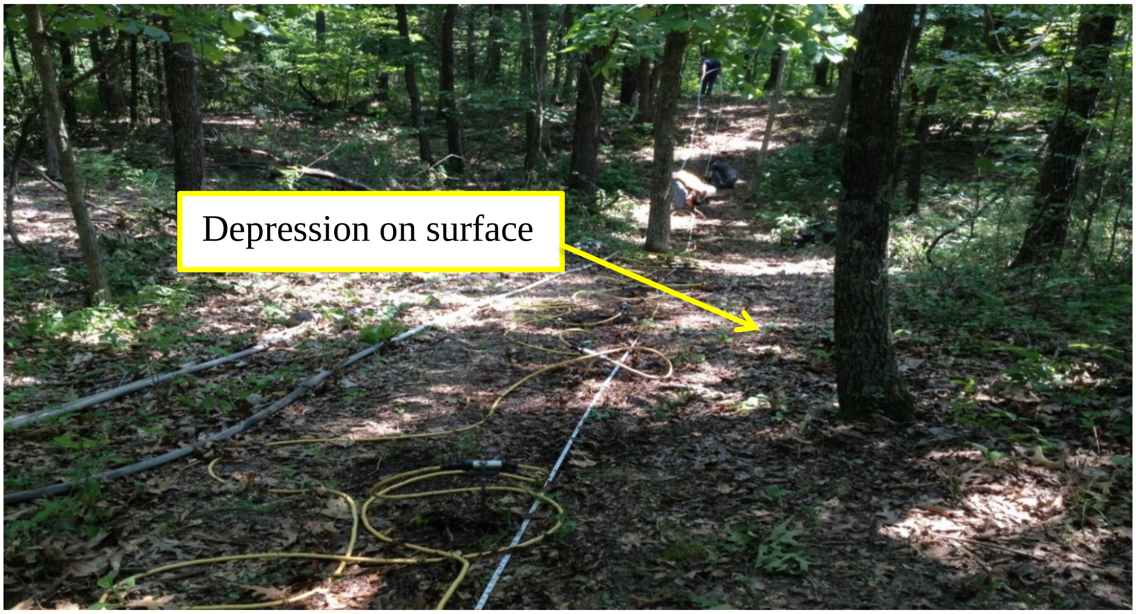

Figure 11.2. Project site showing automated ERT profile 2

There was a depression on the ground surface at the center of the site, close to ERT profile 2, which looks like covered sinkhole, and the area looks like collapsing when the ground was hit with a hammer. The ground was so hard that it was difficult to pound metal stakes into the ground for electrode connections. It was also difficult to insert the geophones firmly in some places because of the difficult terrain.

11.4. DATA ACQUISITION

Three automated electrical resistivity tomography (ERT) profiles were acquired parallel to multichannel analysis of surface waves (MASW) profiles (Figure 11.3). For the ERT, Sixty electrodes with electrode spacing of five feet were used for data acquisition. Dipole-dipole electrode array was used, giving an array length of two hundred and ninety five feet and approximate depth of fifty nine feet.

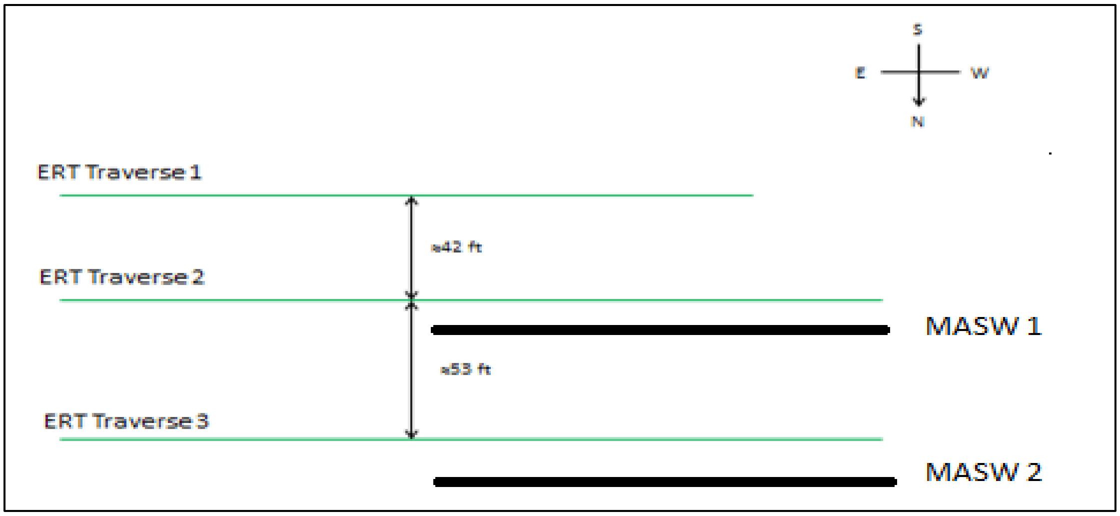

Figure 11.3. Sketch of the investigated area. The green lines are automated electrical resistivity tomography (ERT) profiles while the black lines are that of the multichannel analysis of surface waves (MASW) profiles.

Forty eight electrodes were used in the first profile because of cable problems. For the multichannel analysis of surface waves (MASW) technique, two profiles were acquired parallel to automated electrical resistivity tomography (ERT) profiles two and three starting from the center of the ERT profiles where there is ground depression at about 150 feet mark. Twenty four channels seismograph, twenty four geophones (4.5 HZ. each), a laptop and 20 Lbs. sledge hammer were used for data acquisition. The geophones were spaced five feet apart with an offset distance of thirty feet.

11.5. DATA PROCESSING

Automated electrical resistivity (ERT) data were processed using RES2DINV software, and multichannel analysis (MASW) data were processed using SurfSeis3 software. The data acquired from ERT were not of high quality due to the nature of the site (Figure 11.4); the MASW 2 data were also not of high quality. These problems are attributed to ground condition being too dry and stiff, making electrode contact with the soil difficult, although water tanker was used to wet the ground to minimize the effect. In some instances there were missed data as can be seen from ERT profile 3.

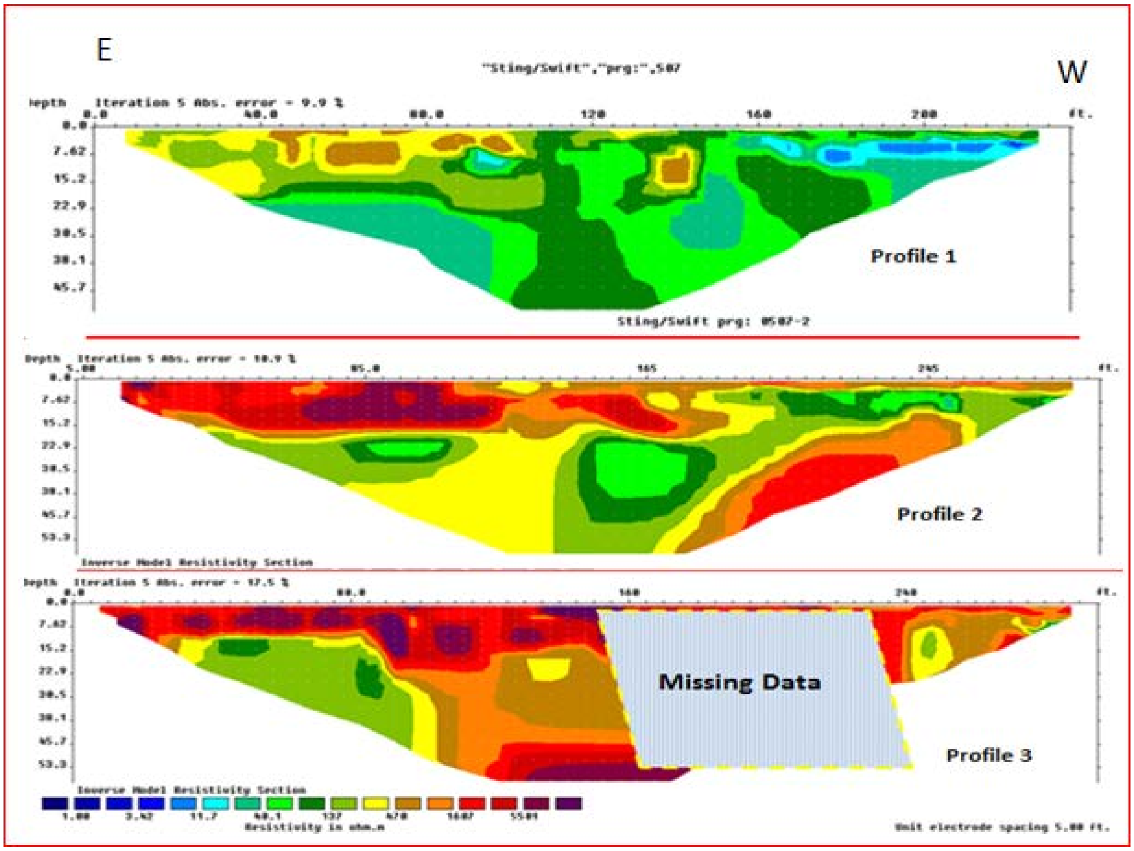

Figure 11.4. Uninterpreted ERT profiles. Profile one was acquired using 48 electrodes to give an array length of 235 feet. Profiles 2 and 3 were acquired using 60 electrodes to give an array length of 295 feet.

11.6. DATA INTERPRETATION

Interpreted ERT data showed that a near-vertical solution-widened joint was mapped in the area, as well as moderately conductive soils which are possible karst infill (Figure 11.5). Depth to top of bedrock was not clearly mapped using ERT but MASW

(Figure 11.6) and borehole data (Figure 11.7) showed that depth to top of bedrock was around 40 to 44 feet.

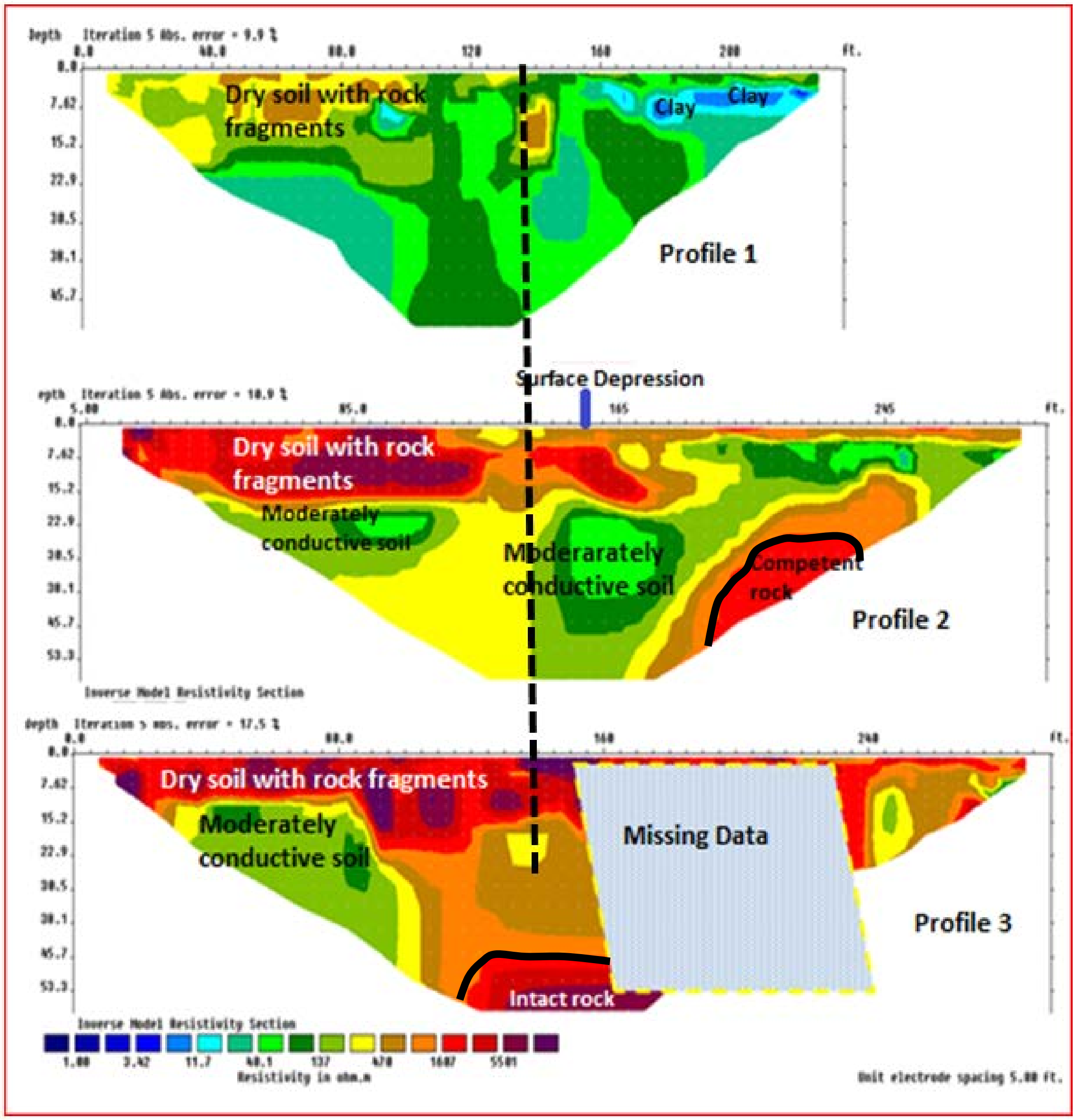

Figure 11.5. Interpreted ERT profile showing a near-vertical (N-S) solution-widened joint. The joint is shown as black dotted line. Moderately conductive soils which are possible karst infills were also mapped. The joint cut across the area where there is surface depression. The black lines represent interpreted depth to top of intact rock which was just above 1600 Ohm-m on the ERT images (profiles 2 and 3).

As a result of poor resistivity contrast between fractured rocks and dry soils, it was difficult to map with confidence, the depth to top of bedrock from the electrical resistivity tomography (ERT) images generated. So, mapping the depth to top of bedrock was based more on multichannel analysis of surface waves (MASW) 1-D shear wave velocity profile generated and the boring logs obtained from Missouri department of natural resources (MDNR) than the ERT images. The interpreted solution-widened joint was superposed on a map of known structural lineaments in the area (Figure 11.8) to show the orientation of the joint in relation to the lineaments.

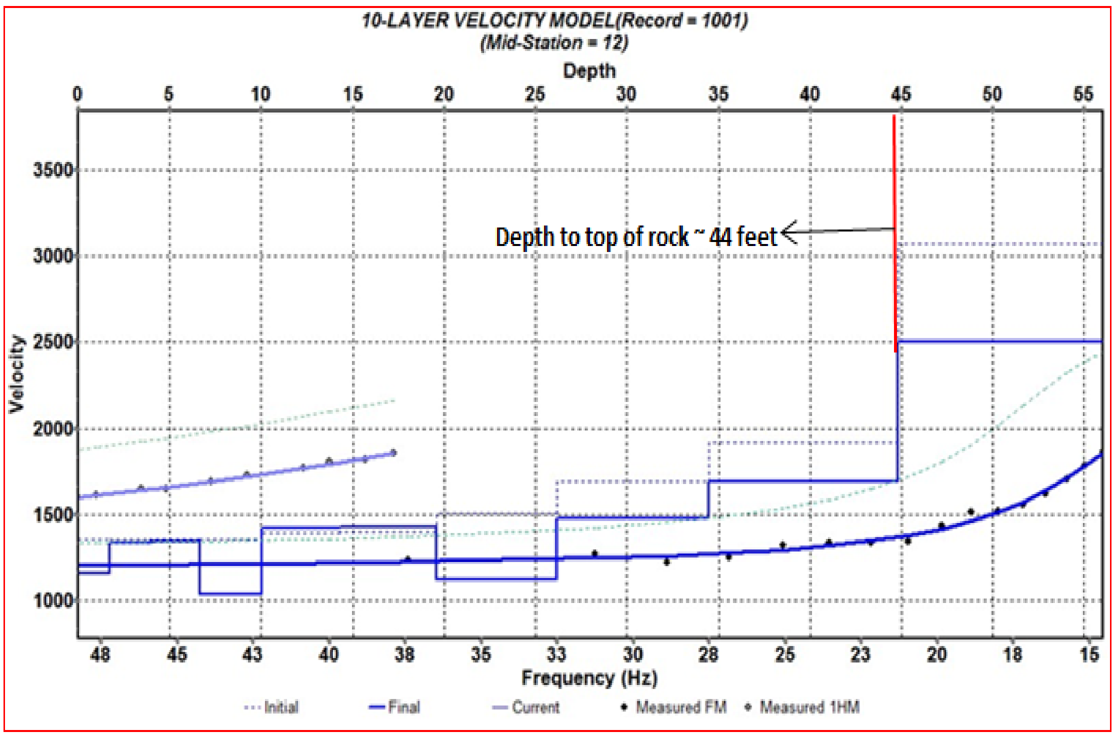

Figure 11.6. 1-D shear wave velocity profile (MASW 1) acquired along ERT profile 2 at 150 feet mark. Depth to top of intact bedrock was around 44 feet and 40 feet on the boring log (figure 11.7) which is a fairly good correlation. The interpreted depth to top of intact rock was just above 1600 Ohm-m on the ERT images. The shear wave velocity of the intact rock was in the region of 1700-2500 ft. /sec. (360-760 m/sec.) which falls within the range of very dense soil and soft rock, based on National earthquake hazards reduction program (NEHRP) table for shear wave velocity of some earth materials.

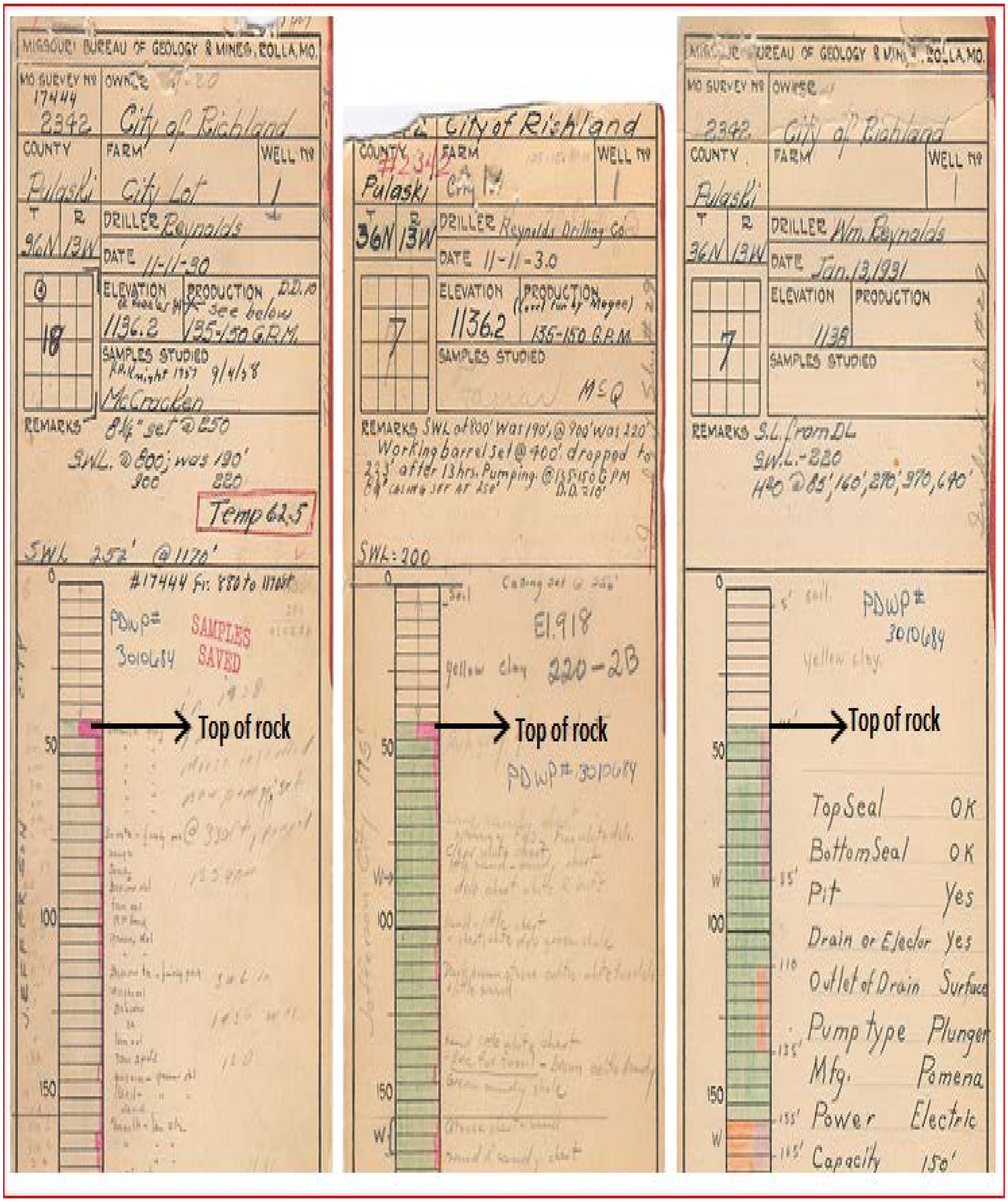

Figure 11.7. Borehole log around the project area obtained from Missouri department of natural resources (MDNR). Depth to top of bedrock was around 40 feet.

The borehole logs were obtained from the closest boreholes drilled around the project site at different times. Depth to top of bedrock in this area has not changed based on the boring logs.

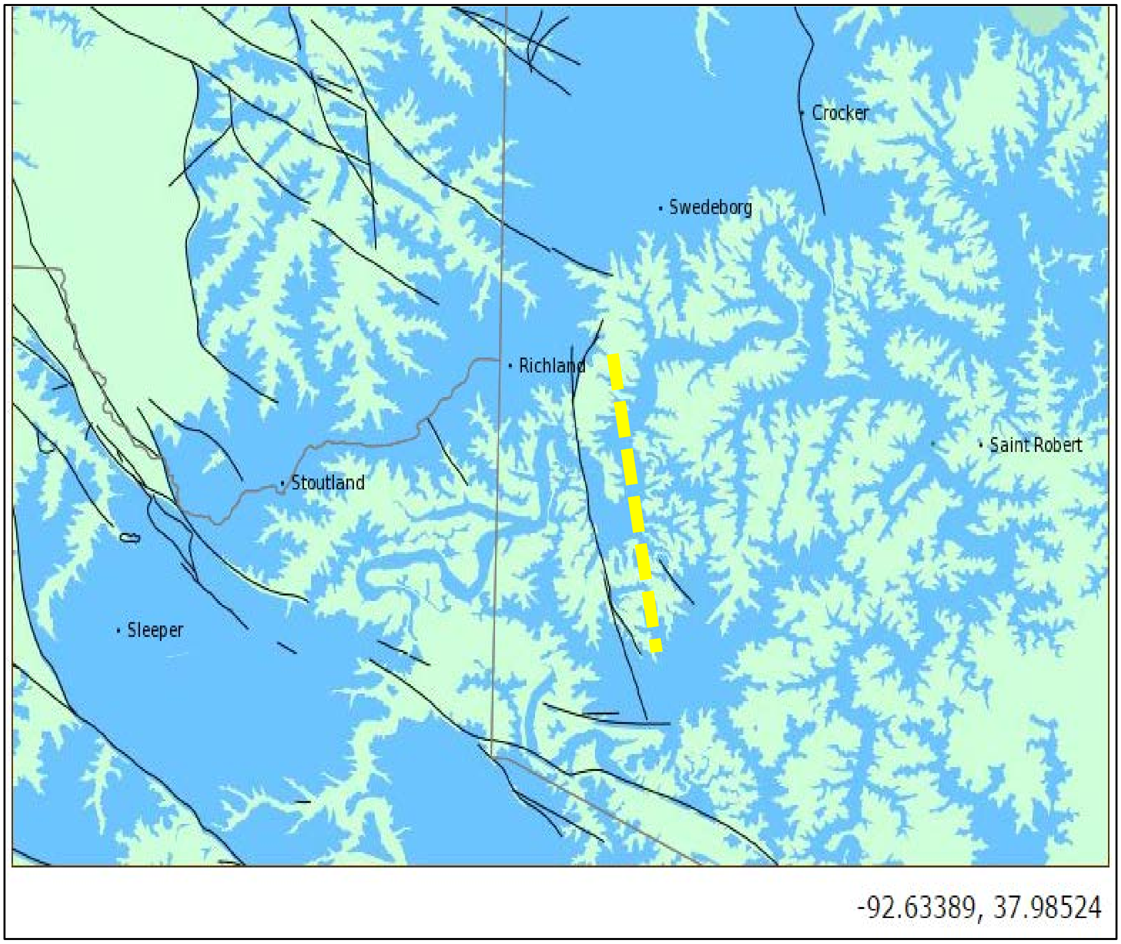

Figure 11.8. Interpreted solution-widened joint superposed on a map of known faults in the area. The near vertical Solution-widened joint (yellow dotted line) trends in the same direction with known faults (black line) in the area.

11.7. CONCLUSION

Interpreted results of the study showed that a near-vertical solution-widened joint was mapped in the area. This joint serves as a channel through which acidic surface water percolates into the subsurface to dissolve the dolomite bedrock. The orientation of the joint conforms with known structural lineaments in the area. The joint cut across a surface depression at 150 feet mark around ERT profile 2, and was interpreted as a possible channel through which surface water percolates into the subsurface. The joint was filled with low resistivity (moderately conductive soils) materials which are possible karst infills.

There is no well defined pattern of the joint encountered based on the automated electrical resistivity tomography images generated, and the density of the interpreted solution widened joint is low. It can be said that karst is poorly developed in this area or on the dolomite bedrock. According to literature on engineering classification of karsts, weaker carbonate rocks lack the strength to span large cavities, and develop limited suites of karst features that are generally smaller than those on stronger carbonate rocks.

The poor resistivity contrast between the fractured rocks and dry soils makes it difficult to map with confidence the depth to top of bedrock using the ERT images generated. But looking at the ERT model available, interpeted depth to top of intact bedrock from profiles 2 and 3 showed a resistivity value of just above 1600 Ohm-m.

So, mapping the depth to top of bedrock on this site/ project was based more on 1-D shear wave velocity profile generated from multichannel analysis of surface waves (MASW) and boring logs obtained from Missouri department of natural resources (MDNR) than the ERT images.

Also, the property was underlain by up to 50 feet of either fractured/weathered rock or competent soil or a combination of both, and depth to top of competent rock was around 40 to 44 feet. Building on the site would cost more money because depth to competent bedrock is high, which would not be case if the depth was shallow. To ascertain this claim, geotechnical approach such as borehole drilling would be a good approach to solve the uncertainty.

12. CONCLUSIONS

The result of the study showed that determining the placement, pattern and density of karst related features like solution-widened joints, clay/sediment-filled voids and water-filled voids would help understand karst processes better in Missouri. Previous works on karst in Missouri were mostly surficial mapping of bedrock outcrops and joints, which are not enough to define the internal structure of karst system, since most critical processes in karst occur underground. The following case studies highlight various problems inherent in karst terrains.

Nixa case study where a storm event increased surface run-off, leading to sinkhole collapse. Interpreted result of the study showed that the two sets of joints trending S-N and NW-SE were mapped in the area. The storm event increased surface run-off which are controlled by these joints. As a result, weak surficial materials are eroded and transported down the subsurface through these joints, resulting in cover-subsidence sinkhole. The point where these joints intersect was where the sinkhole was located. If no immediate remedial measure is taken, the sinkhole will enlarge further and become a major threat to lives and properties in the area.

Gasconade River case study where a void was detected in proximity to a bridge foundation. Interpreted result of automated electrical resistivity tomography (ERT) data with borehole control suggested that the orientation of the set of solution-widened joints (NE-SW) encountered in the project site was perpendicular to known faults and lineaments in the study area which trend NW-SE. The joints are mostly filled by low resistivity wet sand and silt that are washed down to occupy the space vacated by the dissolved bedrock. Low resistivity materials which are possible karst in-fill are mostly found in the south eastern part of the profile where the bedrock was shallow which indicated a possible formation of a less prominent solution-widened joint set in the area. The water-filled voids encountered in the site were not massive enough to threaten the structural integrity of the bridge foundation, and information obtained from the drilling crew in that site revealed that only about 22124 cubic feet (81.94 cubic yards) of grout was used to stabilize the ground around the structure.

Aurora case study involved sinkhole collapse in a parking lot. Interpreted data showed that the sinkhole formed as a result of preferential dissolution of the limestone bedrock along joints and bedding planes. Known structural lineaments around the area trend W-E and NW-SE, and they conform with two of the three interpreted solution-widened joints from ERT. It is possible that past activities near the site such as the abandoned Zin mine and the removal of a large sycamore tree during the construction of the parking lot contributed to the development of the sinkhole. There was a pattern observed where low resistivity clay-filled voids are mostly circular in shape. This type of circular pattern is mostly linked to cover-collapse sinkhole.

Protem case study involved mapping subsurface fractures in a site. Interpreted ERT results showed a set of solution-widened joints trending NE-SW direction which was interpreted as a stream channel through which the nearby sinkhole recharges a creek in the area. The joints are in-filled with low resistivity loose soil and rock materials. There was no structural lineaments shown in immediate proximity to the area from USGS data to know whether the solution-widened joints follow the trend of the lineaments or not. So, bedrrock dissolution was controlled by these joints and depth to top of rock was between 10-20 feet. The presence of the stream channel would be a concern and needs more detailed geotechnical investigations.

Battlefield case study involved site assessment for landfill construction. Interpreted result of the survey showed that near vertical N-S and approximately W-E trending solution-widened joint sets are dominant in the area, and are mostly associated wih man-made features including roads, ponds and drainage ditches. The joint sets occur at least every 400 feet and in some cases every 150 feet (density of the joints), and are infilled with low resistivity (high conductivity) piped clays. A pattern where the joint sets often broaden with depth with lower resistivity values at greater depths was observed in the ERT images. This could be as a result of higher moisture concentrations at depth and the broadening of vertical seepage pathways through fractured rock. Cutter and pinnacle type of karst is most likely in the area especially around the E-W oriented ERT profiles.

Richland case study involved assessment of a private property for karst features. Interpreted results of the study showed that a near-vertical solution-widened joint was mapped in the area, and dissolution of the dolomite bedrock is controlled by this joint, in line with structural lineaments in the area. The joint cut across a surface depression at 150 feet mark around ERT profile 2, and was interpreted as a possible channel through which surface water percolates into the subsurface. The joint was filled with low resistivity (moderately conductive soils) materials which are possible karst infills. Also, the property was underlain by up to 50 feet of either fractured/weathered rock or competent soil or a combination of both, and depth to top of competent rock was around 40 feet and above which would increase the cost of building on the site.

Based on the result of the study from the six case studies it was concluded that karst in Missouri is formed mostly through solution-widened joints where dissolution is intense, and through the process of “piping”.

About 40% of the mapped solution-widened joints (joint orientation) conform with known structural lineaments in the study areas. This showed that preferential surface and groundwater flow direction are mostly controlled by solution-widened joints and structural lineaments in the mapped areas.

In terms of placement, low resistivity clay and soil materials are mostly placed in joints which serve as conduits through which they are transported to the subsurface, and the low resistivity (high conductivity) was as a result of high moisture content at greater depths.

Density of solution-widened joints is high where intense dissolution is taking place, where there is underground depression and where karst features like sinkholes and caves occur or are close to the imaged area. The area with highest karst density in the study was in Battlefield area where one solution-widened joint occurs every one hundred and fifty feet (1/150 feet), and these joints are mostly due to man-made features including roads, parking lots, ponds, hedges and drainage ditches. The type of karst features in the area represent “pinnacle karst”.

Finally, Missouri karst is varied and cannot be classified as a particular type of karst using the criteria for engineering classification of karsts, instead the karst is a combination of kI (juvenile), kIII (mature) and kIV (complex) karsts.

The study has socio-economic implications such as minimizing loss of life and properties through gradual subsidence and sinkhole collapses since people would be enlightened more on activities that are likely to cause sinkholes or ground subsidence. About 40% of sinkhole collapses recorded in Missouri are caused by man-made features including roads, parking lots, ponds, hedges and drainage ditches. These man-made features retain water which percolates into the subsurface through pre-existing fractures which result to sinkhole or subsidence.

The study would also help in decision making while siting boreholes for drinking water to minimize groundwater contamination and pollution through sinkholes, since sinkholes have direct access to groundwater.

The study would create awareness to residents on the need to have the type of insurance that would cover their properties in the event of sinkhole disaster.

Even insurance policy makers would benefit from the study during policy formulation for residents, and in drawing geohazard maps of the area.

It would also serve as a good source of information in geotechnical and civil engineering works related to sinkhole mitigation and remediation.

Karst problems worldwide cause huge annual costs as a result of insufficient understanding of karst processes, and Missouri is recognized as a karst state. Due to complex nature of karst terrain (very strong lateral and vertical changes of physical and lithological properties), subsurface investigation in this area has been a challenge over the years. Typical surficial studies using geological, hydrological and geomorphological methods which have been the case in Missouri are not enough to provide information on degree of karst development, and will not determine the internal structure of karst system. The study has shown that mapping karst related features using geophysical techniques would help understand karst processes better in Missouri.

REFERENCES

A. C. Waltham and P. G. Fookes (2003) “Engineering classification of karst ground conditions”, Re-published from Quarterly Journal of Engineering Geology and Hydrogeology, 36:101-118

Advanced Geosciences, Inc., “Instruction Manual for the SuperSting with Swift Automatic Resistivity and IP System,” 2013.http://www.agiusa.com.

Ahmed S, Carpenter PJ (2003), “Geophysical response of filled sinkholes, soil pipes and associated bedrock fractures in thinly mantled karst, east-central Illinois”. Journal of Environmental Geology, 44:705-716

Bernard R. Wair, Jason T. DeJong and Thomas Shantz (2008) “Guidelines for Estimation of Shear Wave Velocity Profiles”. Pacific Earthquake Engineering Research Center Headquarters at the University of California, Peer Report 2012/08

Cardarelli E, Di Filippo G, Tuccinardi E (2006), “Electrical resistivity tomography to detect buried cavities in Rome: a case study”. Near Surface Geophysics, 4:387-392

Choon B. Park, Richard D. Miller, Jianghai Xia, and Julian Ivanov (2007) “Multichannel Analysis of Surface Waves (MASW)-Active and Passive Methods”. The Leading Edge

Daniel W. Casto, Barbara Luke, Carlos Calderon-Macias and Ronald Kaufmann (2009) “Interpreting Surface Wave Data for a Site with Shallow Bedrock”. Journal of Engineering and Environmental Geophysics, 14:115-127

Debeglia N, Bitri A, Thierry P (2006), “Karst investigations using microgravity and MASW; Application to Orleans, France”. Journal of Near Surface Geophysics, Vol 4, No 4, August 2006, 215-225

Derek Ford and Paul Williams (2007) “Karst hydrogeology and Geomorphology”. John Wiley & Sons, Ltd.

Dewashish Kumar, S. Thiagarajan , S. N. Rai (2011), “Deciphering geothermal resources in Deccan Trap region using electrical resistivity tomography technique” Journal of Geological Society of India, 78:541-548

El-Qady G, Hafez M, Abdalla MA, Ushijima K (2005), “Imaging subsurface cavities using geoelectric tomography and ground-penetrating radar”. Journal of Cave and Karst Studies, 67:174-181

Ezersky M, Bruner I, Keydar S, Trachtman P, Rybakov M (2006), "Integrated study of the sinkhole development site on the western shores of the Dead Sea using geophysical methods". Near Surface Geophysics 4:335-343

Elawadi E, El-Qady G, Nigm A, Shaaban F, Ushijima K (2006), "Integrated geophysical survey for site investigation at a new dwelling area Egypt". Journal of Environmental Engineering Geophysics, 11:249-259

Franjo Sˇumanovac a, Mario Weisser b (2001) "Evaluation of resistivity and seismic methods for hydrogeologicalmapping in karst terrains". Journal of Applied Geophysics, 47:13-28

George V, Harvey D, Nicholas C. Crawford, Christopher G. Groves, George N. Huppert, Ernst H. Kastning, Rick Olson, Betty J. Wheeler (2001) "Living with Karst, A Fragile Foundation". AGI Environmental Awareness Series 4

Gibson PJ, Lyle P, George DM (2004), "Application of resistivity and magnetometry geophysical techniques for near-surface investigations in karst terrains in Ireland". Journal of Cave and Karst Studies, 66:35-38

Jianghai Xia, Richard D. Miller, Choon B. Park, and Julian Ivanov (2000), "Construction of 2-d vertical shear-wave velocity field by the multichannel analysis of surface wave technique": Proceedings of the Symposium on the Application of Geophysics to Engineering and Environmental Problems, Arlington, Va., February 20-24, pp. 1197-1206

Julian Ivanov, Choon B. Park, Richard D. Miller, Jianghai Xia, James A.Hunter, Ron L. Good, and Robert A. Burns (2000) "Joint Analysis of Surface-Wave and Refraction Events from River-bottom Sediments". Society for Exploration Geophysicists Expanded Abstracts

Kansas Geological Survey "Multichannel Analysis of Surface Waves", 2013 http:/www.masw.com/index.html

Kaufmann O, Quinif Y (2001), "An application of cone penetration tests and combined array 2D electrical resistivity tomography to delineate cover-collapse sinkhole prone areas: geotechnical and environmental applications of karst geology and hydrology". Balkema,Lisse, the Netherlands, pp. 359-364

Konstantinos C, Valérie P, Roger G, Rémi V, Frank P. Bosch (2011) "Contribution of Geophysical Methods to Karst-system Exploration: an overview" Hydrogeology Journal 19: 1169-1180

Kruse S, Grasmueck M, Weiss M, Viggiano D (2006), "Sinkhole structure imaging in covered karst terrain". Geophysical Research Letters, 33: L16405

Loke, M. H (2013), “Electrical Imaging Surveys for Environmental and Engineering Studies, “(http://moho.ess.ucla.edu/~pdavis/ess135_2013/literature/ %20%Lokedcresistivity.pdf)

McGrath RJ, Styles P, Thomas E, Neale S (2002), “Integrated high-resolution geophysical investigations as potential tools for water resource investigations in karst terrain”. Journal of Environmental Geology, 42:552-557

NDT Education Resource Center, “The Collaboration for NDT Education” Iowa State University, 2015 www.ndt-ed.org.

Neil L. Anderson, Derek B. Apel and Ahmed Ismail, 2006, “Assessment of Karst Activity at Highway Construction Sites Using the Electrical Resistivity Method,” unpublished report for MoDOT.

Rene P, Maros N, Ivan D, David K (2012) “Determination of Cavities Using Electrical Resistivity Tomography”. Contributions to Geophysics and Geodesy, 42:201-211

Robinson, E.S. and Coruh, C., 1988. “Basic Exploration Geophysics,” Wiley, New York, 562pp.

Šumanovac F, Weisser M (2001) “Evaluation of resistivity and seismic methods for hydrogeological mapping in karsts terrains”. Journal of Applied Geophysics, 47:13-28

Thomas L. Dobecki, Sam B. Upchurch (2006) “Geophysical Applications to Detect Sinkholes and Ground Subsidence”. The leading Edge, 25:336-341

Thomas L. Dobecki (2010) “Sinkholes and Pitfalls in Urban Geophysics” The leading Edge, 944-951

Valois R, Bermejo L, Guérin R, Hinguant S, Pigeaud R, Rodet J (2010), “ Karstic morphologies identified with geophysics around Saulges caves (Mayenne, France)”. Journal of Archaeological Prospection, 17:151-160

Valois R, Camerlynck C, Dhemaied A, Guérin R, Hovhannissian G, Plagnes V, Rejiba F, Robain H (2011), “Assessment of doline geometry using geophysics on the Quercy plateau karst (South France)”. Journal of Earth Surface Processes and Landforms, 36 (9): 1183-1192

Van Shoor M (2002), “Detection of sinkholes using 2D electrical resistivity imaging”. Journal of Applied Geophysics, 50:393-399

Wanfang Zhou, Barry F. Beck, Angela L. Adams (2002) “Effective electrode array in mapping karst hazards in electrical resistivity tomography”. Journal of Environmental Geology, 42:922-928

Zhou W, Beck BF, Stephenson JB (1999), “Investigation of ground water flow in karst areas using component separation natural potential measurements”. Journal of Environmental Geology, 37:19-25

Zhou W, Beck BF, Stephenson JB (2000), “Reliability of dipole-dipole electrical resistivity tomography for defining depth to bedrock in covered karst terranes”. Journal of Environmental Geology, 39:760-766

Zhou W, Beck BF, Adams AL (2002), “Effective electrode array in mapping karst hazards in electrical resistivity tomography”. Journal of Environmental Geology, 42:922-928

VITA

Jeremiah Chukwunonso Obi was born in Ogidi in Anambra state, Southeastern Nigeria. He graduated from Nnamdi Azikiwe University Awka Nigeria in 1997 with Bachelor's degree (BSc. Hons) in Geological Sciences. He gained admission into Missouri University of Science and Technology in 2010 and graduated in 2012 with a Master of Science (MS) degree in Geological Engineering. Shortly after graduation, he was awarded the prestigious Chancellor's Fellowship to pursue his doctorate degree in Geological Engineering.

During his school days, he worked as a teaching assistant (TA) and research assistant (RA). He was involved in various field projects utilizing various geophysical techniques in solving geotechnical and environmental problems. He served as a departmental representative in the council of graduate students (CGS). He was an active member of the Society of Exploration Geophysicists (SEG), American Association of Petroleum Geologists (AAPG) and Association of Environmental and Engineering Geologists (AEG) where he presented abstracts and posters in various conferences. He was a co-author of a paper titled Electrical Resistivity Tomography Investigations.

He graduated in May 2016, and was awarded a doctor of philosophy, PhD. in Geological Engineering.